Summer 2022

Synthesis of model oxepin substrates for comparative two electron oxidation studies with cytochrome P450 and cerium ammonium nitrate to investigate benzene metabolism

Ryan William Fitzgerald

I. Synthesis of Model Oxepin Substrates for Comparative Two Electron Oxidation Studies with Cytochrome P450 and Cerium Ammonium Nitrate to Investigate Benzene Metabolism

II. Attempted Synthesis of 4-Silatranone Lactam Derivatives via Strained Silacyclobutanes

III. Synthesis of a Bifunctional Iron(II)/Iron(III) Hexadentate 8-Hydroxyquinoline-Based Chelator Scaffold

By

Ryan W. Fitzgerald

B.S. Chemistry, University of New Hampshire, 2017

DISSERTATION

Submitted to the University of New Hampshire

in partial fulfillment of

the requirements for the degree of

Doctor of Philosophy

In

Chemistry

September, 2022

This dissertation was examined and approved in partial fulfillment of the requirements for the degree of Doctor of Philosophy in Chemistry by:

Dissertation director, Roy P. Planalp, Associate Professor of Chemistry

Arthur Greenberg, Professor Emeritus of Chemistry

Christopher F. Bauer, Professor of Chemistry

Patricia M. Stone, University Instrumentation Center

Eric M. Gale, Assistant Professor of Chemistry, Massachusetts General Hospital

On 07/28/2022

Approval signatures are on file with the University of New Hampshire Graduate School.

DEDICATION

I dedicate this dissertation to my late siblings William, Thomas, and Amy. Losing the three of them has pushed me to work my hardest in school and research so that I can achieve as many of my goals in life as possible.

I would also like to dedicate this dissertation to my undergraduate assistants Noah Cote and Tristan Hart-Bonville. This journey has had many ups and downs personally and their hard work kept me moving throughout all of life's challenges.

ACKNOWLEDGEMENTS

I would first like to acknowledge my two advisors Dr. Planalp and Dr. Greenberg. Dr. Planalp constantly encouraged me to improve upon my work especially my seminar which would not have been as good without his constant critiques. I feel that I have grown immensely as a chemist because of Dr. Planalp's feedback. Dr. Greenberg has been a real constant in my life since joining his group as an undergrad in the fall of 2014. I really appreciate that Dr. Greenberg took a chance on a student with a sub 3.00 GPA at the time-I would have never gotten this far if he had not noticed my hard work on my advanced organic lab project in his research lab.

Dr. Tomellini provided a lot of insight in the standard addition method for our enzyme experiments as well as with the use of the GCMS. Dr. Holly Weaver-Guevara provided a lot of help characterizing data, worked out the enzymatic protocol almost entirely on her own, and was a great mentor during my time on the project. I owe most of my success to Holly and most of my techniques can be credited to her patient teaching and constant positive reinforcement. I appreciate the members of the Dr. Stacia Sower and Dr. Sherine Elsawa labs in the UNH BMCB (Biochemistry, Cellular and Molecular biology) department for allowing us to use their equipment. I would also like to thank the Anyin Li group and Dr. Jesse Ambrose for all their help with GCMS analysis for my various projects. Dr. Sebastian Pantovich of the Gonghu Li group also helped immensely with headspace analysis in the Li lab for my dibenzo dimer breakdown/coupling reaction. The Department of Chemistry as a whole is also gratefully acknowledged.

It was a real pleasure being a member of the Greenberg group. The small size of the group made gave it a family atmosphere. I would not have accomplished as much as I have without them and my grades in all my chemistry courses increased once I became a member of

the group. I've also grown a lot as a scientist by mentoring Noah Cote and Tristan Hart-Bonville- to see both them succeed as a graduate student and industry worker, respectively, and this has brought me great pride and joy. I would also like to thank my group members in the Planalp group especially Leonid Povolotskiy-his hard work really pushed me to get back in the lab each day to keep up with his growth.

TABLE OF CONTENTS

DEDICATION……iii

ACKNOWLEDGEMENTS……iv

LIST OF SCHEMES…….…….……..viii

LIST OF FIGURES……ix

ABSTRACT……...xi

GENERAL INTRODUCTION…….…….…….……01

CHAPTER PAGE

I. SYNTHESIS OF MODEL OXEPIN SUBSTRATES FOR COMPARATIVE TWO ELECTRON OXIDATION STUDIES WITH CYTOCHROME P450 AND CERIUM AMMONIUM NITRATE TO INVESTIGATE BENZENE METABOLISM…..……....02

Introduction……...02

Results and Discussion……..06

General Conclusions……...……...16

II. SYNTHESIS OF 2,3-BENZOXEPIN FOR COMPARATIVE ENZYMATIC AND OXIDATION STUDIES USING CYTOCHROME P450, MCPBA, AND CERIUM AMMONIUM NITRATE…….17

Introduction……...17

Results and Discussion……..20

General Conclusions……...……...23

III. ATTEMPTED SYNTHESIS OF 4-SILATRANONE LACTAM DERIVATIVES VIA STRAINED SILACYCLOBUTANES…….25

Introduction……...25

Results and Discussion……..27

General Conclusions……...……...31

IV. SYNTHESIS OF FIVE RELATED AMIDES TO MEASURE THE EFFECT OF HYDROGEN BONDING ON AMIDE ROTATIONAL BARRIERS…….33

Introduction……....33

Results and Discussion……..34

General Conclusions……...……...38

V. SYNTHESIS OF A BIFUNCTIONAL IRON(II)/IRON(III) HEXADENTATE 8-HYDROXYQUINOLINE-BASED CHELATOR SCAFFOLD……..……..…39

Introduction……....39

Results and Discussion……..44

General Conclusions……...……...48

VI. EXPERIMENTAL…….....49

General Experimental…….....49

Detailed Experimental……...51

LIST OF REFERENCES……...71

APPENDIX……..I

LIST OF SCHEMES

NUMBER PAGE

1.1. Multistep synthesis of 4,5-benzoxepin……05

1.2. Photochemical synthetic route towards 4,5-benzoxepin……..05

1.3. Synthesis of dibenzodimer comparison……06

2.1. Attempted multistep synthesis of 2,3-benzoxepin……18

2.2. Single step synthesis of 2,3-benzoxepin via in situ benzyne generation……...19

2.3. Comparison of model oxepin substrate 2,3-benzoxepin reaction with cytochrome P450 isoform 1A2 vs. reactions with CAN and *m*CPBA……...19

3.1. Attempted synthesis of novel silatranone lactam derivatives……26

3.2. Quantitative synthesis of 1-methylsilatrane……...27

4.1. One-step syntheses of four of the five related amides. N,N-diethylacetamide (4-2) was purchased. Glycolic acid acetonide (3-3) was synthesized via the same procedure as in chapter 3……35

5.1. Synthesis of tripodal hexadentate chelator linked to a mitochondria targeting tetrapeptide……42

LIST OF FIGURES

NUMBER PAGE

1. Benzene Metabolism via cytochrome P450 oxidation…….....xi

2. Resonance forms of amides and lactams……...xii

3. Novel synthetic approach toward silatranone derivatives via strained silacyclobutane…xii

4. Target molecule for sensing and sequestering intracellular iron……..xiii

1.1. Davies and Whitham proposed mechanism of benzene metabolism towards E,E-muconaldehyde/E,E-muconic acid via a 2,3-epoxyoxepin thermal rearrangement tested by Golding and coworkers and observed by Greenberg and coworkers..…...…...…….02

1.2. Golding and coworkers proposed mechanism of benzene metabolism towards E,E-muconaldehyde/E,E-muconic acid via consecutive one electron oxidation……...……..03

1.3. Dehydrohalogenation to form 4,5-benzoxepin……..07

1.4. Dr. Jessica Morgan's observation of 1H-2-benzopyran-1-carboxaldehyde presumably via a 2,3-epoxyoxepin and di-aldehyde intermediates…….08

1.5. Potential mechanism of breakdown of dimer 1-7 into isocoumarin with 146 M/Z and 174 M/Z peaks via Electron Impact Mass Spectrometry……..09

1.6a. Proposed mechanism for the formation of dimer 1-7……11

1.6b. Proposed mechanism for the formation of dimer 1-10……..12

1.7. Typical enzyme reaction protocol……..13

1.8. A) Total Ion Chromatogram (TIC) for reaction of 4,5-benzoxepin 5 with P450 1A2; B) Mass spectra of compounds 5, 6, and "fraction 1" product, respectively……..14

2.1. A.) Past group member's model oxepin 2,7-dimethyloxepin. B.) Versatility of 2,3-benzoxepin as a model oxepin substrate……18

2.2. In situ generation of benzyne from anthranilic acid……..…..…..20

2.3. ^{1}H NMR of the A.) mCPBA reaction with 2,3-benzoxepin and B.) the CAN reaction with 2,3-benzoxepin……...21

2.4. Electron impact mass spectra of CYP1A2 reaction with 2,3-benzoxepin……22

3.1. Left to right: Adamantane lactam derivative synthesized and computational analyzed via Dr. Jessica Morgan; Silatrane derivatives computationally analyzed by Azaline Dunlop-Smith and synthesized in this work; 1-methyl-4-silatranone, the target molecule of this work……...25

3.2. ^{1}H NMR of potential 1-methyl-4-silatranone in a mix of $CDCl_3$ and CD_3OD…….29

3.3. ^{1}H-^{1}H COSY NMR of potential 1-methyl-4-silatranone in a mix of $CDCl_3$ and CD_3OD..……...29

3.4. Electron impact mass spectrum of reaction towards 1-methyl-4-silatranone……31

4.1. Five related amides synthesized and purchased for testing amide rotational barriers and number of hydrogen bond donors/acceptors……..…...33

4.2. Derivatives of the Eyring equation that relates coalescence temperature (Tc) and change in chemical shift (in Hz) with transition state Gibbs free energy ($\Delta G^{\ddagger}$ in kJ/mol above or kcal/mol below)…….34

4.3. Variable temperature NMR data for A) 3-5 and B) 3-5 1/10 dilution……...36

4.4. Calculated $\Delta G^{\ddagger}$ values (shown in kcal/mol with uncertainty ±0.1-0.2 kcal/mol) from coalescence temperatures (shown in °C) for the five related amides in this study……37

5.1. Fenton chemistry……40

5.2. Inspiration for the hexadentate iron chelator. Left to right: Hider and coworkers catecholic peptide design, Planalp and coworkers Fe2+ tamepyr ligand, and Serratrice and workers conjugatable tripodal hexadentate ligand CacCAM for Fe3+……...41

5.3. Synthesis of imine trinitrile/first tripodal structure……45

5.4. A.) Imine hydrolysis of imine trinitrile in aldehyde trinitrile and B.) spectral evidence of aldehyde formation……45

5.5. Synthesis for converting aldehyde trinitrile into alcohol trinitrile……47

5.6. Synthesis of the TBS protected alcohol trinitrile tripod via TBS-OTf reflux of the alcohol trinitrile……..47

5.7. Synthesis of the TBS alcohol triamine tripod via Raney Ni/NaBH4 reduction……47

ABSTRACT

Two model oxepins were synthesized in an attempt to model the metabolism of benzene in the human liver. 4,5-Benzoxepin was subjected to similar enzyme reactions that the oxepin metabolite itself would encounter if one was exposed to benzene. In addition, a synthesis of 2,3-benzoxepin was completed in order to compare enzyme and non-enzyme catalyzed reactions with that of 4,5-benzoxepin. In an attempt to test the validity of the enzyme reactions, the model oxepins were also reacted with a two single electron oxidizing inorganic salt, cerium (IV) ammonium nitrate (CAN) to see if the intermediates following the enzyme reaction were consistent. Other chemists in the past have postulated that oxepin undergoes further epoxidation in metabolism instead of two single electron oxidations, so a test with dimethyldioxirane (DMDO) was also performed on the model oxepins to observe if their products closer matched the enzyme reactions. Research suggests that oxepin can follow both the two single electron oxidation and further epoxidation metabolic pathways when exposed to enzymes CYP1A2 and CYP3A4 under multiple concentrations of enzyme with a fixed concentration of model oxepin substrate.

Keywords: *1-benzoxepin, 2,3-benzoxepin, 3-benxoxepin, 4,5-benzoxepin, benzene metabolism, oxepin, cytochrome P450, isoform 1A2, isoform 3A4, isoform 2E1, pHLM*

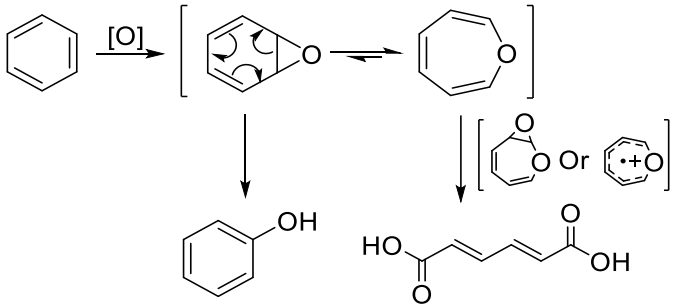

Figure 1. *Benzene Metabolism via cytochrome P450 oxidation. Some possible products are phenol (left) and E,E-muconic acid (right).*

Amides and lactams are common structural motifs found in a variety of natural products and construct the backbone of amino acid chains, proteins, and enzymes. Amides have 3 major resonance contributors (see **Figure 2**). 4-Silatranones have been calculated previously to have the nitrogen lone pair delocalized like in normal amides vs. having a coordinate covalent bond with silicon as in silatranes, which is a bridged bicyclic amine dependent upon conformation. This research aims to synthesize strained lactams known as 4-silatranones (**Figure 3**) and to help elucidate who wins the competition for nitrogen's lone pair-the silicon via dative bond or delocalization into the amide carbonyl.

Keywords: *Silatranone, strained lactams, amide resonance, silacyclobutane*

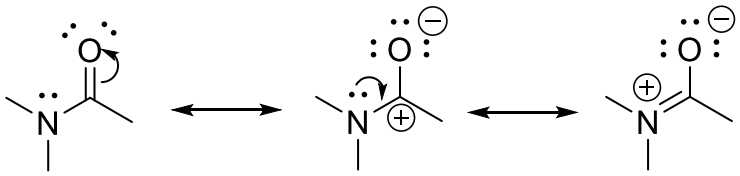

Figure 2. *Resonance forms of amides and lactams.*

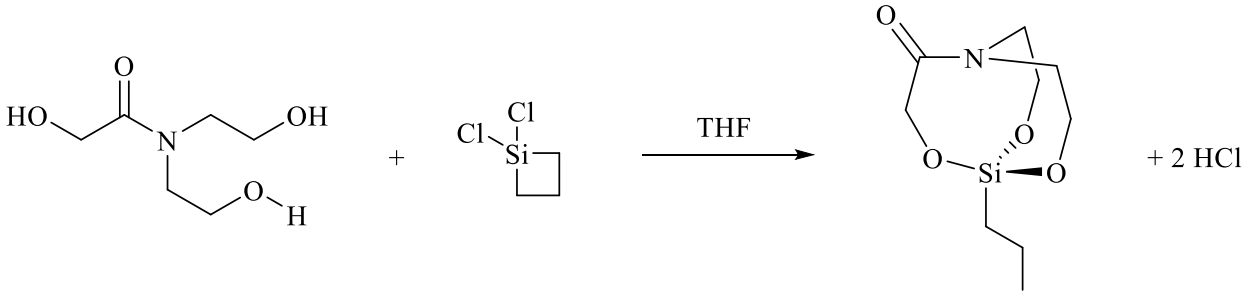

Figure 3. *Novel synthetic approach toward silatranone derivatives via strained silacyclobutane. Note: IUPAC name for structure shown: 1-propyl-2,8,9-trioxa-5-aza-1-silabicyclo[3.3.3]undecane-4-one*

Iron chelators have many biological applications including the treatment of iron overload disease, the suppression or promotion of reactive oxygen species production and even the ability

to sense the iron status in the cell. Development of a chelator that can modulate and sense intracellular iron is the goal of this research. 8-hydroxyquinoline has been shown as a powerful chelating agent for iron in the past when three equivalents of 8-hydroxyquinoline have been tethered to a tripodal linker allowing for a hexadentate chelator to completely sequester iron. This portion of the project focuses on the synthesis of a tripodal linker with a carboxylic acid handle (**Figure 4**) to attach the chelator to lysine residue of a SS-peptide (synthesized by a research group member) that targets the mitochondria of a cell which contain labile iron pools.

Keywords: *Tripodal linker, tripodal chelator, hexadentate chelator, chelation therapy, SS-peptide, 8-hydroxyquinoline, 7-carboxy-8-hydroxyquinoline, iron metabolism, bifunctional iron chelator*.

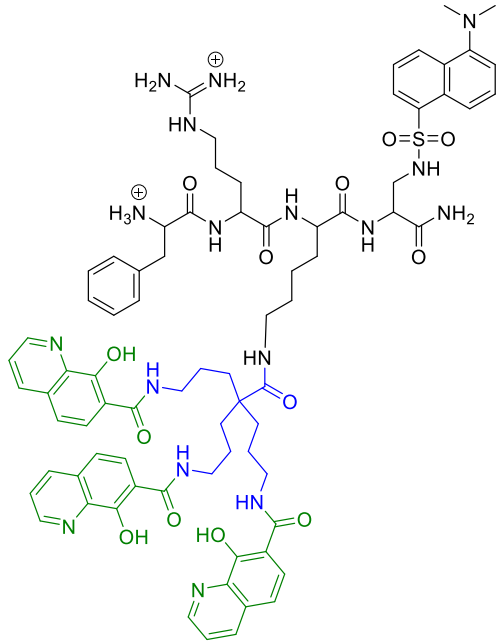

Figure 4. *Target molecule for sensing and sequestering intracellular iron. Mitochondria targeting peptide with fluorescent sensor shown in* ***black****, 7-carboxy-8-hydroxyquinoline pendants shown in* ***green****, and triamine tripodal linker with carboxylic acid handle shown in* ***blue*** *(target portion of this research).*

GENERAL INTRODUCTION

This thesis is divided into six chapters: 1) Synthesis of model oxepin substrates for comparative two electron oxidation studies with enzymes and cerium ammonium nitrate to investigate benzene metabolism; 2) Synthesis of 2,3-benzoxepin for comparative enzymatic and oxidation studies using cytochrome P450, *m*CPBA, and cerium ammonium nitrate; 3) Attempted synthesis of 4-silatranone derivatives via strained silacyclobutanes; 4) Synthesis of five related amides to measure the effect of hydrogen bonding on amide rotational barriers; 5) Synthesis of a bifunctional iron(II)/iron(III) hexadentate 8-hydroxyquinoline based chelator scaffold; 6) Experimental Section. Chapter one contains an introduction, results and discussion, and conclusions sections of the exploration of oxepin route benzene metabolism modeled by 4,5-benzoxepin with potential work that could be performed on other model substrates. Chapter two details oxidation testing on another model oxepin substrate-2,3-benzoxepin. Chapter three shows attempts at a novel synthesis of 4-silatranone lactams. Chapter four shows the variable temperature NMR studies on five related amides to measure amide rotational barriers. Chapter fives entails the synthesis of a linker scaffold for attaching a hexadentate iron (II)/(III) chelator to a mitochondria targeting peptide. Chapter six contains relevant experimental details to support the results revealed in chapters one-five.

Chapter 1

Synthesis of Model Oxepin Substrates for Comparative Two Electron Oxidation Studies with Cytochrome P450 and Cerium Ammonium Nitrate to Investigate Benzene Metabolism

Introduction

Benzene is a known carcinogen and toxic chemical used in industry and as an industrial byproduct.[1,3-7] Knowing the mechanistic pathways which potential toxin substances break down in the body is useful to prevent illnesses and help those ailing presently.[1,3-7] The hypothesis by Davies and Whitham that epoxidation of oxepin to a reactive 2,3-epoxyoxepin intermediate furnished the major focus for this study.[2] Oxepin derivatives are, therefore, useful models in investigating the ring opening mechanism of oxepin as postulated in benzene metabolism.[2-7] 4,5-Benzoxepin (aka. 3-benzoxepin) is a good substrate for use in enzymatic oxidation studies with cytochrome P450.[25,26,28] This project focuses on improving the synthesis of 4,5-benzoxepin for use in enzymatic reactions by the Greenberg research group at UNH to establish the eukaryotic metabolic, ring-opening pathway of benzene and adding a new trial substrate in 2,3-benzoxepin (discussed in chapter 2) to further reveal how oxepin derivatives react when exposed to enzymes.[2,30,45,46]

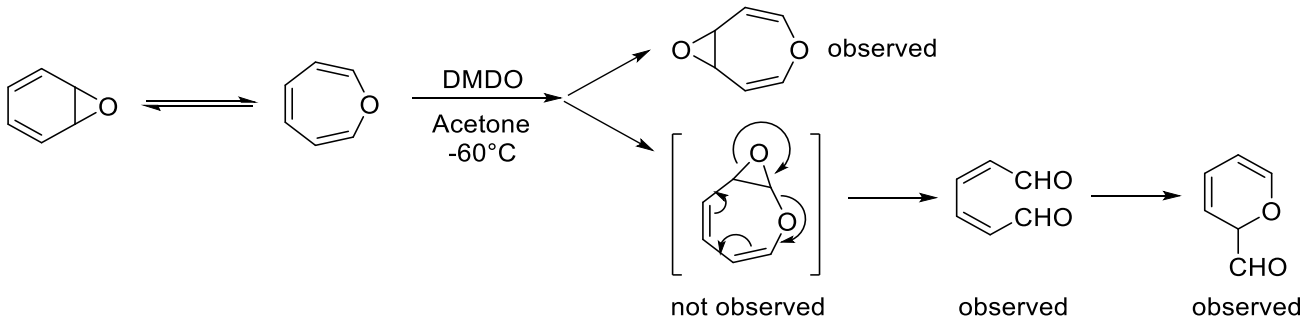

Figure 1.1. *Davies and Whitham proposed mechanism of benzene metabolism towards E,E-muconaldehyde/E,E-muconic acid via a 2,3-epoxyoxepin thermal rearrangement tested by Golding and coworkers and observed by Greenberg and coworkers in the present study*[2,48]

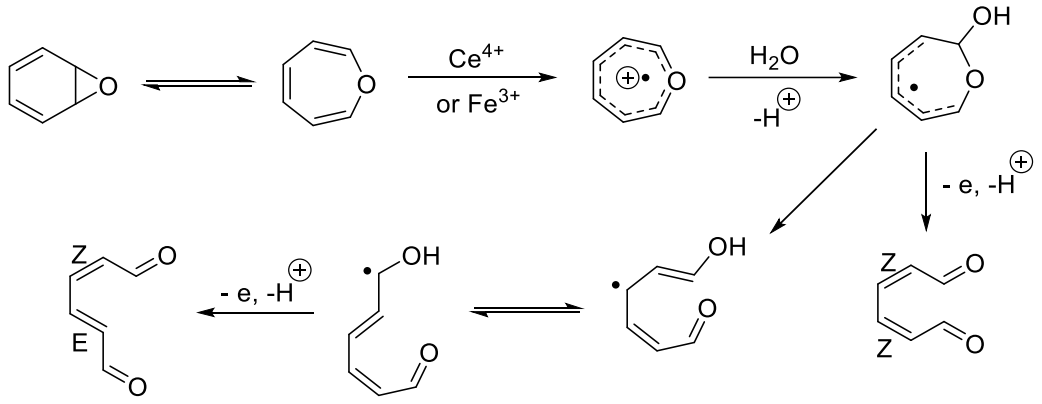

Figure 1.2. *Golding and coworkers proposed mechanism of benzene metabolism towards E,E-muconaldehyde/E,E-muconic acid via consecutive one electron oxidation*[29]

Investigation of benzene metabolism via the oxepin route goes back several decades. Vogel and coworkers demonstrated that benzene is first epoxidized to benzene oxide and undergoes a rapid valence tautomerization with oxepin in 1967.[1] In 1977 Davies and Whitham postulated that the oxepin intermediate may undergo further epoxidation via a 2,3-epoxyoxepin intermediate followed by thermal rearrangement to Z,Z-muconaldehyde and isomerization to E,E-muconaldehyde/E,E-muconic acid (via aldehyde dehydrogenase).[2] In 1982 Tochtermann and coworkers observed a stable 2,3-epoxyoxepin via epoxidation of an alkyl bridged oxepin.[24] In 1997 Golding and coworkers observed Z,Z-muconaldehyde and a ring closed pyrancarboxaldehyde of muconaldehyde after DMDO low temperature epoxidation of oxepin but were unable to observe the 2,3-epoxyoxepin intermediate via their methods.[27] Greenberg and coworkers observed a simple 2,3-epoxyoxepin via low temperature NMR oxidation of 2,7-dimethyloxepin which rearranges to a diketone structure upon gentle heating in 1998.[26] In

2010, Golding and coworkers suggested that oxepin could ring open via a consecutive single electron oxidation (two electrons removed from oxepin total) mechanism via tests with Ce^{4+} and Fe^{3+} yielding muconaldehyde isomers.[29] Finally, in 2020, we published our GC/MS findings of cytochrome P450 oxidation with that of cerium (IV) ammonium nitrate (CAN) and dimethyldioxirane (DMDO) showing evidence for both mechanisms.[48]

Benzene metabolism via the oxepin route can be studied through the synthesis of model substrates containing a derivate of oxepin. The two studied were: 2,3-benzoxepin and 4,5-benzoxepin. Synthesis of 2,3-benzoxepin and synthesis of 4,5-benzoxepin have been completed and tested. The two model substrates can be made through multistep syntheses and can further be employed in enzymatic reactions and two electron oxidations with CAN. **Scheme 1.1** and **Scheme 1.2** show the two synthetic routes toward model oxepin 4,5-benzoxepin.

4,5-Benzoxepin had been earlier reacted with dimethyldioxirane leading to the observable 2,3-epoxyoxepin at low temperatures by our group.[25] Subsequently reacted with cerium (IV) ammonium nitrate which resulted in dimeric products (this work).[48] To further validate this dimer, a synthesis of a dibenzodimer derivative synthesis was performed and can be seen via **Scheme 1.3**.

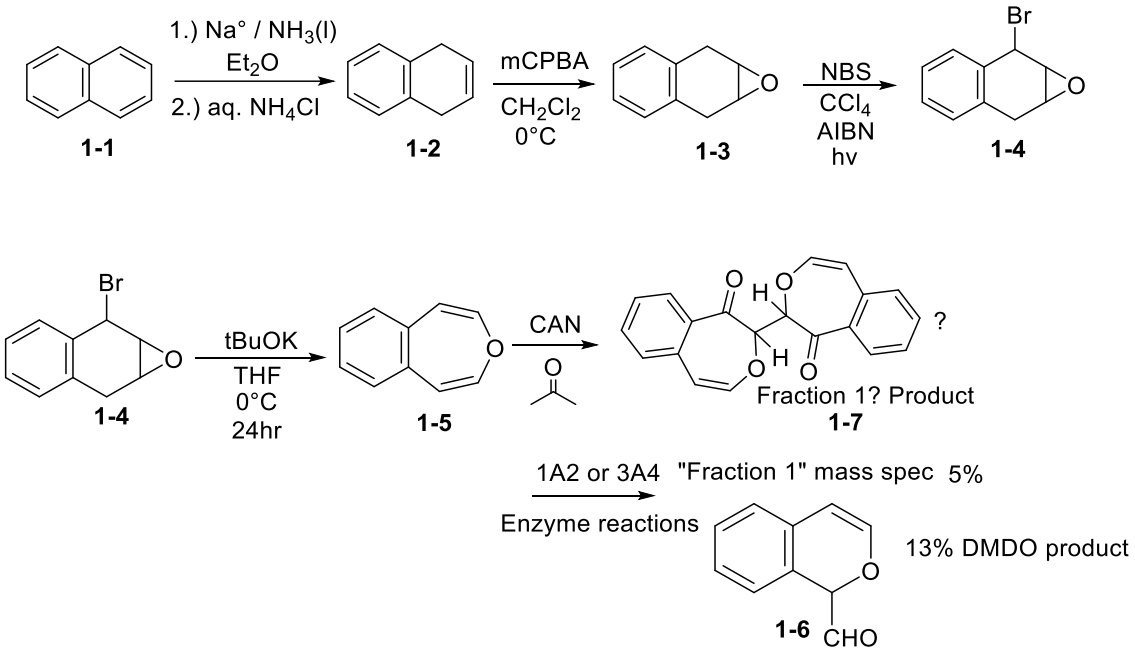

Scheme 1.1: *Multistep synthesis of 4,5-benzoxepin.*[48]

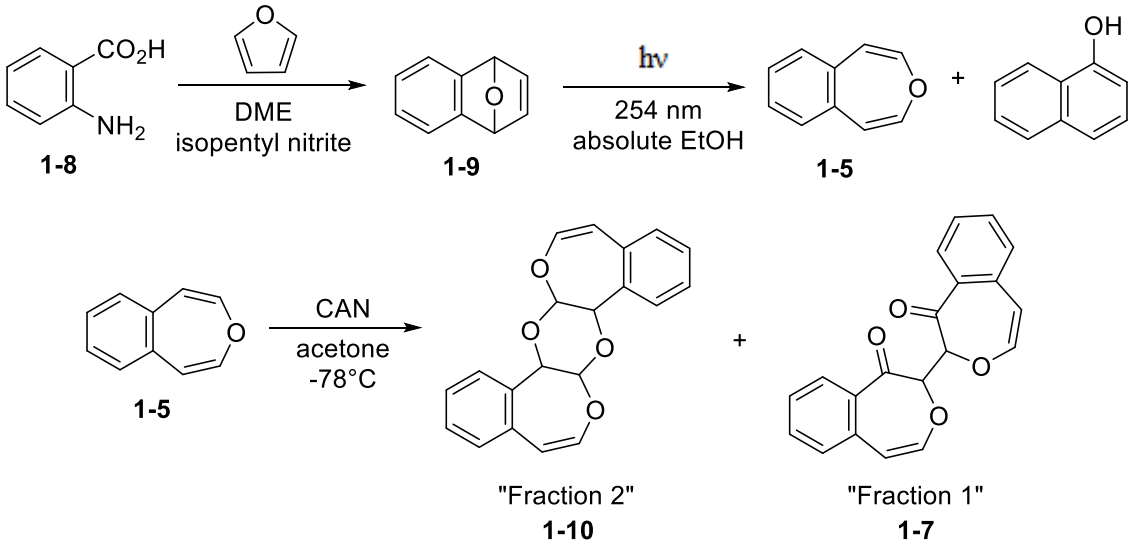

Scheme 1.2: *Photochemical synthetic route towards 4,5-benzoxepin.*[48]

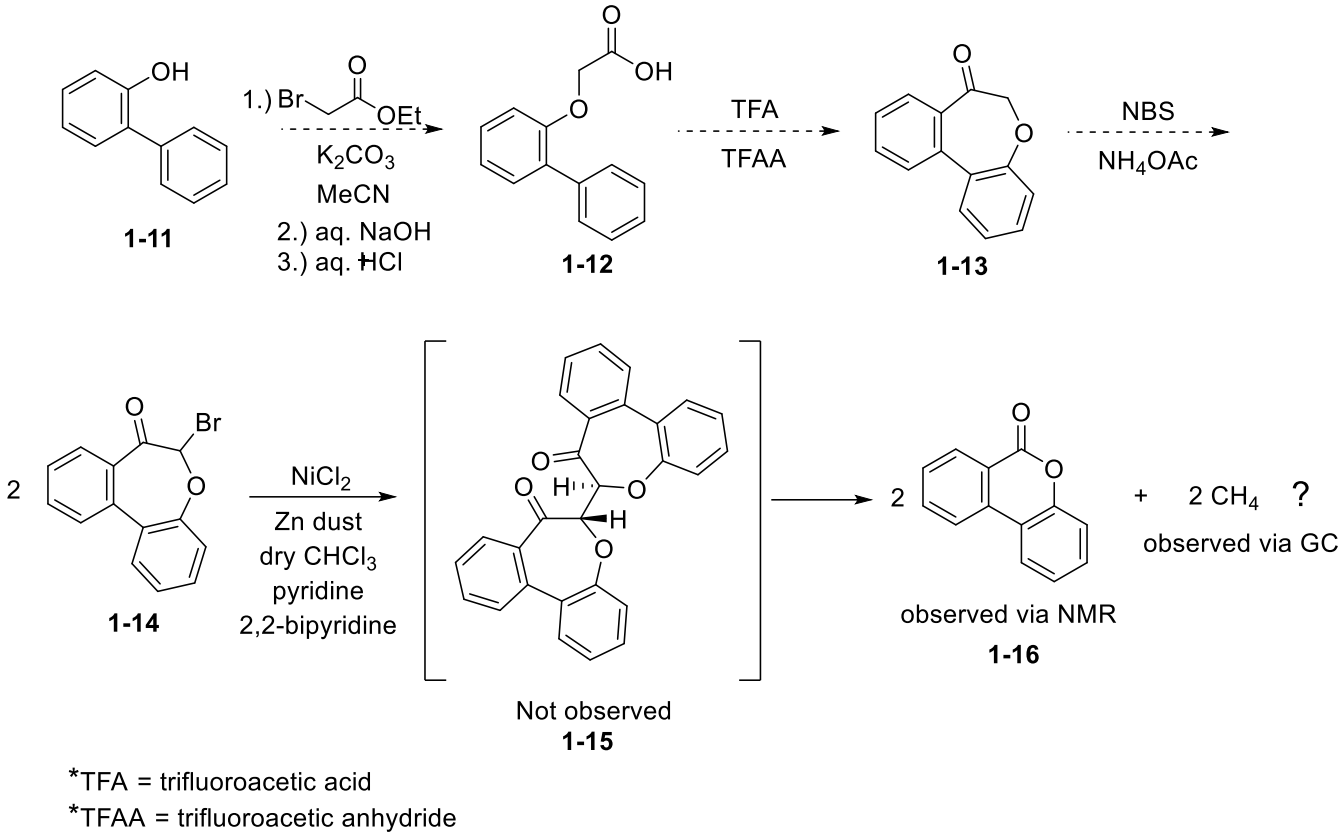

Scheme 1.3: *Synthesis of dibenzodimer comparison.*[48]

Results and discussion

4,5-Benzoxepin was the target model oxepin in this study and can be obtained via two different synthetic pathways. The original multistep synthesis involved starting with naphthalene (**1-1**) as the building block molecule. Naphthalene (**1-1**) first underwent a Birch reduction using sodium metal in liquid ammonium to yield 1,4-dihydronaphthalene (**1-2**). 1,4-dihydronaphthalene (**1-2**) has a free alkene not conjugated into the aromatic system which can be epoxidized using *m*CPBA to yield epoxide (**1-3**). Epoxide (**1-3**) is then subjected to benzylic bromination via NBS (N-bromosuccinimide) to install a good leaving group and to afford brominated epoxide (**1-4**). Brominated epoxide (**1-4**) can be converted to 4,5-benzoxepin (**1-5**)

via a dehydrohalogenation reaction using potassium t-butoxide as the hindered base. The mechanism for dehydrohalogenation is shown in **Figure 1.3** below.[48]

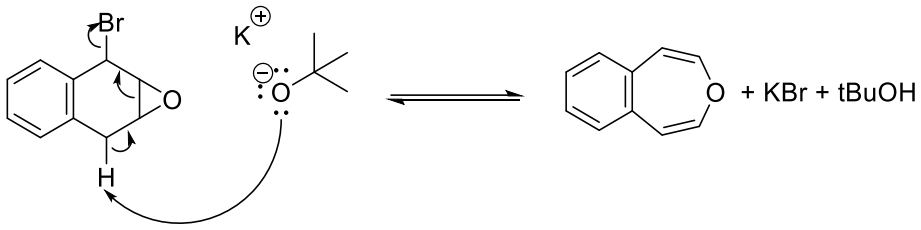

Figure 1.3. *Dehydrohalogenation to form 4,5-benzoxepin.*[1,48]

An alternative synthesis for 4,5-benzoxepin (**1-5**) was developed that was more succinct involving only two steps (**Scheme 1.2**). Anthranilic acid (**1-8**) proved to be a highly useful synthon as it allowed for *in situ* generation of benzyne which can undergo a Diels-Alder reaction with furan to yield bridged oxide (**1-9**). When dilute **1-9** was exposed to 254nm light in absolute ethanol, it afforded 4,5-benzoxepin (**1-5**) in approximately 10% yields after silica column to remove 82% 1-napthol byproduct.

4,5-benzoxepin (**1-5**) was subjected to epoxidation conditions using dimethyldioxirane by former Greenberg group members Jessica Morgan and Holly Guevara so it did not require repeat experiments as it afforded 1*H*-2-benzopyran-1-carboxaldehyde (**1-6**) product each time completed presumably via ring opened di-aldehyde and 2,3-epoxyoxepin intermediates as shown in **Figure 1.4** to study the further epoxidation mechanism of oxepin.[25]

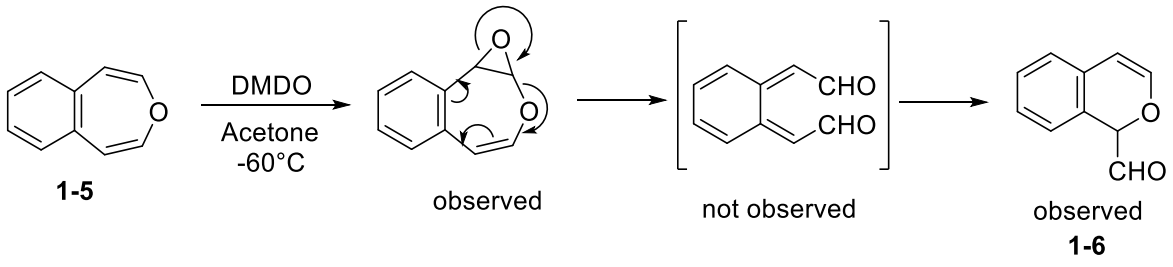

Figure 1.4. *Nauduri's observation of 1H-2-benzopyran-1-carboxaldehyde presumably via a 2,3-epoxyoxepin and di-aldehyde intermediates*.[25]

4,5-benzoxepin (**1-5**) was tested for consecutive single electron oxidation mechanism by using two equivalents of cerium (IV) ammonium nitrate (CAN) in the presence adventitious water from the solvent, acetone.[29] The two major products of the CAN reaction are known as "fraction 1" (**1-7**) and "fraction 2" (**1-10**) due to their fraction appearance upon silica flash chromatography. NMR experiments using deuterated acetone and excess CAN showed that **1-7** does not turn into **1-10** or vice versa over time. Dimeric product **1-7** was proposed by the group because of the integrations on the ^{1}H NMR (H=7), number of unique carbons (C=10), presence of ketone C=O on IR at 1666 cm^{-1}, and absence of O-H on IR. 2D NMR shows no coupling of the C-H proton of the dimeric linkage to other protons on the structure (via COSY) and no through space interactions (via NOESY). This led our group to the conclusion that there is a C-C bond in a dimeric fashion. Unfortunately, upon electron impact mass spectrometry analysis, dimer **1-7** appeared to decompose into isocoumarin with a mass/charge of 146 m/z. A potential mechanism for this breakdown is shown in **Figure 1.5**.[48]

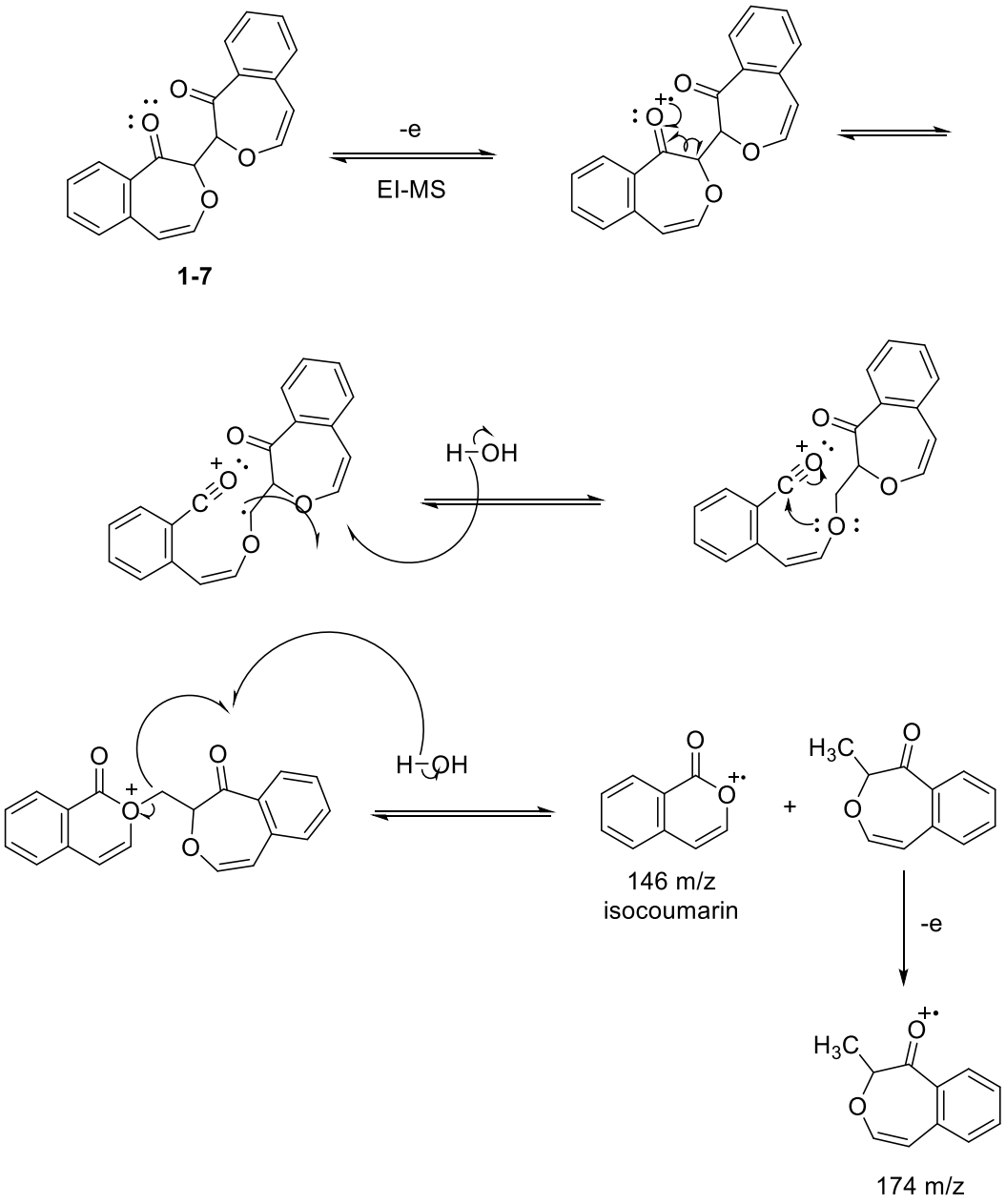

Figure 1.5. *Potential mechanism of breakdown of dimer **1-7** into isocoumarin with 146 m/z and 174 m/z peaks via Electron Impact Mass Spectrometry*.

An attempt to validate the structure of dimer **1-7** ("fraction 1") was undertaken. This was attempted by synthesis of bromo-dibenzo monomer **1-14** and attempted nickel homocoupling for two alkyl bromide sp^3 carbon centers. **1-13** had been made previously in the

literature so we brominated it selectively with NBS and ammonium acetate to afford **1-14**. **1-13** can be made in two steps starting with building block 2-phenylphenol (**1-11**). **1-11** can be alkylated with 2-bromoacetic acid ethyl ester and base/acid work ups to yield the carboxylic acid derivative **1-12**. Acid **1-12** can be cyclized using strong acid trifluoroacetic acid with trifluoroacetic anhydride into **1-13**. Enough **1-14** was synthesized by former group member Dr. Holly Guevara to allow testing. An unexpected and puzzling observation was the formation benzoisocoumarin (**1-16**) rather than dimeric **1-15** (see **Scheme 1.3**). Where did the two CH groups go? Were they simply eliminated as acetylene? This suggested investigating analysis of the headspace in the reaction vessel. With assistance of the equipment in the Gonghu Li lab at UNH, the coupling reaction was tested out in a test tube under argon and the headspace gas identified via syringe removal and GC analysis. Surprisingly, the headspace appeared to indicate methane as the gaseous byproduct even as ^{1}H NMR showed the same rearrangement product that Dr. Guevara had found to be benzoisocoumarin (**1-16**) with no isolation of dimer **1-15** at all. We were hoping to isolate the dibenzodimer to validate our dimer findings but it was very interesting and promising to see a similar rearrangement akin to what was shown on the mass spec with "fraction 1" and its potential breakdown to a 146m/z isocoumarin (**Figure 1.5**). At this time, the mechanism for the formation of benzoisocoumarin (**1-16**) through the seeming thermal decomposition of expected product **1-15** (**Scheme 1.3**) and the observation of isocoumarin (146 m/z) in the EI mass spectrum of the homologue dimer **1-7** (see **Figure 1.5**). **Figure 1.6a** shows the proposed mechanism for the formation of dimeric product "fraction 1" **1-7** and major product "fraction 2" dimer **1-10** has its mechanism shown in **Figure 1.6b**.

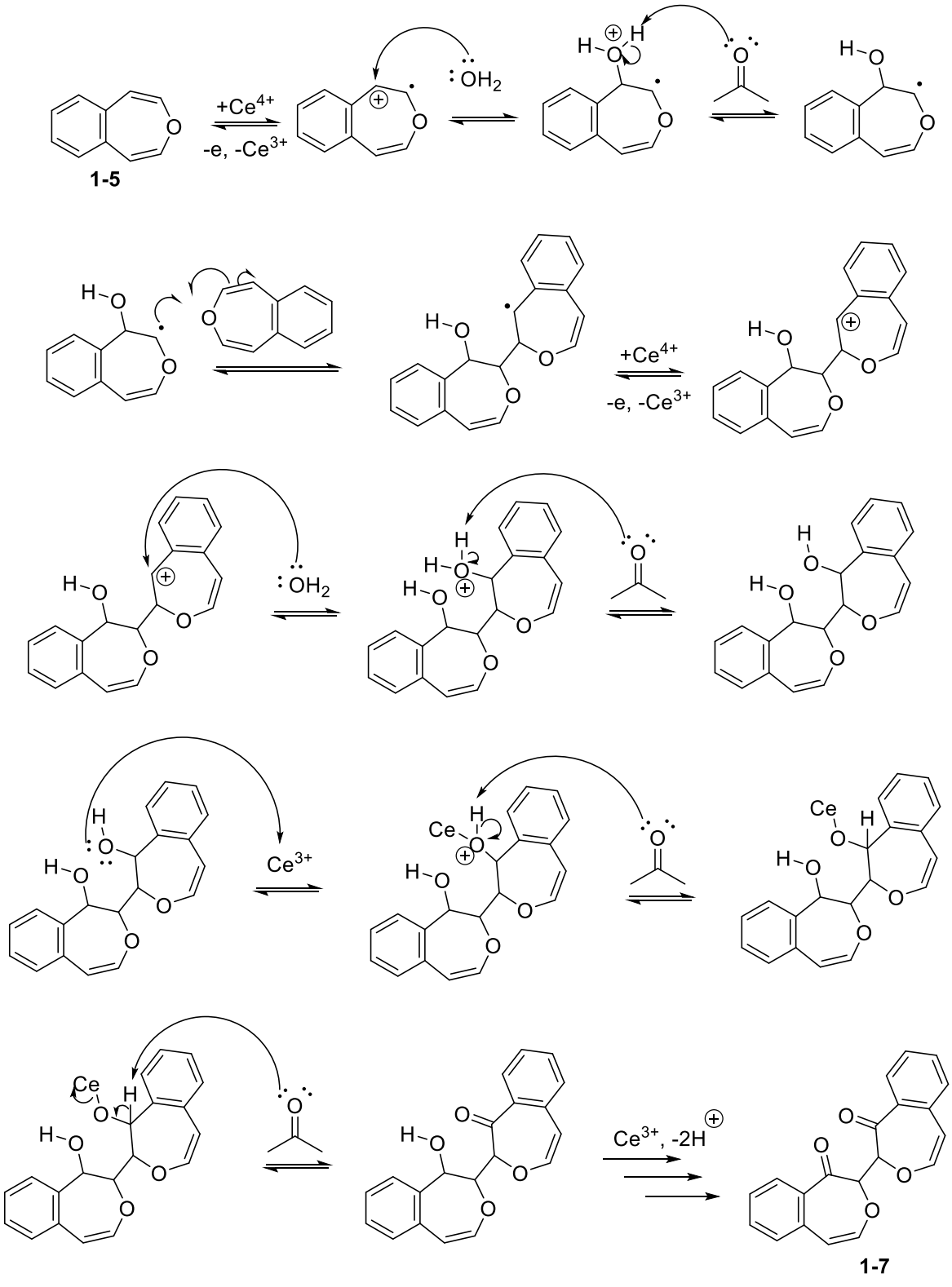

Figure 1.6a. *Proposed mechanism for the formation of "fraction 1" dimer* ***1-7***.[48]

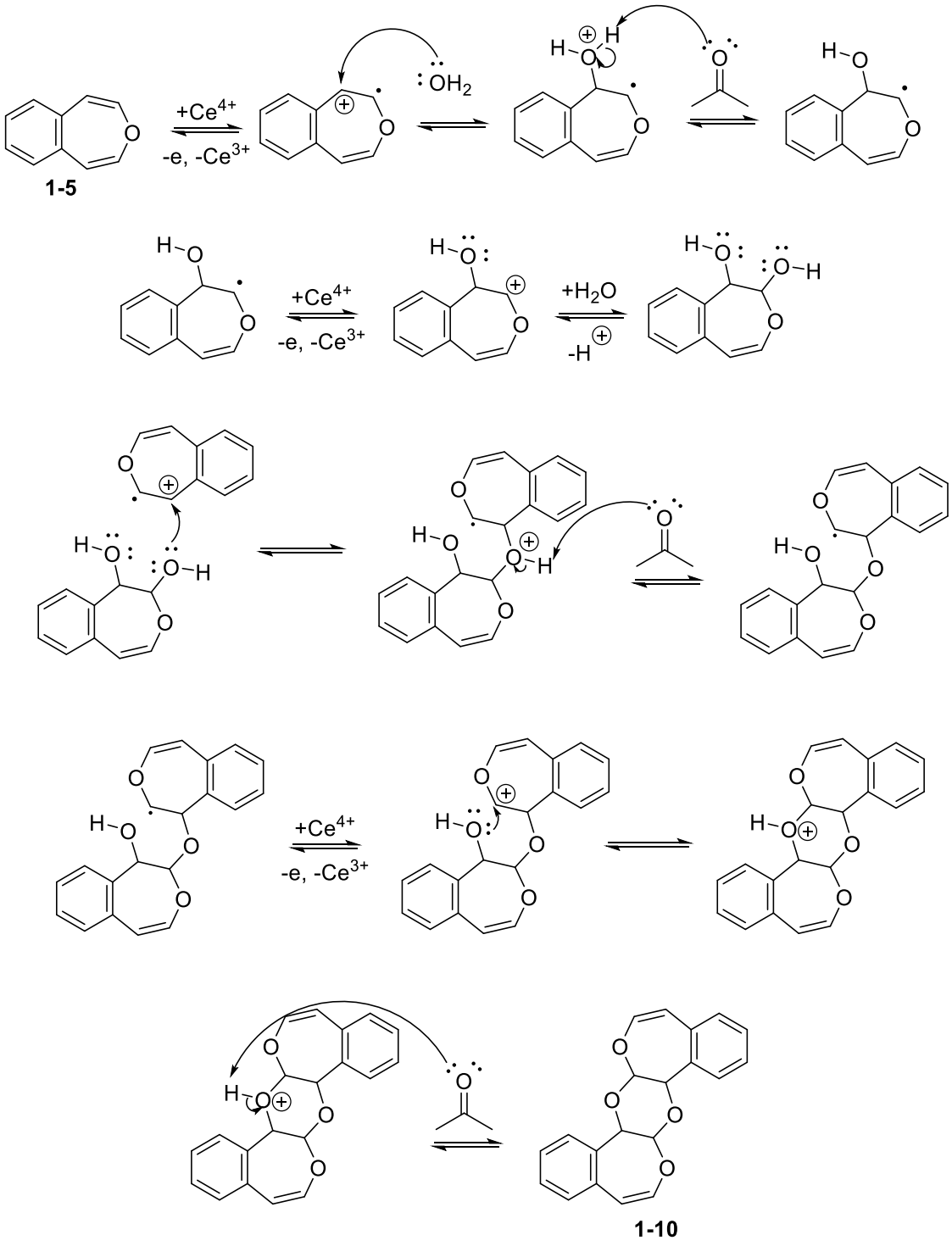

Figure 1.6b. *Proposed mechanism for the formation of "fraction 2" dimer* ***1-10***.[48]

Enzymatic oxidation was tested on 4,5-benzoxepin (**1-5**) using cytochrome P450 isoforms 2E1 (smaller active site isoform known to metabolize benzene), 1A2 (known to metabolize naphthalene which is of similar size to **1-5**), 3A4 (larger active site able to metabolize a myriad of substrates), and pHLM (pooled human liver microsomes).[45] In nearly a 3:1 ratio 1*H*-2-benzopyran-1-carboxaldehyde (**1-6**):"fraction 1" (**1-7**) shows that cytochrome P450 appears to follow both epoxidation and consecutive single electron oxidation mechanisms. A typical enzyme protocol is shown in **Figure 1.7** and all reactions were diluted to correct concentration and 1mL reaction volume with MilliQ water.

Enzyme	Substrate	[Substrate]	[Enzyme]	[NADPH]	[$MgCl_2$]
2E1	4,5-benzoxepin	300 µM	50 pmol/mL	1.0 mM	3.3 mM
1A2	4,5-benzoxepin	300 µM	35 pmol/mL	1.0 mM	4.4 mM*
3A4	4,5-benzoxepin	300 µM	35 pmol/mL	1.0 mM	3.3 mM
pHLM	4,5-benzoxepin	300 µM	0.5 mg/mL	1.0 mM	3.3 mM

Figure 1.7. *Typical enzyme reaction protocol. *Optimized amount-complete substrate consumption.*[48]

A series of organic syntheses and enzymatic reactions were run and improved. Every step of the 4,5-benzoxepin synthesis now has a satisfactory yield. The free radical bromination improved to a 64% yield from 9.81% in past reactions, which significantly improved the multistep synthesis productivity. Epoxide starting material from that reaction was recovered from column chromatography and was reused. An aprotic solvent was used with carbon tetrachloride instead of dichloromethane and also AIBN was used instead of benzoyl peroxide with light as an initiator instead of heat and now yields are regularly 60% or better. To improve the dehydrohalogenation of brominated epoxide to 4,5-benzoxepin, a few simple changes were made. Diethyl ether was replaced with dry THF because potassium t-butoxide is more soluble in it and 4 equivalents of potassium t-butoxide were also used. Along with these two minor changes the apparatus was changed as well. Originally, a solid addition of potassium t-butoxide

was done to brominated epoxide stirring in the flask. In the second attempt, the potassium t-butoxide was placed in the flask to stir to improve solubility and the brominated epoxide (dissolved in THF) was added drop wise through a dropper funnel and all of these improvements helped ensure that all reactants were in the same phase to react.

Studies were completed on the metabolism of 4,5-benzoxepin, benzene, and naphthalene. A reaction was performed on benzene as a control reaction to test enzyme purity and effectiveness. This reaction did not work, but it provided invaluable experience in enzymatic reactions. Two different reactions with 4,5-benzoxepin with enzymes or CAN yielded promising results but required further analysis and purification at the time. The enzymatic reactions may require further concentration adjustments, but a lower limit of substrate concentration has been established due to low concentration reactions with enzymes 1A2 and pHLM. The enzyme reactions worked more optimally due to the addition of excess Mg^{2+} (4 equivalents consumed all starting materials) to the system for naphthalene and 4,5-benzoxepin metabolism with enzyme isoform 1A2 or 3A4. Product **1-6** and the "fraction 1" product (**1-7**) have been shown in small concentrations in the GCMS chromatograms (see **Figure 1.8**) when compared to their standard samples.

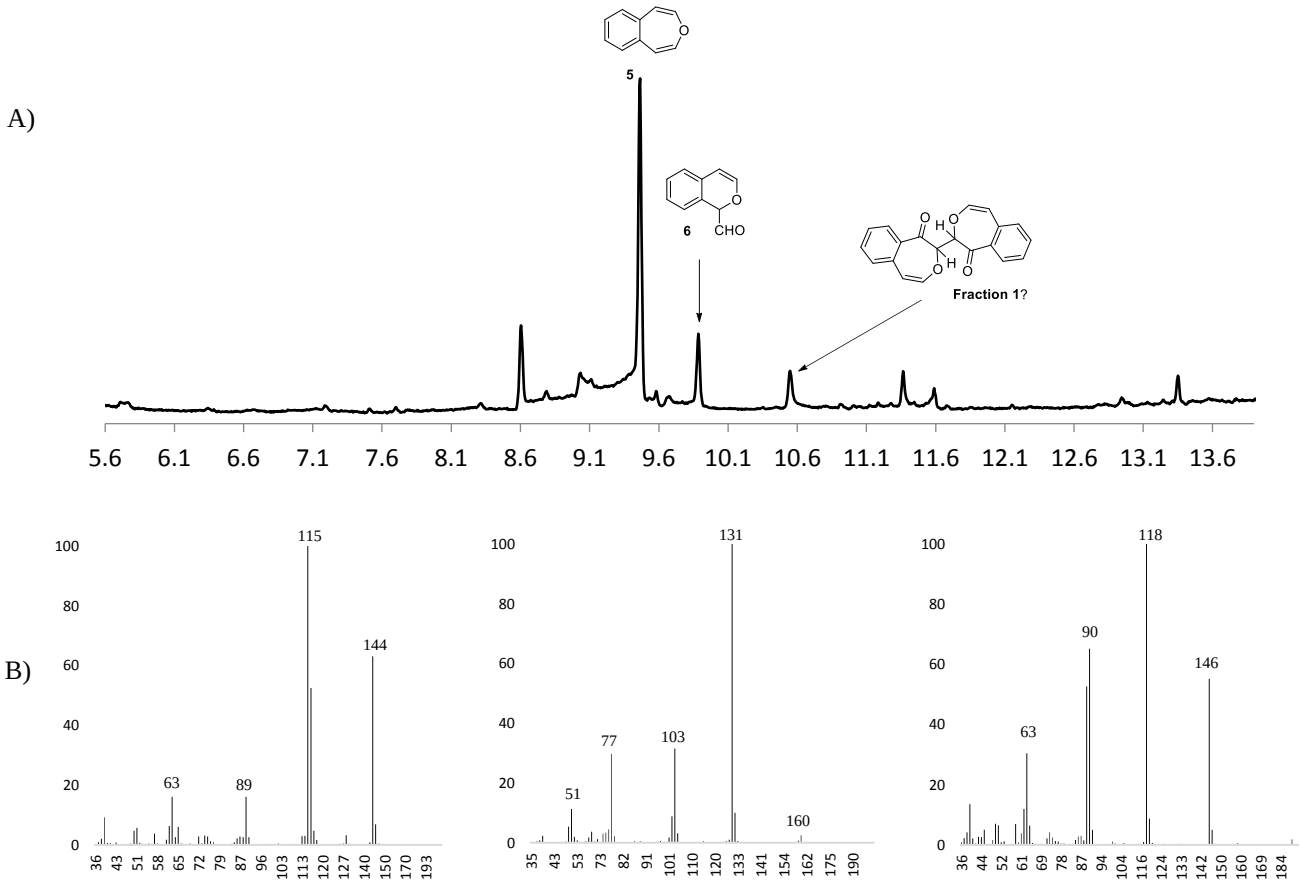

Figure 1.8. *A) Total Ion Chromatogram (TIC) for reaction of 4,5-benzoxepin **1-5** with P450 1A2; B) Mass spectra of compounds **1-5**, **1-6**, and "fraction 1" **1-7** products, respectively*

General conclusions

An attempt to elucidate the mechanism of benzene to ring opened metabolite Z,Z-muconaldehyde/Z,Z-muconic acid via cytochrome P450 was undertaken. This research aimed to determine if oxepin metabolized via a 2,3-epoxyoxepin or radical cation/two electron oxidation mechanism. Model oxepin substrate 4,5-benzoxepin was the focus of this research and it afforded evidence of 2,3-epoxyoxepin via low temperature NMR using DMDO by prior group members (Nauduri) as well as promising dimeric products that underwent rearrangement when exposed to cerium (IV) ammonium nitrate as the electron oxidizing agent. P450 studies were introduced with this project-researchers (Golding et. al and Davies et. al.) in the past have postulated these mechanisms but were missing the actual enzyme data for comparison. Various P450 isoforms yielded a mixture of the product of the DMDO epoxidation and CAN consecutive single electron oxidation providing some evidence that both mechanisms are in play. Optimizations of the enzyme protocol were also performed and when four equivalents of $MgCl_2$ were used relative to the NADPH and glucose-6-phosphate, all of the substrate was able to be consumed by the P450 enzyme isoform.

Chapter 2

Synthesis of 2,3-benzoxepin for comparative enzymatic and oxidation studies using Cytochrome P450, *m*CPBA, and Cerium Ammonium Nitrate

Introduction

The 4,5-benzoxepin project provided the inspiration for oxidation studies on other oxepins. Dr. Holly Guevara of the Greenberg group did both enzyme, epoxidation, and two electron oxidation reactions on 2,7-dimethyloxepin which localizes the carbocation on the tertiary carbon adjacent to the oxygen as Golding and coworkers proposed would occur upon reaction with CAN making it an excellent model oxepin.[2,29,48] This project spawned from the 4,5-benzoxepin and 2,7-dimethyloxepin substrates as another way to find out if competitive enzymatic epoxidation would occur in an oxepin at the 2,3-olefinic or 4,5-olefinic positions as shown in **Figure 2.1**.[48-51] This project also set out to set if similar dimeric products will form when exposed to CAN and enzymes as with the 4,5-benzoxepin project. As shown in **Figure 2.1**, 4,5-benzoxepin (**1-5**) only contains a 2,3 functionalizable olefin without breaking aromaticity of the benzene ring whereas 2,3-benzoxepin (aka. 1-benzoxepin, **2-7**) contains both a free 4,5-olefinic group and a 2,3-olefinic group akin to that of an oxepin intermediate metabolite.[48] Enzymatic testing on 2,3-benzoxepin would serve as a means to further complete out knowledge on the epoxidation and consecutive two electron oxidation of oxepin intermediates.

The synthesis of 2,3-benzoxepin (**2-7**) is outlined in **Scheme 2.1** (multistep) and **Scheme 2.2** (one-pot synthesis). Further reactions of 2,3-benzoxepin with consecutive two electron oxidizing agent CAN, epoxidizing agent *m*CPBA, and enzyme cytochrome P450 isoform 1A2 are shown in **Scheme 2.3**.

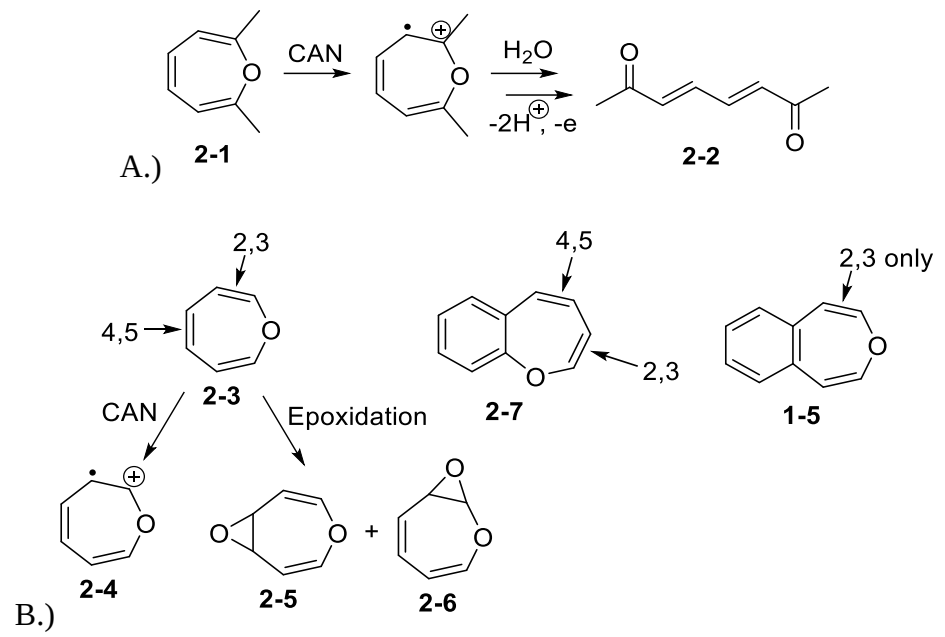

Figure 2.1. *A.) Past group member's model oxepin 2,7-dimethyloxepin. B.) Versatility of 2,3-benzoxepin as a model oxepin substrate*

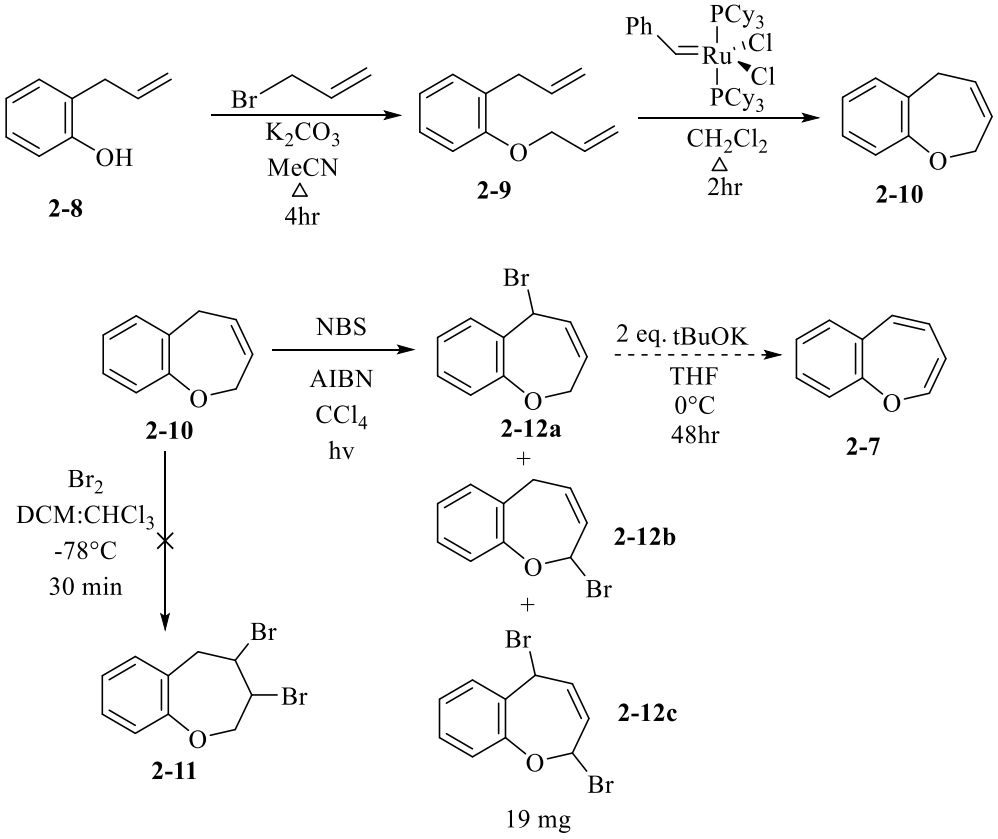

Scheme 2.1: *Attempted multistep synthesis of 2,3-benzoxepin*

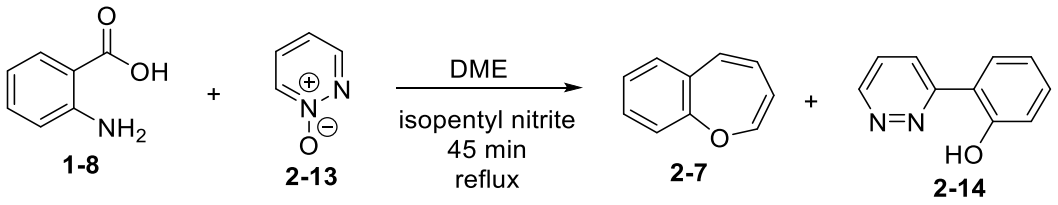

Scheme 2.2: *Single step synthesis of 2,3-benzoxepin via in situ benzyne generation*

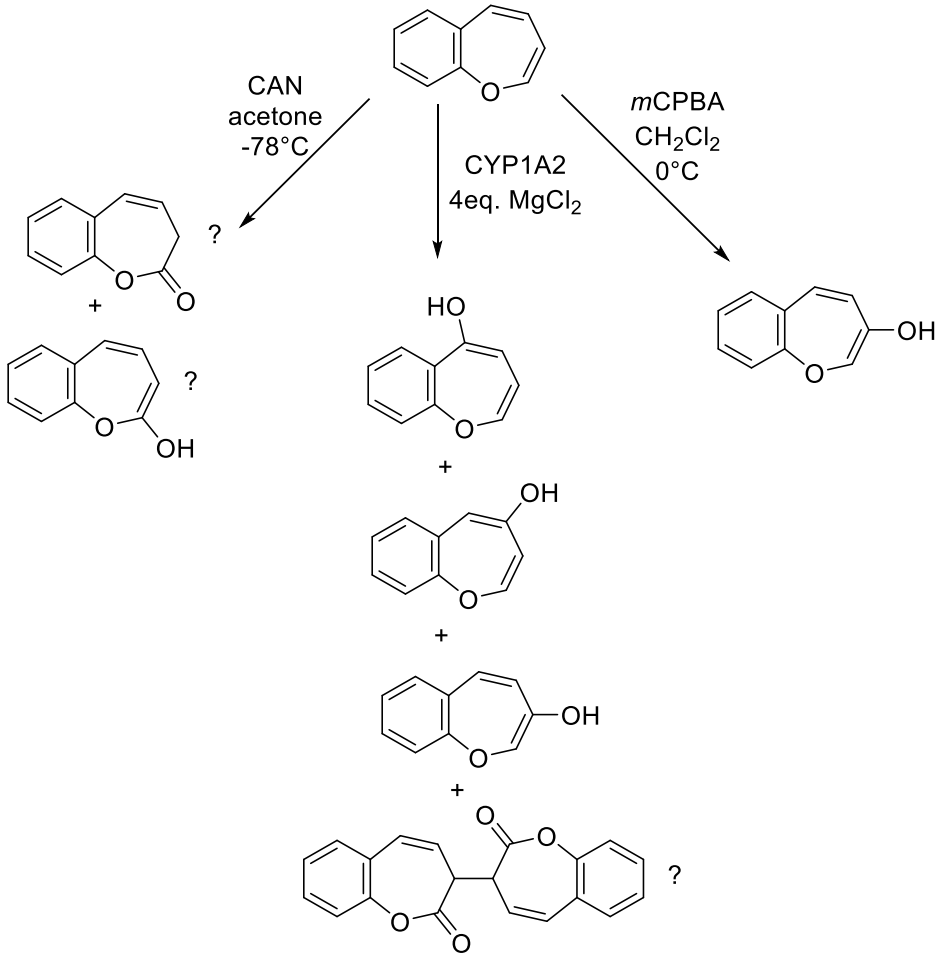

Scheme 2.3: *Comparison of model oxepin substrate 2,3-benzoxepin reaction with cytochrome P450 isoform 1A2 vs. reactions with CAN and mCPBA*

Results and discussion

An attempt to synthesize model intermediate metabolite 2,3-benzoxepin (**2-7**) was underwent. The multistep synthesis shown in **Scheme 2.1** ended with a mixture of mono- and dibrominated dihydrobenzoxepins. The original synthesis involved an o-allylation of 2-allylphenol (**2-8**) followed by ring-closing metathesis of 1-allyloxy-2-allylbenzene (**2-9**) to afford 2,5-dihydro-1-benzoxepin (**2-10**) as the oxepin framework.[48-50] Relocation of the double bond was required to generate 2,3-benzoxepin (**2-7**) and was attempted to be done via NBS monohalogenation and subsequent dehydrohalogenation. Preliminary mass spec data done by the Anyin Li group at UNH showed the presence of both monobrominated products **2-12a** and **2-12b** as well as a dibrominated product (**2-12c**). It was decided that this mixture of products would make dehydrohalogenation difficult, so it was not attempted.

A new approach for the synthesis of 2,3-benzoxepin was attempted inspired by the 4,5-benzoxepin synthesis involving a benzyne Diels-Alder reaction. Anthranilic acid (**1-8**) can be used to generate benzyne *in situ* when combined with isopentyl nitrite because it transforms the Ar-NH_2 substituent into a diazonium Ar-N_2^+ leaving group. Subsequent deprotonation of the Ar-CO_2H group sets off elimination of CO_2 and N_2 as gases leaving a triple bond in their place which is shown in **Figure 2.2**. This newly generated benzyne can be combined with pyridazine N-oxide to form 2,3-benzoxepin in a one-pot reaction.

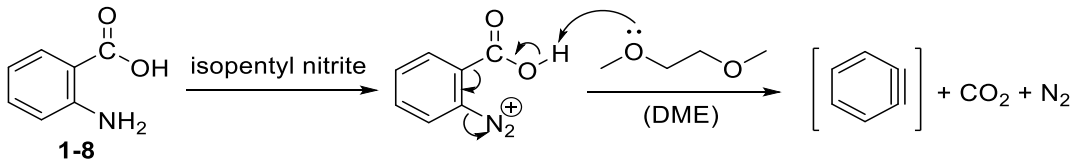

Figure 2.2. *In situ generation of benzyne from anthranilic acid*

A reaction with cerium (IV) ammonium nitrate and *m*CPBA were tested on 2,3-benzoxepin. The *m*CPBA reaction appears to yield mono-hydroxylated products as shown by the two doublet and two singlet patterns in the NMR shown in **Figure 2.3**. Integrations of the singlets come out to 1H and 1H leading to the enol assignment for the structure vs the keto tautomer. The CAN reaction tells a similar story appearing to yield a monohydroxylated enol in equilibrium with its keto tautomer as seen in **Figure 2.3**.

2,3-benzoxepin was also tested with cytochrome P450 isoform 1A2 (CYP1A2) and the products were analyzed via electron impact mass spectrometry. The reaction appeared to yield 3 monohydroxylated species as shown by the three 162-163 m/z peaks shown in chromatograms in **Figure 2.4**. There were also 3 similar retention time GC peaks further supporting this conclusion. Also, as a very minor product with retention time of 20.29 minutes was a potential dimeric product with a 318 m/z ratio that was elusive in the 4,5-benzoxepin project for "fraction 1" dimeric product **1-7**.

A.)

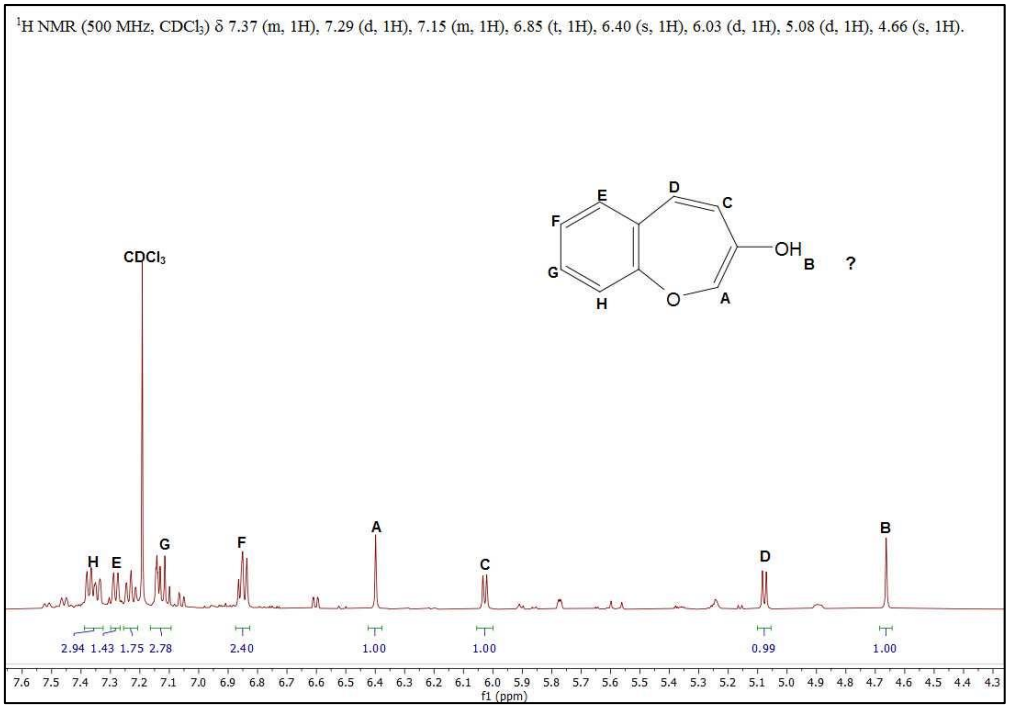

B.)

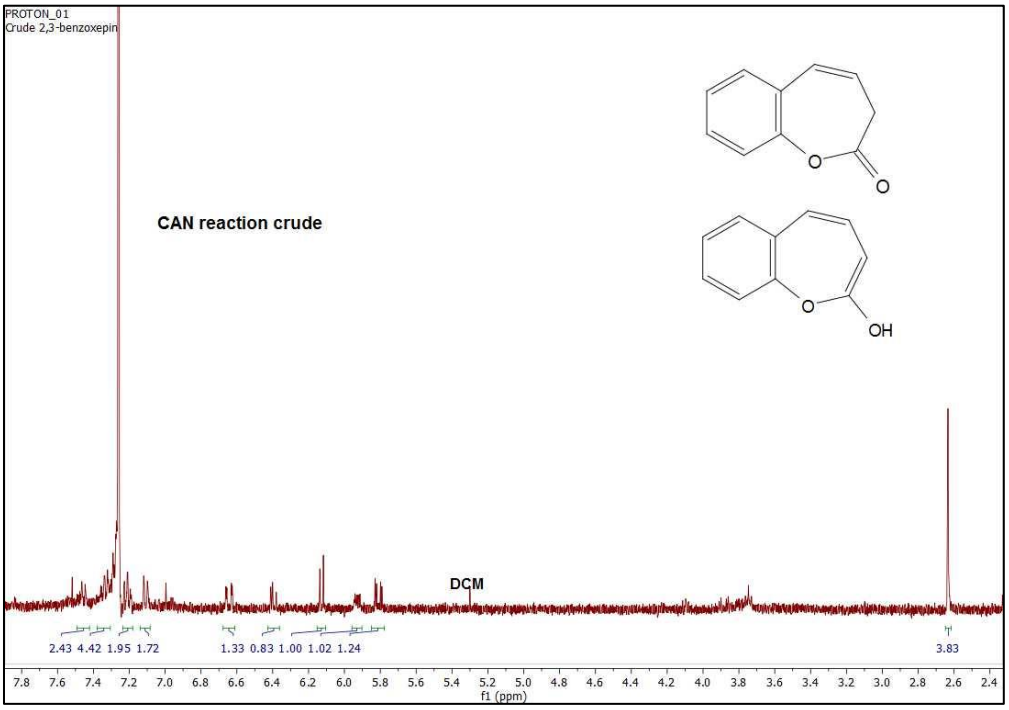

Figure 2.3. *^{1}H NMR of the A.) mCPBA reaction with 2,3-benzoxepin and B.) the CAN reaction with 2,3-benzoxepin*

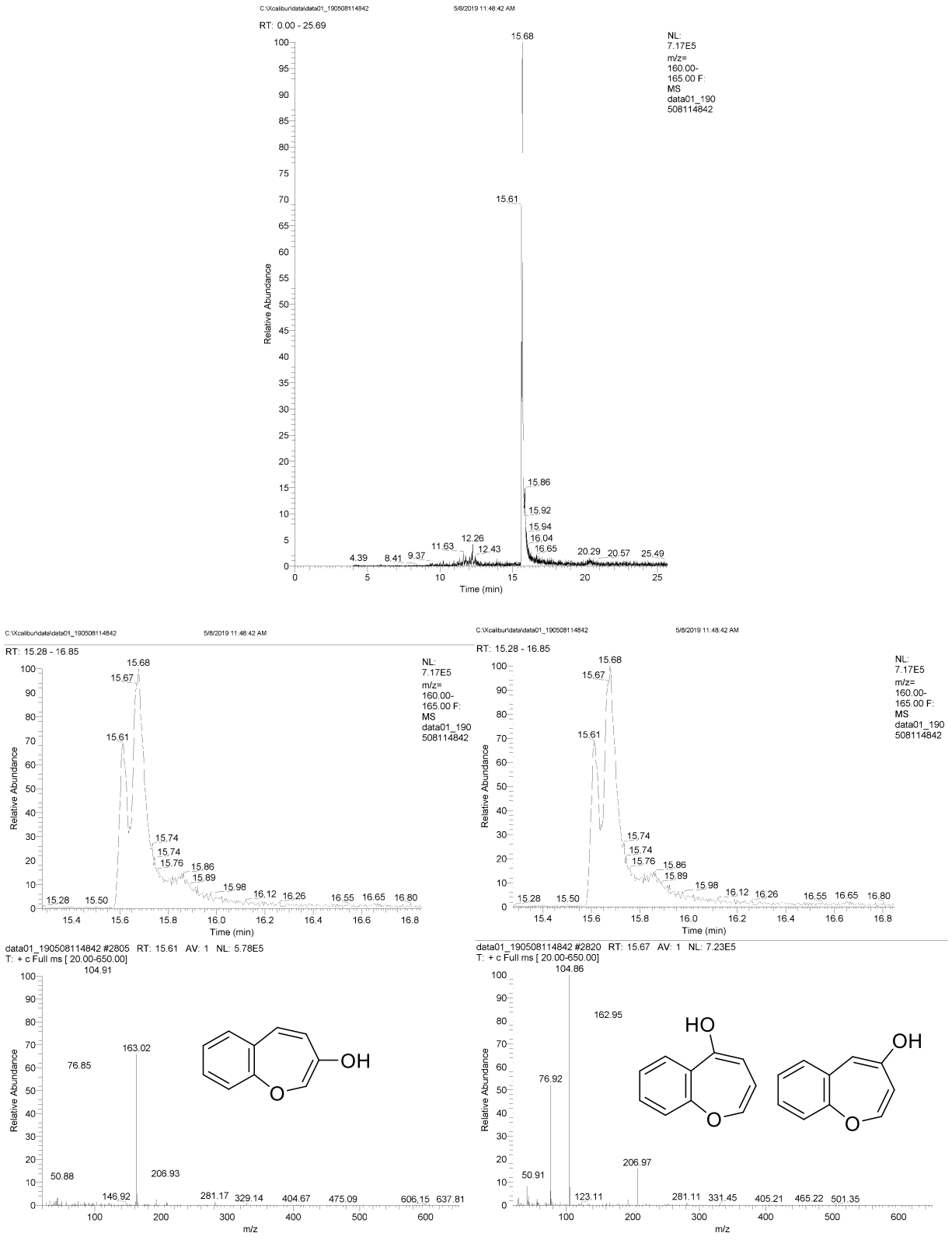

Figure 2.4. *Electron impact mass spectra of CYP1A2 reaction with 2,3-benzoxepin*

General conclusions

An attempt to add another model oxepin substrate to our mechanistic studies of cytochrome P450 was undertaken. Our one-pot synthesis of the model substrate 2,3-benzoxepin proved to be very effective but also expensive because the high cost of pyridazine N-oxide limited the quantity of 2,3-benzoxepin synthesized. The multistep synthesis had excellent yields up to the bromination step by either Br_2 or NBS which caused the major shift in synthetic strategy. The 2,3-benzoxepin project was completed but purification was challenging due to the small scale of the *m*CPBA and CAN reactions. Each reaction had changes in the proton NMR but both did not yield enough material for adequate carbon NMR making identification difficult. The enzyme reactions were more successful with excellent signal to noise on the GC trace and 3 clear peaks with chromatograms of 162 M/Z indicative of monohydroxylations in three different locations.

Chapter 3

Attempted synthesis of 4-silatranone lactam derivatives via strained silacyclobutanes

Introduction

Strained lactams and amides have been an area of interest for Greenberg and coworkers for years. Dr. Jessica Morgan synthesized several strained lactams as well as carrying out the computational aspects of silatranes with amide linkages (**Figure 3.1**).[52,53,59] Former undergraduate Azaline Dunlap-Smith did an honors thesis on the computational aspects of both silatranes and silatranones derivatized at the 1-position (off the silicon) that helped pave the way for this synthesis project.[52,58]

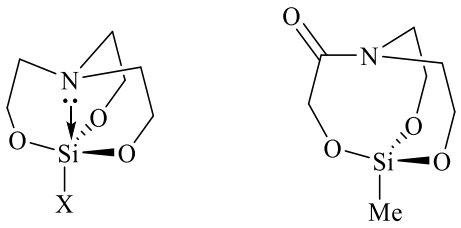

Figure 3.1. *Left: Silatrane derivatives computationally analyzed by Azaline Dunlop-Smith and synthesized in this work; Right: 1-methyl-4-silatranone, a target molecule of this work*

Silatranes come from a family of molecules called atranes which contain three 5-membered rings in a bridged tricyclic fashion.[52,56-58,60-62] A silatrane itself is a bridged tricyclic amine whereas a 4-silatranone is the presently unknown lactam derivative of a silatrane.[52,56-58] Silatranes were first discovered by Frye and coworkers as white solid mixed within polymeric material.[52,56] 3-Silatranones have been made in the past to make the ester/lactone.[58,60-61] A 4-silatranone provides a lot of molecular complexity and challenge to synthesize because it may change the geometry of the nitrogen to planar and can delocalize the lone pair which normally

stabilizes a silatrane and locks it together with a tetrahedral nitrogen and bipyramidal silicon via a dative/coordinate covalent bond.[52,58]

This work set out to improve the access of silatrane derivatives via rotary evaporator (rotovap) synthesis and hopefully uncover the first synthesis of a 4-silatranone (**Scheme 3.1**) either by conventional reflux methods or the rotovap approach used for silatranes.

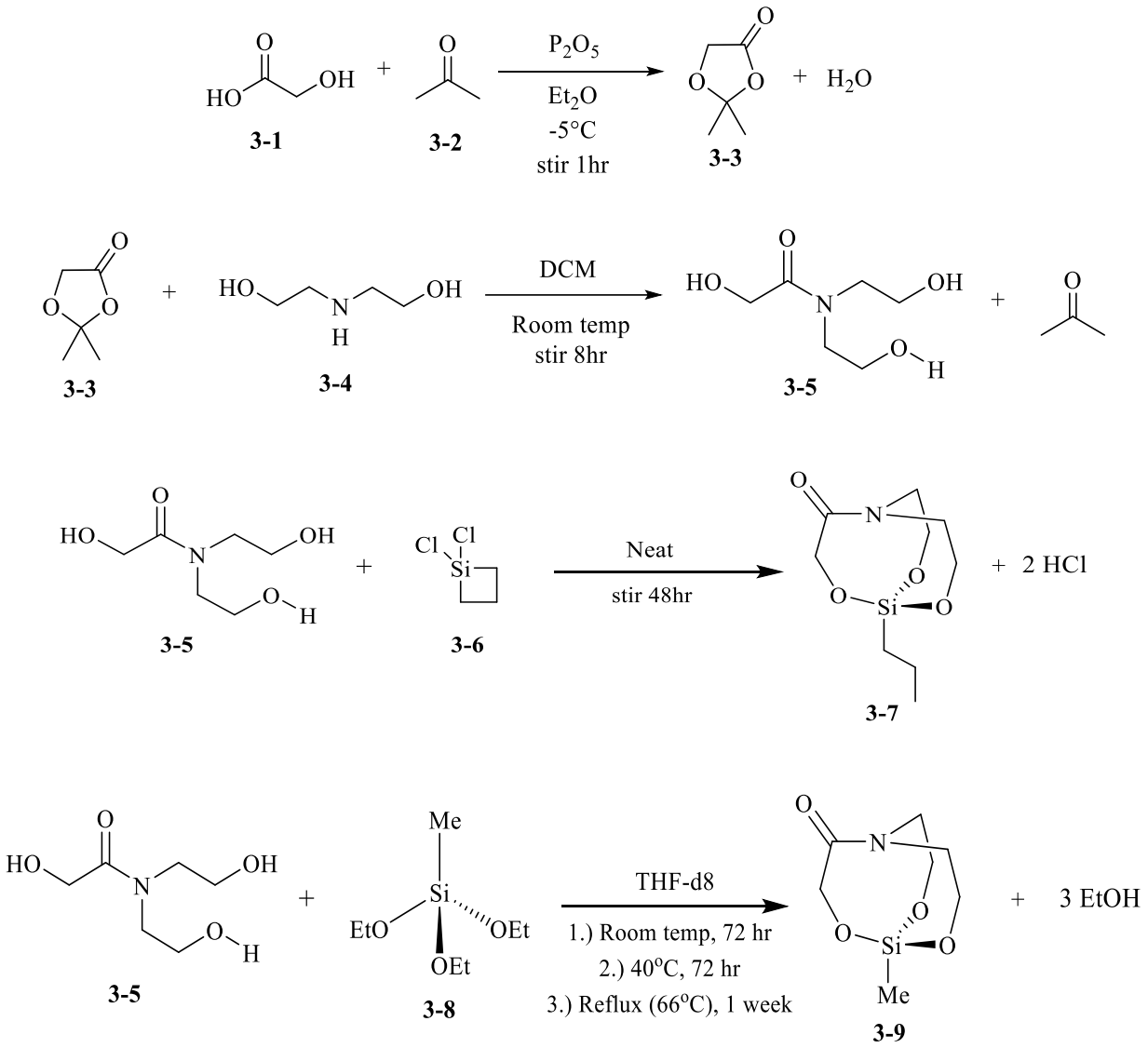

Scheme 3.1: *Attempted syntheses of novel silatranone lactam derivatives **3-7** and **3-9***

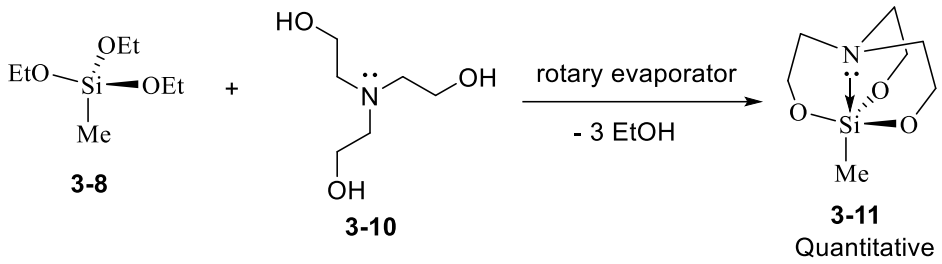

Scheme 3.2: *Quantitative synthesis of 1-methylsilatrane*

Results and discussion

Two multistep syntheses were explored in an attempt to synthesize the novel silatranone lactams 1-methyl-4-silatranone (**3-9**) and 1-propyl-4-silatranone (**3-7**). GC/MS analysis suggests promising but inconclusive data for the synthesis of the methyl derivative alongside oligomeric polysiloxane byproducts. The propyl derivative was less successful but the 1,1-dichlorosilacyclobutane (**3-6**) provides energy to aid in overcoming the uphill, endergonic barrier (21 kcal/mol calculated via B3LYP/6-31G*) to forming the desired 4-silatranone in the form of releasing ring strain (26 kcal/mol).[33]

Both 1-methyl-4-silatranone and 1-propyl-4-silatranone required the synthesis of the tertiary amide, N-glycolyldiethanolamine (**3-5**), as a building block to serve as the top of the lactam structure. This amide can be obtained via a two-step synthesis. The first step entails the acetal protection of acetone using glycolic acid as the source of a diol to afford 2,2-dimethyl-1,3-dioxolan-4-one (**3-3**, aka. glycolic acid acetonide). Successful synthesis of 2,2-dimethyl-1,3-dioxolan-4-one (**3-3**) could only be achieved with the addition of P_2O_5 as a drying agent because the reaction is completely reversible, and any trace water would give clear, white solid glycolic

acid precipitate in the flask. This lactone serves as a glycolic acid donor when reacted diethanolamine (**3-5**) in the next step with acetone as the byproduct. This is an advantageous byproduct because reduced pressure in the form of the rotary evaporator can help drive the reaction to completion by removal of acetone. Silica column using two polar eluents (4:1 Methanol:ethyl acetate) gave good yields of the desired amide.

N-glycolyldiethanolamine (**3-5**) can then be reacted with triethoxymethylsilane (**3-8**) via three nucleophilic substitutions of the three primary alcohols of the amide and three successive deprotonations by the ethoxide leaving groups to generate the desired lactam and three equivalents of ethanol. This proved to be a very challenging reaction. Excessive heating or moisture promoted the formation of polysiloxane polymers forming networks/gels to immediately precipitated out of solution. **Figure 3.2** and **Figure 3.3** show the most promising NMR data for synthetic attempts for 1-methyl-4-silatranone. **Figure 3.4** shows the GC/MS total ion chromatogram and mass spectrum showing a mass/charge ratio of 202 m/z short of the 203 g/mol of 1-methyl-4-silatranone (**3-9**), which is potentially due to an instrument calibration issue. While this is promising, the results should be interpreted with caution. There is potential that 1-methyl-4-silatranone was synthesized and it lost a proton in the electron impact mass spec process. Similar systems containing a methylene alpha to both an ether and amide carbonyl have been calculated to have a pKa of -0.77, which is very easily deprotonated. At this time, we believe that it is unlikely that the methyl derivative was made successfully but these results were promising.

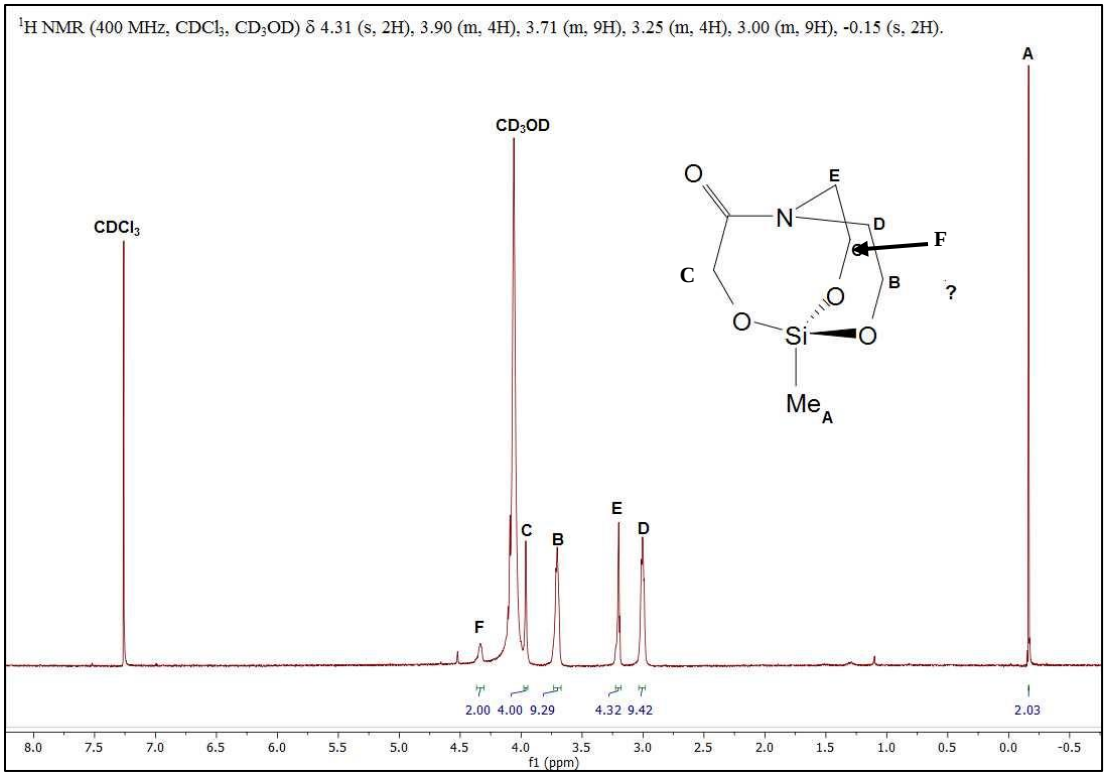

Figure 3.2. *[1]H NMR of potential 1-methyl-4-silatranone in a 1:1 mix of $CDCl_3$ and CD_3OD.*

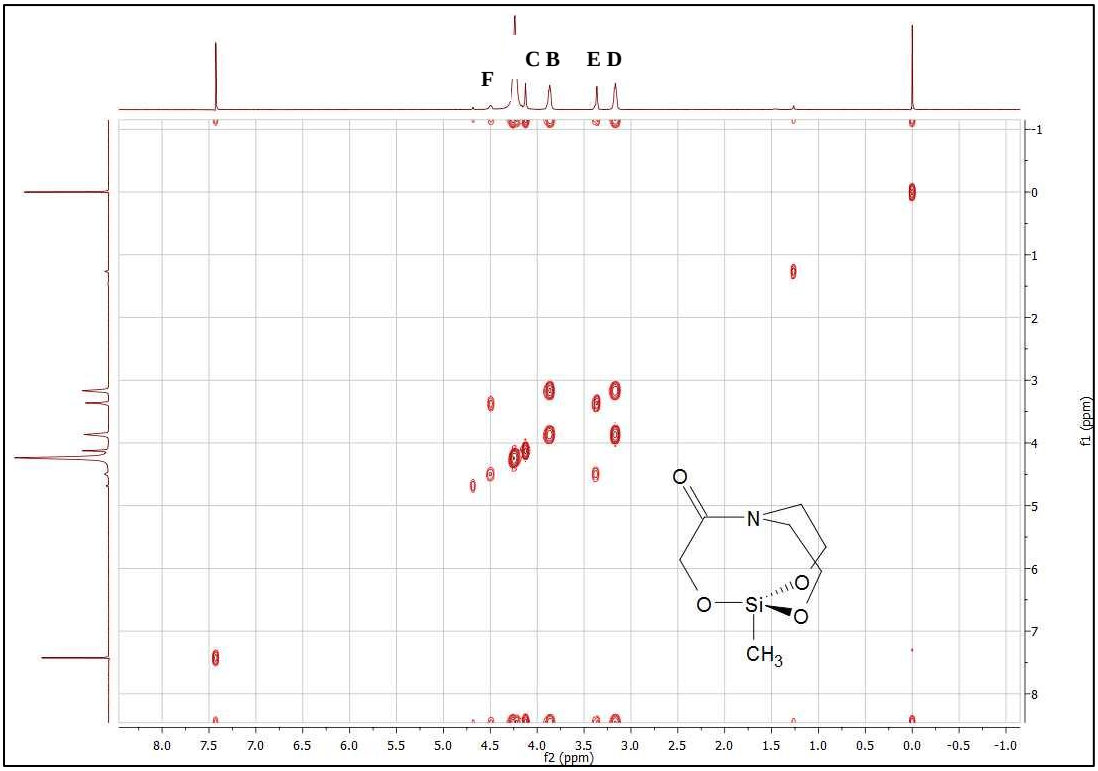

Figure 3.3. *^{1}H-^{1}H COSY NMR of potential 1-methyl-4-silatranone in a 1:1 mix of $CDCl_3$ and CD_3OD.*

1-propyl-4-silatranone (**3-7**) has been more elusive with NMR peaks for the alkyl chain integrating much higher than it should indicative of polysiloxane oligomer formation. This was not unexpected however, the 1,1-dichlorosilacyclobutane starting material was very reactive and could be seen fuming as soon as the cap of the bottle was removed. Preliminary electron impact mass spec showed only high molecular weight oligomer formation, but the reactivity of this reagent shows promise towards generating a strained molecule in the form of a n-propyl-4-silatranone.

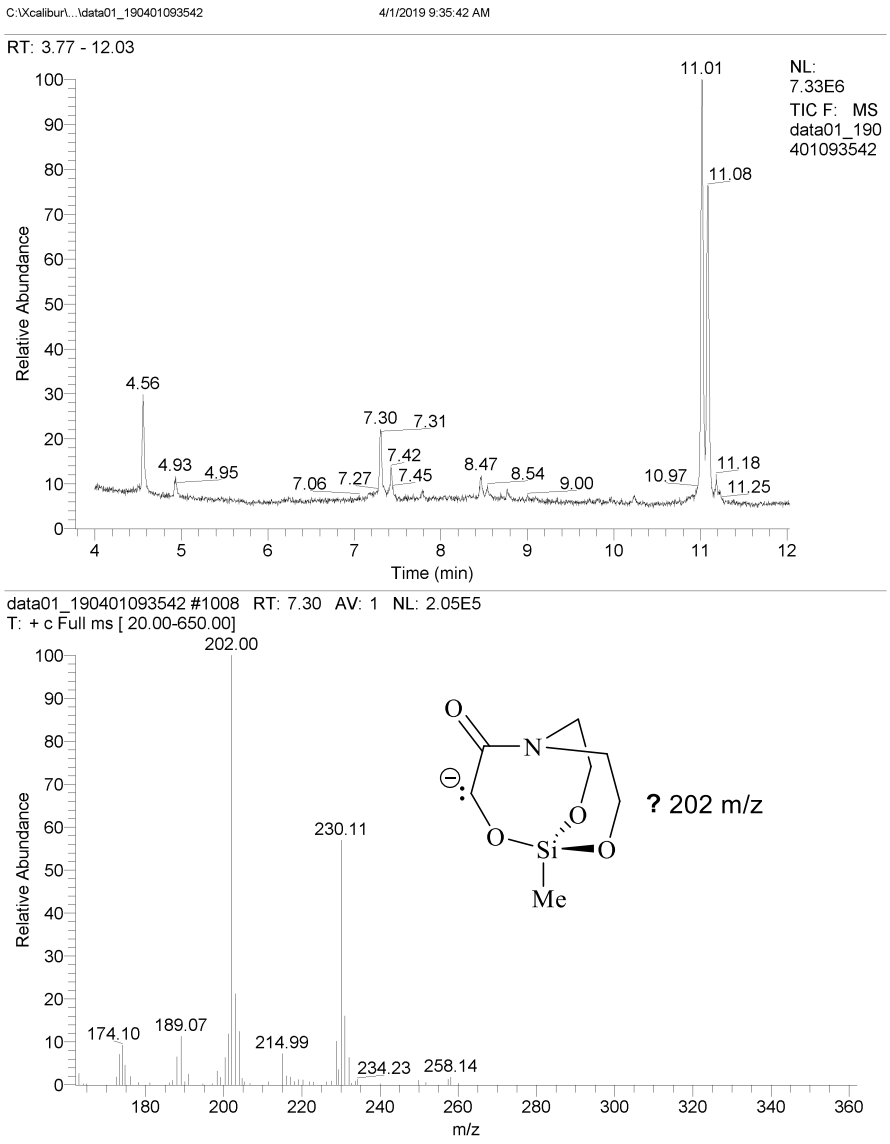

Figure 3.4. *Electron impact mass spectrum of reaction towards 1-methyl-4-silatranone*

General conclusions

Strides have been made towards a successful synthesis of a novel 4-silatranone derivative with a mass to charge of 202 m/z appearing on electron impact mass spec potentially of a deprotonated 1-methyl-4-silatranone. Attempts to synthesize the n-propyl derivative continue to provide polymers and gel networks, but the added reactivity of silacyclobutanes is a very

tempting synthesis avenue. The rotovap synthetic method for generating 1-methylsilatrane is very efficient and viable for synthesizing 4-silatranones as well but there are so many conditions to consider (eg. heating, when to lower pressure, how to prevent polymerization). Stirring a room temperature and gradually heating to reflux over the course of a few days was not effective. There is a possibility that there is a better silane starting material that we have not consider as well. Ultimately this project has left us with far more questions than answers but the low pKa of methylene protons alpha to the lactam carbonyl could a source of confusion about the success of the synthesis of the methyl derivative.

Chapter 4

Synthesis of five related amides to measure the effect of hydrogen bonding on amide rotational barriers

Introduction

The questions that arose from the 4-silatranone project provided a desire for more knowledge on the amide starting materials.[52,55] N-glycolyldiethanolamine (**3-5**) has a uniquely lower carbonyl frequency of 1590 cm^{-1}, which we postulated was due to many sources of intramolecular hydrogen bonding restricting the amide rotation.[55] To see if this was the case, related amides were synthesized and purchased that were lacking terminal OH groups and contained methyl groups in their place into each possible combination (**Figure 4.1**).[55]

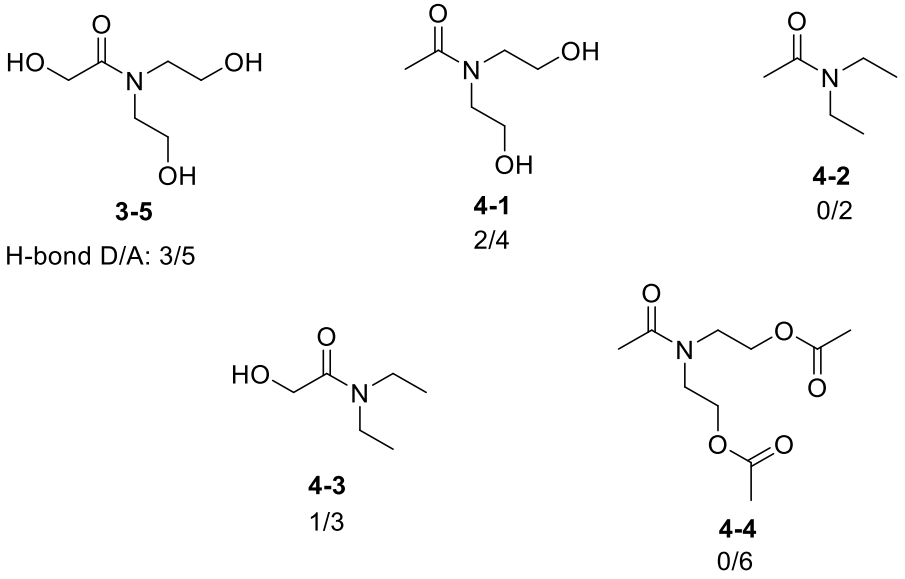

Figure 4.1. *Five related amides synthesized and purchased for testing amide rotational barriers and number of hydrogen bond donors/acceptors.*[55]

Each amide was able to be dissolved in acetonitrile-d3 and tested for their rotational barrier via variable temperature NMR. The coalescence temperature was measured and this temperature was used to back calculate $\Delta G^{\ddagger}$ of the rotational barrier using a derivative of the Eyring equation. This equation (shown in **Figure 4.2**) also factors in the change in frequency/chemical shift that occurs in the heating process. The coalescence temperature is recorded when the two peaks merge and smooth out.

$$(\Delta G^{\ddagger} / RT_c) = (22.96 + \ln(T_c / \Delta\nu))$$

For $\Delta G^{\ddagger}$ in kJ/mol with T_c in Kelvin (K) and $\Delta\nu$ in Hz.

or:

$$\Delta G^{\ddagger} = -RT \ln (k_r h/k_B T_c) = 1.987\ T_c\ (23.06 + \ln (T_c/k_r))$$

For $\Delta G^{\ddagger}$ in kcal/mol with T_c in K.

$$\Delta H^{\ddagger} = -1.9872\ (\text{slope})$$

$$\Delta S^{\ddagger} = 1.9872\ (\text{intercept} - \ln(\kappa k_B/h)\ (\kappa = \text{transmission coefficient} = 1/2)$$

$$\ln (\kappa\ k_B/h) = 23.06\ (\text{where } \kappa = ½)$$

where:
k_r = rate constant
T_c = temperature (K)
h = Planck's constant
k_B = Boltzmann constant
R = gas constant (1.987 cal/degC mol)

Figure 4.2. *Derivatives of the Eyring equation that relates coalescence temperature (T_c) and change in chemical shift (in Hz) with transition state Gibbs free energy ($\Delta G^{\ddagger}$ in kJ/mol above or kcal/mol below).*[55,76,81]

Results and Discussion

Five related amides were either synthesized or purchased and studied by variable temperature NMR analysis. Coalescence temperatures were measured and were used to calculate the $\Delta G^{\ddagger}$ of the amide rotational barrier. N,N-diethylacetamide (**4-2**) was purchased and used as is for this experiment. The other four amides were synthesized in an efficient one-step synthesis for each amide (shown in **Scheme 4.1**).

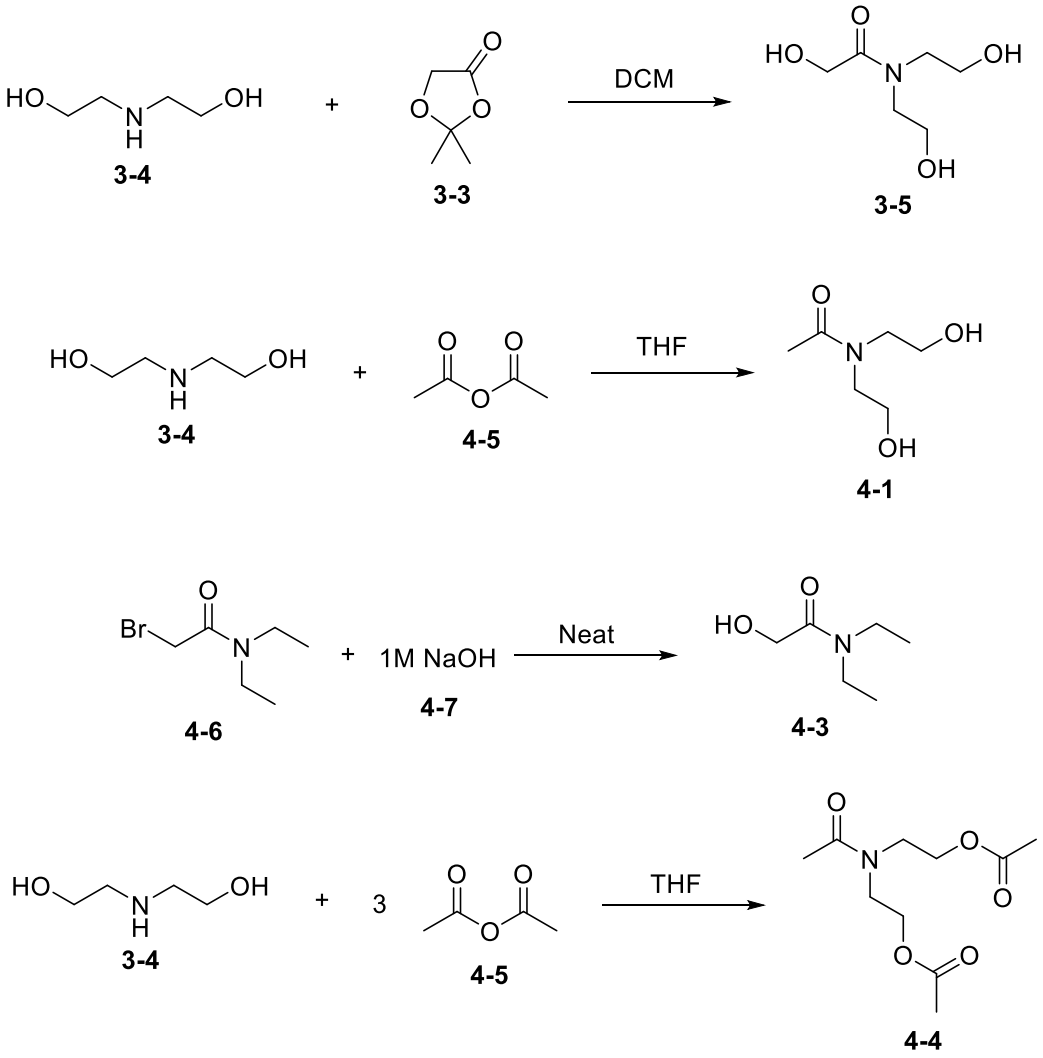

Scheme 4.1: *One-step syntheses of four of the five related amides. N,N-diethylacetamide (**4-2**) was purchased. Glycolic acid acetonide (**3-3**) was synthesized via the same procedure as in chapter 3.*[55,76-81]

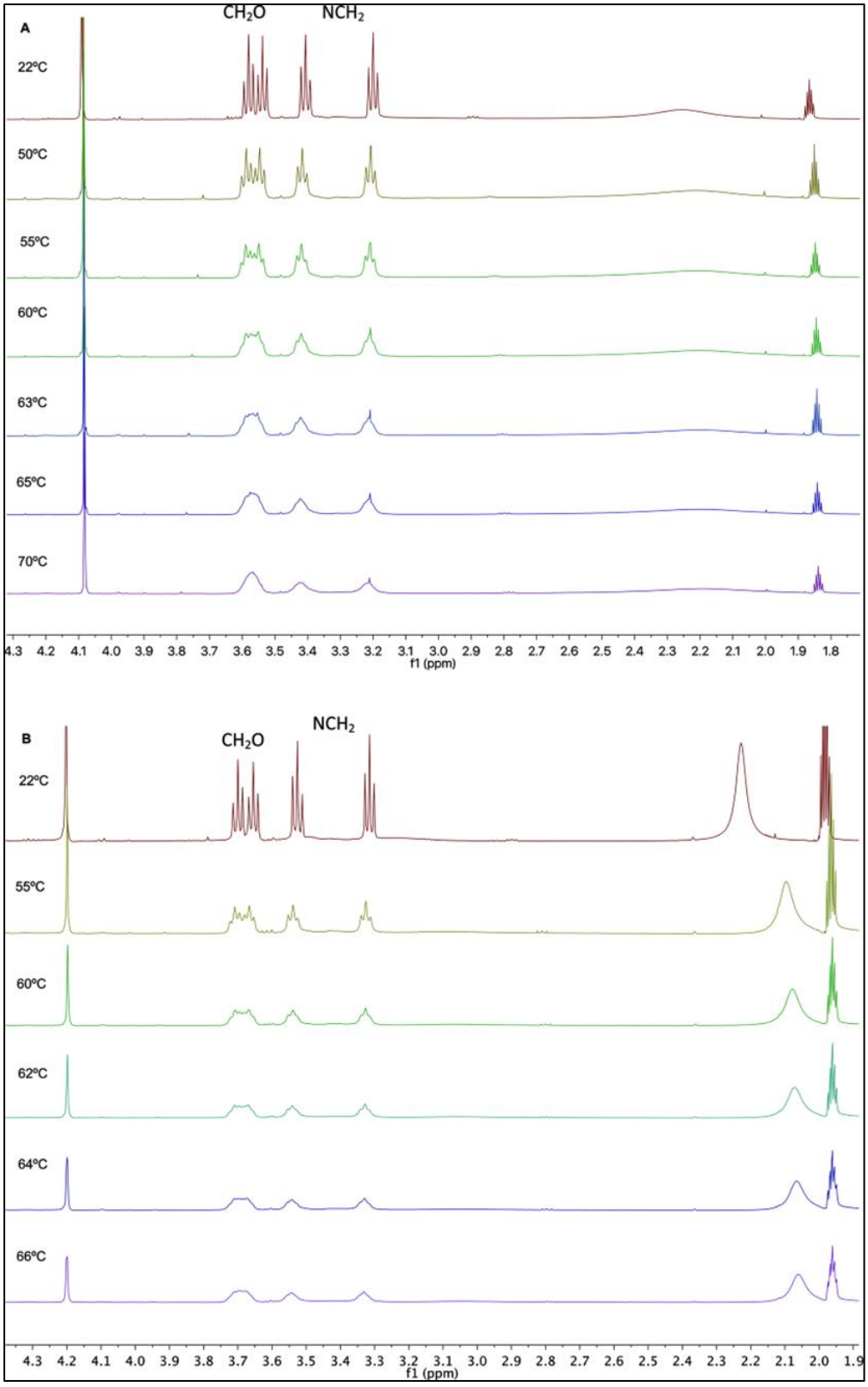

Figure 4.3. *Variable temperature NMR data for A)* ***3-5*** *and B)* ***3-5*** *1/10 dilution.*[55]

Four amides were synthesized in this work. First, N-glycolyldiethanolamine (**3-5**) was synthesized via the same approach as in chapter 3-protection of acetone with glycolic acid to form glycolic acid acetonide (**3-3**) followed by stirring of diethanolamine (**3-4**) with the acetonide to form the desired amide **3-5**. Next, N-acetyldiethanolamine (**4-1**) was synthesized by combining acetic anhydride (**4-5**) with diethanolamine (**3-4**) in a mono-acetylation reaction. N-glycolyldiethylamine (**4-3**) was generated via S_N2 reaction of sodium hydroxide (**4-7**) with 2-bromo-N,N-diethylacetamide (**4-6**). Finally, N,N-bis[2-(acetyloxy)ethyl]acetamide (**4-4**) was created by combining excess acetic anhydride (**4-5**) with diethanolamine (**3-4**) in a tri-acetylation reaction.

Each amide underwent variable temperature NMR (400 MHz) heating to find their coalescence temperature (T_c) and an example of this is shown in **Figure 4.3**.

Amide	Protons	T_c (°C)	k_r (sec^{-1})	$\Delta G^{\ddagger}$ (kcal/mol)	ν_{CO} (cm^{-1}) (neat)	ν_{CO} (cm^{-1}) (CH_3CN)
3-5	NCH_2	63	6.81	18.0	1590	1631
3-5	CH_2O	63	9.01	17.8		
3-5 (1/10 conc)	NCH_2	64	7.70	18.0		
3-5 (1/10 conc)	CH_2O	64	14.2	17.6		
4-1	NCH_2	35	1.21	17.5	1606	1639
4-1	CH_2O	72	8.41	18.4		
4-1 (in DMSO)	NCH_2	77	25.8	17.85 (DMSO)		
4-1 (in DMSO)	CH_2O	77	24.5	17.89 (DMSO)		
4-2	NCH_2	30	(2.5)	(16.8)	1634	1633
4-2	$CH_2C\mathbf{H}_3$	74	34.8	17.5		
4-3	NCH_2	63	28.9	17.0	1633	1647
4-3	$CH_2C\mathbf{H}_3$	63	15.6	17.4		
4-4	NCH_2	70	20.1	17.7	1638	1643
4-4	CH_2O	72	17.6	17.9		
4-4	$COCH_3$	70	20.8	17.6		

Figure 4.4. *Calculated $\Delta G^{\ddagger}$ values (shown in kcal/mol with uncertainty ±0.1-0.2 kcal/mol) from coalescence temperatures (shown in °C) for the five related amides in this study.*[55]

As shown in **Figure 4.4**, the $\Delta G^{\ddagger}$ values range from 17.0 kcal/mol to 18.4 kcal/mol, which does not demonstrate a large change in the rotational barrier despite varying degrees of hydrogen bonding of the five related amides.[55] Amide **4-2** lacks the extra OH groups and has a $\Delta G^{\ddagger}$ of 17.5 kcal/mol whereas amide **3-5** has the most OH groups/hydrogen bonding ability has its barrier increase to only 18.0 kcal/mol.[55] This culminated in us concluding that hydrogen bonding is not a major contributor to the amide rotational barriers at least when it comes to these systems.[55]

General conclusions

The amide rotational barrier of five related amides was determined to evaluate the effect/if there was an effect related to intramolecular hydrogen bonding. Variable temperature NMR in acetonitrile-d3 proved to be an invaluable technique in measuring these rotational barriers. Intramolecular hydrogen bonding appears to have little to no effect on the amide rotational barrier resulting in $\Delta G^{\ddagger}$ of only 1.4 kcal/mol in difference at most. Though this might not be the most interesting result, it helps further complete our knowledge on amides and their barriers.

Chapter 5

Synthesis of a bifunctional iron(II)/iron(III) hexadentate 8-hydroxyquinoline-based chelator scaffold

Introduction

Cellular labile iron plays a pivotal role in many biological processes through its role in the Fenton reaction.[66,67,69,75] Strongly bound iron, as in heme, is not Fenton active, but the intracellular transit of iron involves weakly bound, Fenton-active iron, referred to as the labile iron pool.[66,67,69,75,82] The Fenton reaction (shown in **Figure 5.1**) is responsible for the generation of reactive oxygen species (ROS) including hydroxyl radical.[69,72,73,75] These reactive oxygen species can go on to damage cellular components including lipids and DNA.[69,72-73,75] In the ferroptosis process of programmed cell death, oxidized lipids (lipid ROS) are produced.[66,69,72,73,75] Iron chelators can prevent Fenton chemistry.[66,68] Labile Fe^{3+} found in reducing environments should also be considered as targets for chelation as reduction from Fe^{3+} to Fe^{2+} can cascade into the Fenton reaction process.[63,66-69,75]

This project addresses chelators of use in two areas, the understanding of ferroptosis and the treatment of iron overload disease.[75] Iron overload disease can result in a shortened life span, decreased quality of life, and increased Fenton chemistry.[75] The subject chelator should be capable of sequestering both iron(II) and iron(III), and be usable *in vitro* and *in vivo* for these purposes. The most important site of intracellular iron metabolism is the mitochondrion.[83] By targeting the chelator to the mitochondria with an appropriate peptide, these two areas are addressed.[66]

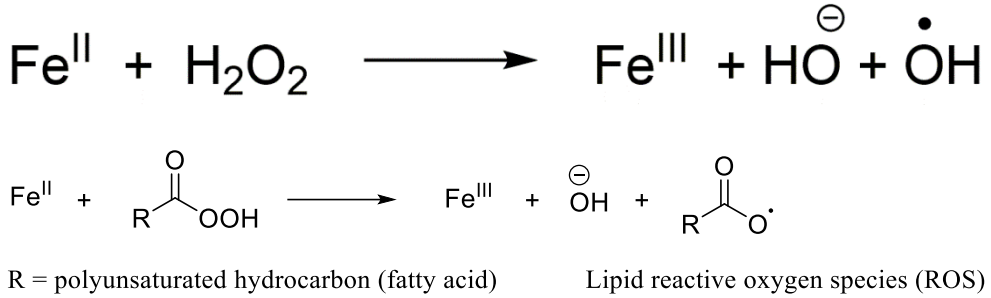

Figure 5.1. *Fenton chemistry*

Great strides have been made towards iron chelators by Serratrice et al. through the use of catechol chelating pendants on tripodal scaffolds (**Figure 5.2**).[63,66,68] Hider and coworkers made the same tetrapeptide sequence as ours (**Figure 5.2**) with a catechol conjugated to the lysine residue capable of coordinating Fe^{3+}. In order to chelate both Fe^{2+} and Fe^{3+} intracellularly, we are studying 8-hydroxyquinoline-based chelators (**Figure 5.2**).[67] Previous studies of tripodal iron chelators in our group focused on Fe^{2+} chelators, namely the tamepyr and tachpyr ligands, which are based on aminopyridyl pendant groups, and have inspired the current project (**Figure 5.2**).[71,84]

Catechol pendants groups are good at chelating the harder acid Fe^{3+} through phenolic oxygens and amide carbonyl donors whereas tamepyr and tachpyr ligands chelate through imino-pyridyl and amino-pyridyl groups resulting in a higher affinity for the softer acid Fe^{2+}.[67,71] 8-Hydroxyquinoline-chelating pendant groups used in this study offer both a pyridyl nitrogen and phenolic oxygen to complex iron, and two potential binding modes which bind both Fe(II) and Fe(III) when tethered by TREN (tris(2-aminoethyl)amine) in a tripodal fashion.[66] In this work, we replace TREN with a new tripod scaffold capable of conjugation to a lysine residue of a targeting peptide via a carboxylic acid group.[66]

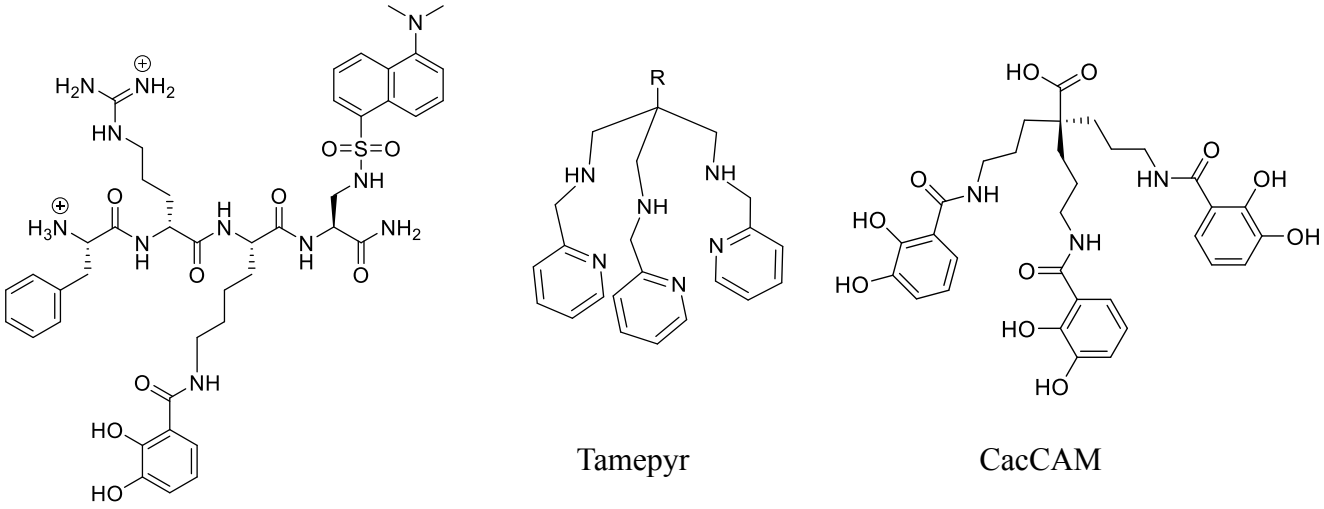

Figure 5.2. *Inspiration for the hexadentate iron chelator. Left to right: Hider and coworkers catecholic peptide design, Planalp and coworkers Fe^{2+} tamepyr ligand, and Serratrice and coworkers conjugatable tripodal hexadentate ligand CacCAM for Fe^{3+}.*

There are limitations to our three inspirational molecules. Firstly, the Hider and coworkers tetrapeptide has the ability to target the mitochondria of a cell due to its unique cationic hydrophobic repeating residues (a member of the Szeto-Schiller peptide family).[74] The Hider molecule also contains the catechol iron chelating pendant which is only selective for Fe^{3+}, thus cannot fully shut down Fenton chemistry which is driven by the transformation of Fe^{2+} to Fe^{3+} via peroxides.[67,75] It would also require three equivalents of catechol (a bidentate ligand) and peptide to coordinate one Fe^{3+} by filling all six coordination sites. Hexadentate coordination is achieved by the tamepyr ligand, but the softer nitrogen chelates favor Fe^{2+} solely so labile Fe^{3+} in the mitochondria could still be reduced and participate in Fenton chemistry.[71,75] The tamepyr ligand also lacks a targeting group such as a peptide but one could be feasibly attached in the future.[71] Finally, CacCAM developed by Serratrice and coworkers achieves hexadentate binding of Fe^{3+} completely but is not a soft enough ligand to accommodate Fe^{2+} as well. The 7-carboxy-

8-hydroxyquinoline pendant ligand attached via amide bonds should, in principle, provide the happy medium needed to coordinate both Fe^{3+} and Fe^{2+}.[67] It can bind Fe^{2+} via the pyridyl nitrogen and phenolic/phenoxide oxygen in a 5-membered chelate and it can bind Fe^{3+} via coordination of the amide carbonyl and phenolic/phenoxide oxygens in a 6-membered chelate.[67]

The outline for the synthesis of this novel hexadentate chelator scaffold is outlined in **Scheme 5.1** including its future prospective attachment to our group's mitochondria targeting peptide synthesis via solid phase peptide synthesis by group member Leonid Povolotskiy.[66,74]

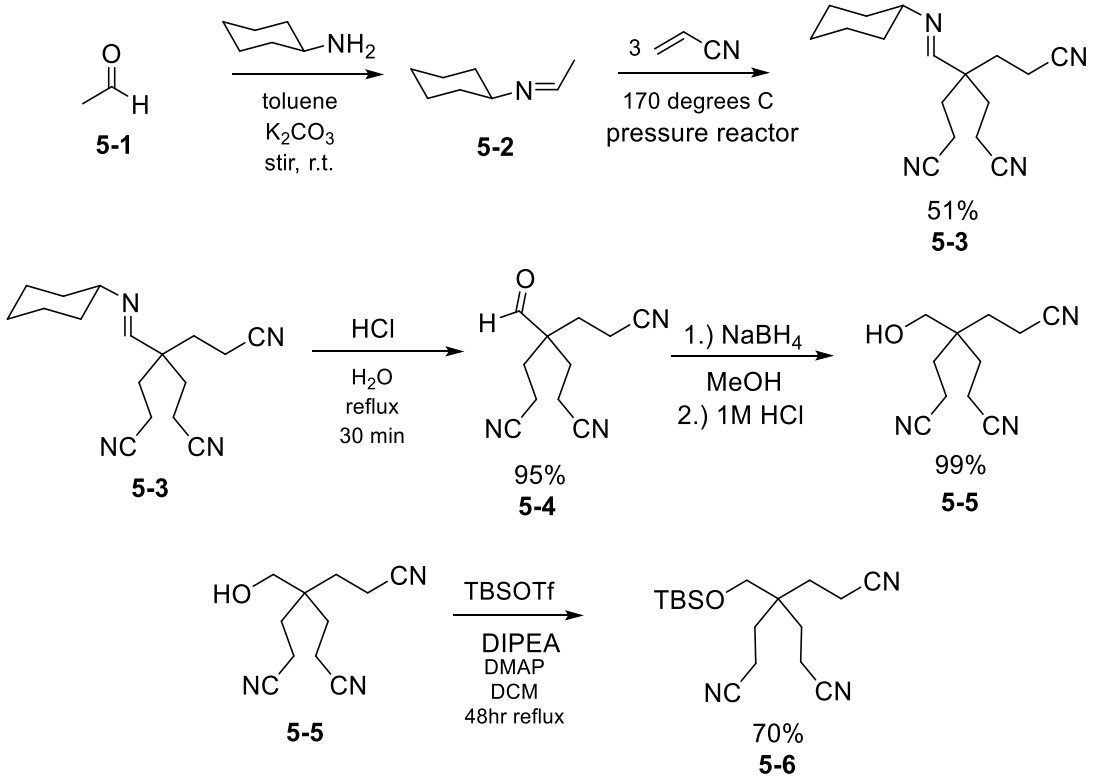

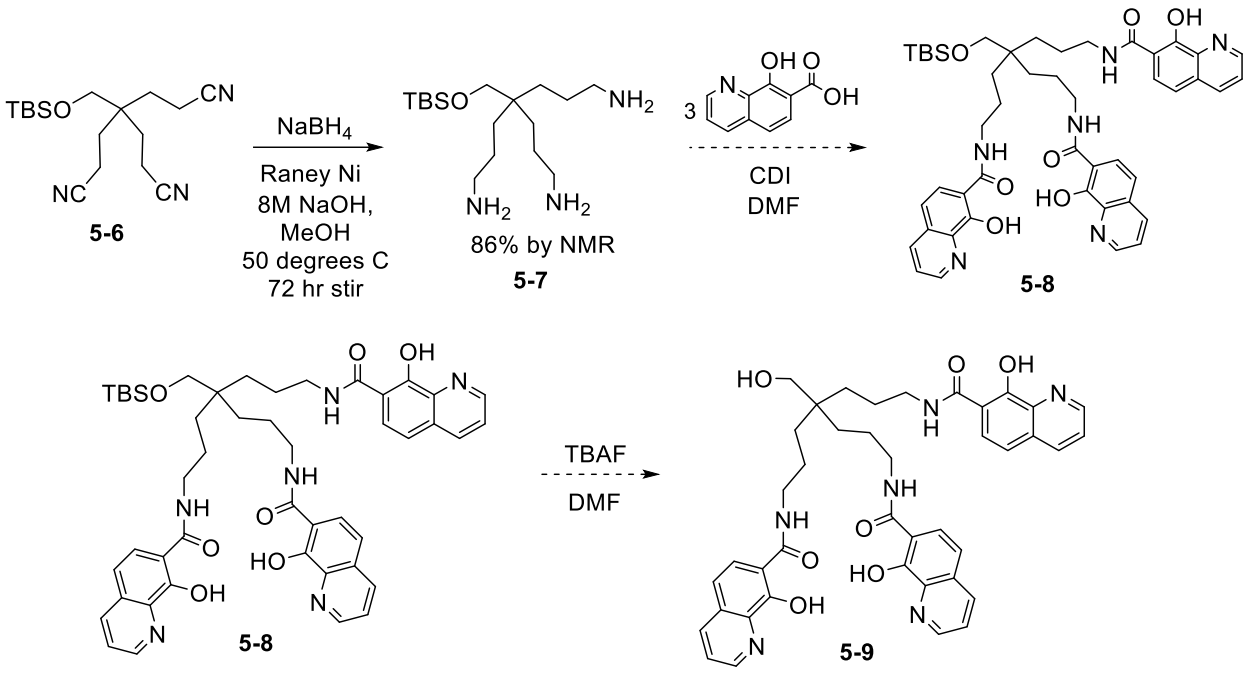
TBSO
CN
NC
CN
5-6
NaBH4
Raney Ni
8M NaOH,
MeOH
50 degrees C
72 hr stir
TBSO
NH2
NH2
NH2
86% by NMR
5-7
3
OH O
N
OH
CDI
DMF
TBSO
O
OH
N
H
N
NH
O
NH
O
HO
OH
N
N
5-8
TBSO
O
OH
N
H
N
NH
O
NH
O
HO
OH
N
N
5-8
TBAF
DMF
HO
O
OH
N
H
N
NH
O
NH
O
HO
OH
N
N
5-9

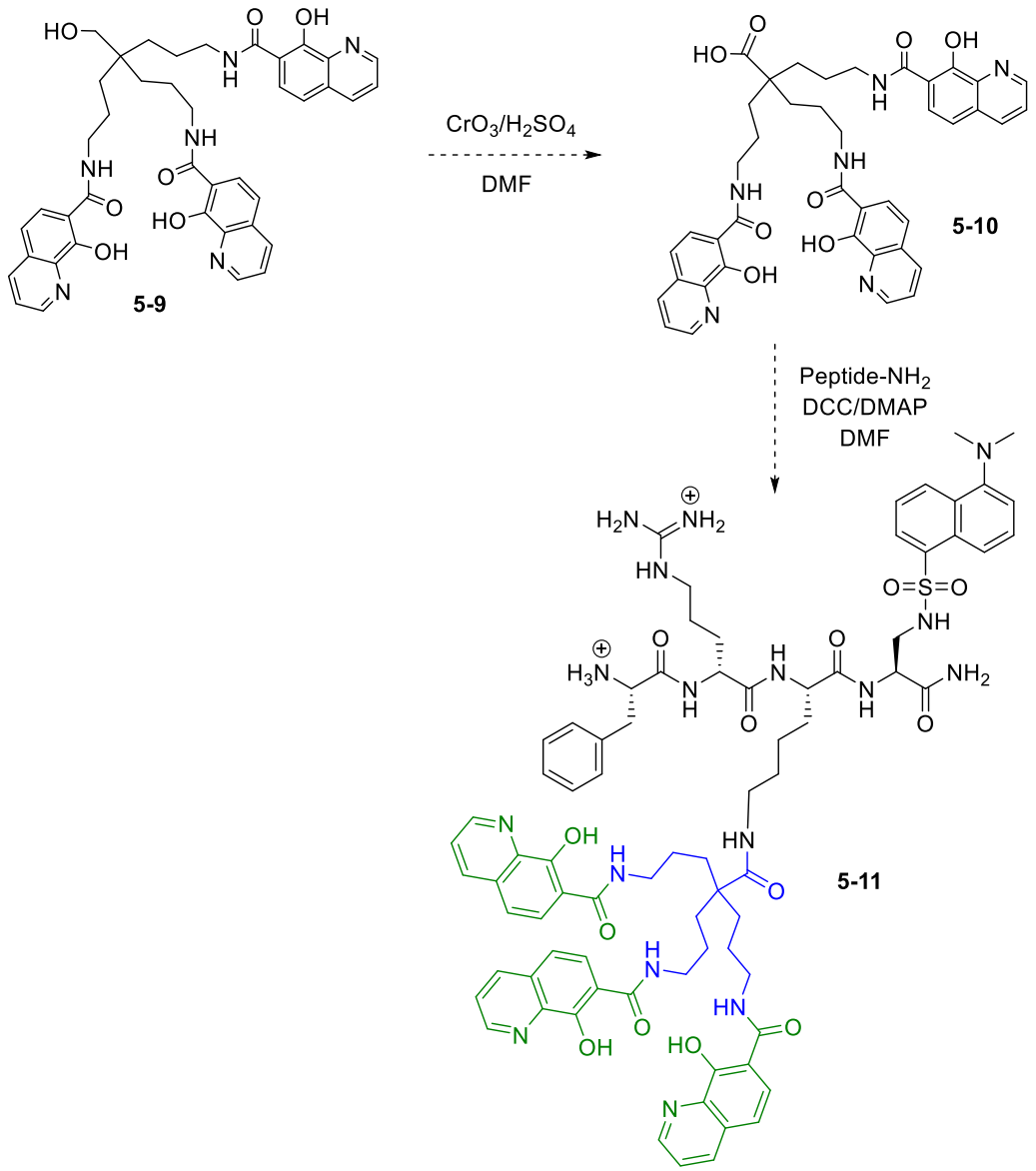

Scheme 5.1: *Synthesis of tripodal hexadentate chelator linked to a mitochondria targeting tetrapeptide. Mitochondria targeting peptide with fluorescent sensor shown in* ***black****, 7-carboxy-8-hydroxyquinoline pendants shown in* ***green****, and triamine tripodal linker with carboxylic acid handle shown in* ***blue*** *(target portion of this research).*

Results and discussion

The synthesis of a triamine tripodal linker has been completed to this point, with the final step being amide condensation to chelating pendant group firstly, 7-carboxy-8-hydroxyquinoline.

Two synthetic steps remain to obtain the peptide conjugate which are a TBS deprotection step and oxidation of the resulting alcohol to a carboxylic acid, enabling amide condensation of the ligand to a peptide lysine group.

The triamine ligand scaffold has been prepared by a multistep synthesis. Condensation of acetaldehyde and cyclohexylamine afforded an imine (**5-2**) which was subjected to enamine Michael addition of three equivalents of acrylonitrile, achieved via a pressure reactor at 170 degrees Celsius to overcome the barrier to forming the first tripodal structure (**5-3**) seen in **Figure 5.3**.

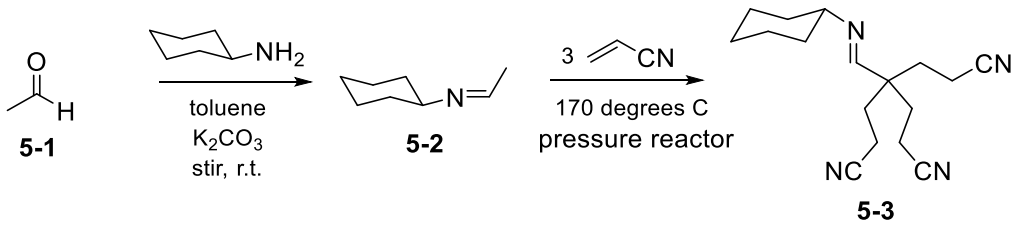

Figure 5.3. *Synthesis of imine trinitrile/first tripodal structure*

This imine trinitrile (**5-3**) was hydrolyzed into aldehyde trinitrile (**5-4**) via water and concentrated HCl and is shown in **Figure 5.4**. This transformation can also be monitored by ^{1}H and ^{13}C NMR as the number of peaks drastically reduce to 3 proton NMR signals and 5 carbon NMR signals.

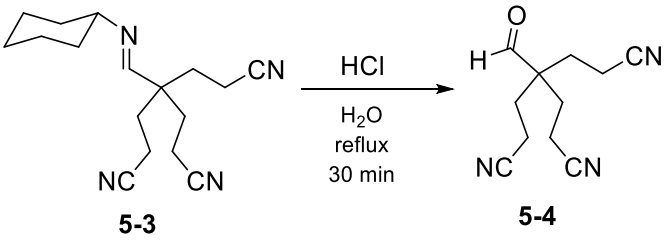

A.)

B.)

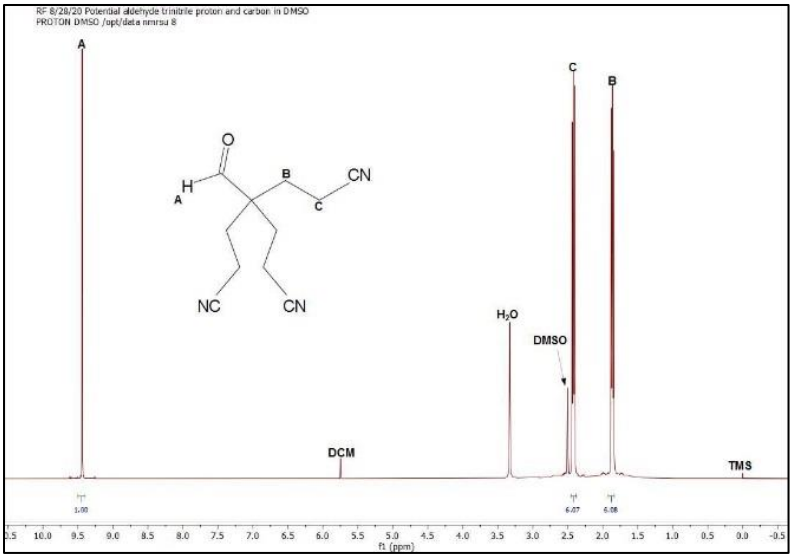

B.)

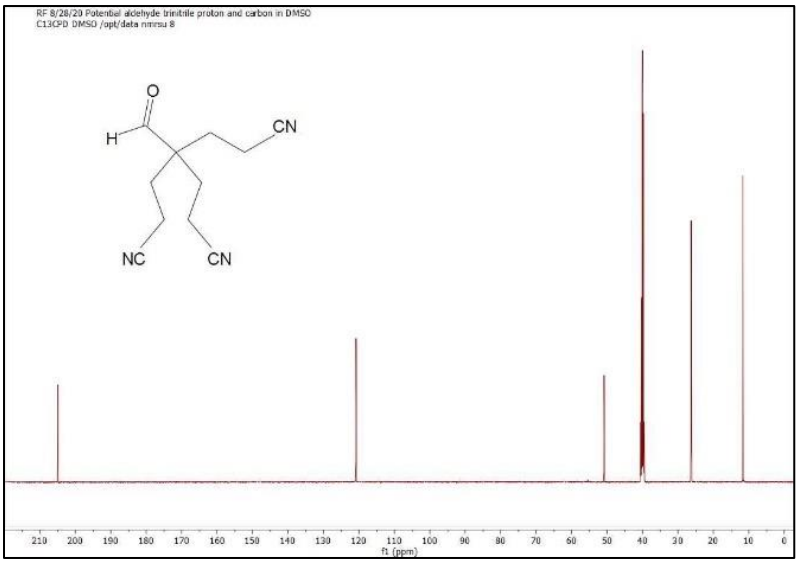

Figure 5.4. *A.) Imine hydrolysis of imine trinitrile in aldehyde trinitrile and B.) spectral evidence of aldehyde formation [^{1}H NMR (500 MHz, DMSO-d6); ^{13}C NMR (125 MHz, DMSO-d6)]*

The aldehyde trinitrile (**5-4**) was treated with sodium borohydride subsequently and alkoxide intermediate was quenched with HCl to afford the alcohol trinitrile (**5-5**) shown in **Figure 5.5**.

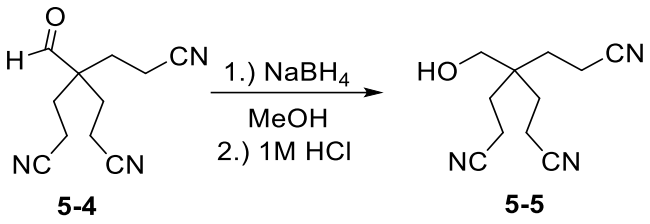

Figure 5.5. *Synthesis for converting aldehyde trinitrile into alcohol trinitrile*

Prior to reduction, the primary alcohol handle of the alcohol trinitrile (**5-5**) tripodal structures was protected via a 48-hour reflux with TBS triflate to yield the TBS protected alcohol trinitrile (**5-6**) shown in **Figure 5.6**.

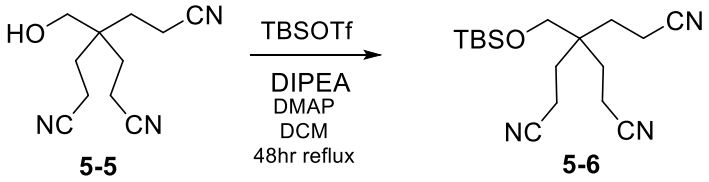

Figure 5.6. *Synthesis of the TBS protected alcohol trinitrile tripod via TBS-OTf reflux of the alcohol trinitrile*

This TBS protected alcohol trinitrile (**5-6**) can then be reduced via a combination of excess sodium borohydride, Raney nickel, and 8M sodium hydroxide to form the TBS protected alcohol triamine (**5-7**) (shown in **Figure 5.7**) for linking to chelating pendants.

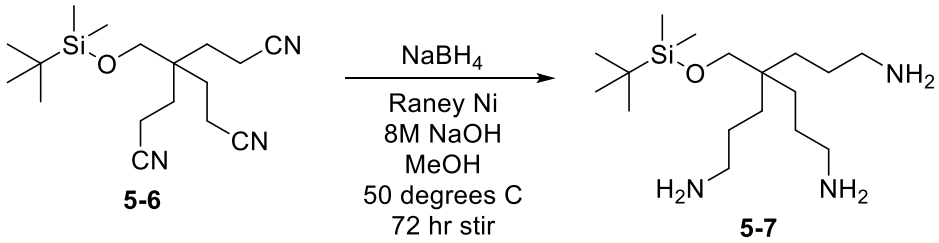

Figure 5.7. *Synthesis of the TBS alcohol triamine tripod via Raney Ni/$NaBH_4$ reduction*

General conclusions

Synthesis of the TBS protected alcohol triamine has been completed to this point and is ready for coupling to the 7-carboxy-8-hydroxyquinoline chelating pendants. The biggest hurdle in this synthesis was getting the nitrile groups to reduce into primary amines successfully-the Raney Ni, $NaBH_4$, and NaOH conditions finally broke through this barrier after many attempts with other reducing conditions. Also, another big improvement was switching the imine trinitrile synthesis from a reflux in DMF approach to a pressure reactor in toluene approach, which allowed for yields of 50% and large-scale reactions moving forward for easier transformations.

Chapter 6

Experimental

General Experimental

INSTRUMENTATION

^{1}H NMR

All intermediates and final products were characterized by NMR. ^{1}H NMR and ^{13}C NMR were acquired with a Varian Mercury 400 BB NMR, a Bruker 500 BB NMR, and/or a Bruker 700 NMR. Chemical shifts are reported in parts per million (ppm) relative to tetramethylsilane (TMS) unless otherwise noted. Chloroform-d, dimethylsulfoxide-d6, methanol-d4, and tetrahydrofuran-d8 were purchased from Cambridge Isotope Labs and were stored over molecular sieves (4Å).

GCMS

Shimazdu GCMS-QP2010 equipped with a 30.0 m SHRX1-5MS column (thickness: 0.25 μm, diameter: 0.25 μm) and 70 eV electron impact detector. The injector temperature (splitless injection) was held at 250 °C and the detector at 260°C. The column temperature increased from 45°C to 250°C at 15°C /min and held at 250°C for 0 min, after a solvent delay of 5.5 min. Flow rate was 1 mL/min and total run time was 14.67 minutes.

SOLVENTS AND REAGENTS

All solvents and reagents were purchased from Fisher, Alfa Aesar, Sigma Aldrich, Pharmco Aaper, and Acros. All chemicals were used as is and required no further purification.

CHROMATOGRAPHY

Reaction products were purified by flash column chromatography using Silicycle Inc. silica gel (60 Å, 230–400 mesh). Thin layer chromatography was performed on Agela Technologies TLC Silica plates (silica gel 60 GF254) and visualization was accomplished with UV light.

ENZYMATIC INCUBATIONS

NADPH and magnesium dichloride were purchased from Sigma Aldrich. Potassium phosphate buffer (0.5 M), pooled human liver microsomes, and cytochrome P450 isoforms 1A2, 3A4, and 2E1 were purchased from Corning Life Sciences in Woburn, MA. MilliQ water was used in all incubations, which were carried out in a 37°C water bath.

DETAILED EXPERIMENTAL

Synthesis of 1,4-dihydronaphthalene (**1**-**2**) *via Birch Reduction:*

A Dewan condenser apparatus was constructed filled with solid CO_2 and acetone bath to condense liquid ammonia (NH_3). Glassware was extensively dried to prevent against potential fire hazards. A three-neck flask was filled with naphthalene (5.0175g) and dry diethyl ether (Et_2O) (80mL); and the flask was fitted with two rubber septa, magnetic stir bar, nitrogen atmosphere, and Dewan condenser. Sodium metal (Na°) (1.62g) was added to the 3-neck flask in fine chunks after being rinsed in hexanes to remove trace mineral oil, which Na° is stored in. The flask was hastily sealed to maintain dryness and safety. The solution changed from clear to blue to green back to deep blue. The reaction was stirred for 20 minutes. Some brown precipitate formed during the reaction indicative of iron contamination from rust in the NH_3 gas cylinder.

The reaction was quenched by adding NH_4Cl (15mL) dropwise. After the first 7mL the solution turned blue back to green and turned a tinged green at 8mL total. Solution was blue again after 9mL total of mild acid and the solution was completely clear after all 15mL was added.

Clear solution was transferred to a round bottom flask and condenser by vacuum and reduced pressure for 60 minutes to remove liquid NH_3 to yield white solid with brown iron precipitate contaminate.

Solution was extracted with Et_2O (2 x 30mL) to yield a brown aqueous layer containing inorganic iron precipitate salt and a clear organic layer containing crude product. Organic layer was dried with anhydrous Na_2SO_4 and was condensed to a bright white solid (3.25g crude, 49%

yield), which was determined to be a 2:1 mixture of 1,4-dihydronapthalene (**1-2**) and naphthalene (**1-1**).

1,4-dihydronapthalene (**1-2**) as a crude white solid mixture: ^{1}H NMR (400 MHz, $CDCl_3$) δ 7.10 (m, 4H), 5.91 (t, 2H), 3.40 (d, 4H).

Synthesis of epoxide (**1-3**) *using mCPBA:*

1,4-dihydronapthalene (1.625g) was dissolved in dichloromethane (DCM) (30mL) in 250mL 3-neck flask fitted with a nitrogen inlet and magnetic stir bar. The flask was placed in an ice bath at 0°C. The solution turned pale yellow. To this solution, *m*CPBA (2.76g) dissolved in another portion of DCM (30mL) was added dropwise via a dropper funnel. Residual *m*CPBA in the dropper funnel was rinsed into the reaction solution. A thick white and yellow precipitate formed in the flask. KI paper was used to see if the oxidizing agent (*m*CPBA) was working. The reaction was allowed to stir for 18 hours total before filtering off the precipitate. The filtrate was washed with $NaHSO_3$ (2 x 25mL), $NaHCO_3$ (2 x 50mL) and brine (NaCl) (2 x 25mL) before being condensed via vacuum into crude epoxide (**1-3**) and 1,4-dihydronapthalene (**1-2**) mixture (2.24g) as a yellow/orange solid. TLC analysis (3:1 hexanes:diethyl ether solvent system) indicated that the epoxide required further purification.

Crude epoxide was purified via silica column to yield pure epoxide (1.03g, 63.9%). Epoxide (**1-3**) as a yellow-white solid: ^{1}H NMR (400 MHz, $CDCl_3$) δ 7.14 (m, 2H), 7.04 (m, 2H), 3.48 (m, 2H), 3.31 (d, J=16.16Hz, 2H), 3.17 (d, J=13.84Hz, 2H).

Synthesis of brominated epoxide (**1-4**) *via photochemical NBS bromination*:
AIBN radical initiator was dissolved in carbon tetrachloride (CCl_4) (10mL) and left in hood overnight. Epoxide (0.160g, 1eq.) was combined with NBS (0.234g, 1.1eq.) in a 3-neck flask fitted with a nitrogen inlet, magnetic stir bar and reflux condenser. AIBN solution was added to the flask. Then, CCl_4 (30mL) was added to completely dissolve all solids for a total amount of 40mL of CCl_4. Once all of the solids were dissolved via stirring, an intense visible light source was shined onto the 3-neck flask and solution. The light source heated the solution while activating the AIBN to a reflux. Reaction was run for 8 hours and at reflux after 1 hour due to immense heat from the light source. TLC analysis (3:1 hexanes:diethyl ether solvent system) indicated that the brominated epoxide formed after the first hour and in concentrated amounts after the full 8 hours.

Crude brominated epoxide was purified via column to yield pure brominated epoxide (0.160g, theoretical yield 0.250g, 64.0% yield). Brominated epoxide (**1-4**) as a yellow oil: ^{1}H NMR (400 MHz, $CDCl_3$) δ 8.08 (dd, 1H), 7.68 (dt, 1H), 7.53 (dt, 1H), 7.25 (dd, 1H), 5.54 (d, 1H), 3.78 (t, 1H), 3.65 (t, 1H), 3.29 (d, 2H).

Synthesis of 4,5-benzoxepin (**1-5**) *via dehydrohalogenation of brominated epoxide*:
Potassium t-butoxide (0.224g, 4 eq.) was dissolved in dry THF (20mL) in a 3-neck flask fitted with a nitrogen inlet, magnetic stir bar and dropper funnel. The 3-neck flask was placed in an ice bath. Solution was allowed to stir to ensure better solubility of potassium t-butoxide. Brominated epoxide (0.114g, 1eq.) dissolved in dry THF (5mL) was added drop wise in portions to the solution every 10 minutes for 50 minutes total. After the 50 minutes was up, dry THF (1mL) was added to the dropper funnel to rinse residual brominated epoxide starting material into the solution and then the dropper funnel was replaced with a calcium chloride drying column.

Reaction was stirred for 24 hours and ice was allowed to melt after the first 8 hours. Using TLC analysis (3:1 hexanes:diethyl ether solvent system), it was determined that 4,5-benzoxepin formed after 1 hour in trace amounts and in concentrated amounts after 20 hours.[1,3,5]

Crude 4,5-benzoxepin was purified via column to yield pure 4,5-benzoxepin (0.060g, theoretical yield 0.072g, 83.3% yield). 4,5-benzoxepin (**1-5**) as a yellow powder solid: ^{1}H NMR (400 MHz, $CDCl_3$) δ 6.90 (m, 2H), 6.63 (m, 2H), 5.64 (d, J=7.52Hz, 2H), 5.01 (d, J=8.20Hz, 2H).

Two electron oxidation of 4,5-benzoxepin (**1-5**) *using cerium (IV) ammonium nitrate (CAN)*:
4,5-benzoxepin (0.060g) was combined with CAN (0.457g) in a scintillation vial fitted with a small magnetic stir bar and were dissolved in acetone (5mL). The vial was wrapped in foil so that the reaction could be stirred in the dark. After one hour diethyl ether (2mL) was added to fully dissolve products. The reaction stirred for 48 hours to yield crude "fraction 1" unidentified product (0.100g crude yield). The reaction was placed in a freezer to avoid decomposition of products and was purified via 3:1 hexanes:diethyl ether silica flash column under N_2 after 1 week. ^{1}H NMR indicates the presence of "fraction 1" when compared to a standard ^{1}H NMR of "fraction 1" **1-7** (0.057g, 43.0% yield). ^{1}H NMR (500 MHz, $CDCl_3$) δ 8.01 (dd, 2H), 7.61 (dt, 2H), 7.40 (dt, 2H), 7.34 (d, 2H), 6.67 (s, 2H), 6.48 (d, 2H), 5.94 (d, 2H).

Enzymatic reactions using enzymes pHLM and 2E1 with benzene substrate:
Benzene (64mM) underwent enzymatic reactions in 4 trials with either cytochrome P450 isoforms 2E1 (50pmol/mL or 5.0pmol/mL for trials 1 and 2) or pHLM (12.5µL or 1.25µL for trials 3 and 4). Each was combined buffer (100µL), $NADP^+$ solution A (25µL), NADPH solution B (5µL), and milli-Q water (355.16µL). Enzymes were pre-incubated for 5 minutes prior to

addition to the solution. Solution was heating in a water bath at a constant 37°C for 30 minutes. Each trial was extracted with dichloromethane (3 x 600µL) and the organic layer was kept each time. Organic layers were stored at -80°C before analysis.

GCMS analysis was performed on the final products to see if muconic acid or phenol formed as products as a control experiment and neither product was seen. ^{1}H NMR could not be performed due to the scale of the reaction.[48]

Enzymatic reactions using enzymes pHLM and 1A2 with 4,5-benzoxepin (**1-5**) *substrate*: Enzymatic reactions with 4,5-benzoxepin (**1-5**) were explored using different concentrations of substrate (4,5-benzoxepin) and using a standard addition method using "fraction 1" standard as the expected product. The concentrations of 4,5-benzoxepin that were tested were 50µM, 100µM, 150µM and 200µM with cytochrome P450 isoform 1A2 (25pmol/mL, 25µL) for trials 1-4, respectively and were repeated for trials 5-8 with isoform pHLM (0.25mg/mL, 12.5µL). All 8 trials had the same amounts of buffer (200µL), $NADP^{+}$ solution A (50µL) and NADPH solution B (10µL) combined with substrate, enzyme, and milli-Q water. Milli-Q water was added to dilute to the proper concentrations with the amounts for a total 1mL reaction volume. Enzymes were pre-incubated for 5 minutes prior to addition to the solution. Solution was heating in a water bath at a constant 37°C for 30 minutes. Each trial was extracted with dichloromethane (3 x 600µL) and the organic layer was kept each time. Standard "fraction 1" (143mM, 2.4µL) was added half of each trial in a separate container for 16 total samples. Organic layers were stored at -80°C before analysis.

GCMS analysis was performed on the final products to see if "fraction 1" formed as products as a control experiment and analysis indicated that "fraction 1" formed and unreacted

4,5-benzoxepin remained for substrate concentrations of 150μM and 200μM whereas the 50μM and 100μM could not be determined because their respective peaks are buried in the baseline.

Enzymatic reactions using enzyme P450 1A2 with naphthalene substrate and revised regenerating system:

Revisions were made to the NADPH regenerating system to include excess $MgCl_2$ as a divalent cation to balance negative charges on the phosphate groups of ATP and this allowed for mass spectrometry analysis of the metabolism of naphthalene to naphthol, which is the known metabolite of naphthalene and the product was compared to a pure standard of naphthol with a yield in excess of 50%.

Enzymatic reactions using enzymes P450 1A2 and P450 3A4 with 4,5-benzoxepin substrate and revised regenerating system:

The new regenerating system employed in the naphthalene to naphthol control experiment was used in the same reaction as all other enzymes reactions with 4,5-benzoxepin as a substrate again to yield carboxaldehyde **1-6** and "Fraction 1" as products in a 2:1 ratio (product **1-6** : "Fraction 1" product **1-7**) when compared to standards of the two compounds. Standard additions were not done in this procedure.

Attempted synthesis of dimer (**1-15**) *and resulting synthesis of benzoisocoumarin* (**1-16**) *via nickel homocoupling:*

A test tube was fitted with a small magnetic stir bar and monomer 6-bromo-dibenz[b,d]oxepin-7(6H)-one (0.050 g, 1 eq.), anhydrous $NiCl_2$ (0.0224 g, 1 eq.), Zn dust (0.0113 g, 1 eq.), and

2,2'-bipyridine (0.0540g, 2 eq.) were added. Dry pyridine (0.0139 mL, 1 eq.) and dry $CHCl_3$ (15 mL) were added via pipette to the test tube. The test tube was fitted with a septum and sealed with parafilm. The test tube was then purged for 5 minutes with argon and then sealed with an argon atmosphere. Solution was stirred overnight and the headspace was analyzed via GC and was identified with a methane standard to be generating methane. Solution was gravity filtered into a separatory funnel and was washed with 1M HCl (3 x 25 mL) and the organic layer was dried with sodium sulfate. The organic layer/$CHCl_3$ was evaporated via rotary evaporator and high vacuum to yield an orange solid mixture of benzoisocoumarin (**1-16**) and dibenz[b,d]oxepin-7(6H)-one (**1-13**) (0.0352g) with no starting material remaining. A crude NMR was obtained for the product (in Appendix). Products were not separated because it demonstrated repeatability of group member Dr. Guevara's work.

Synthesis of 2-allyl-1-allyloxybenzene (**2-9**) *via o-allylation:*

Building block starting material 2-allylphenol (**2-8**) (1.500g, 1.458mL, 1.0eq) was combined with allyl bromide (1.158mL, 1.2eq) and K_2CO_3 (1.854g, 1.2eq) and dissolved in acetonitrile (35.0mL) in a 250mL round bottom flask. Solution was refluxed under a nitrogen atmosphere for 4 hours. Acetonitrile was evaporated and the liquid and white solid were redissolved in Et_2O (25mL) for washes. The organic layer was washed with brine (3 x 25mL), water (3 x 25mL), and sodium bicarbonate (10% w/v) (3 x 25mL). A crude NMR was run and it was determined that all of the 2-allylphenol (**2-8**) was converted to the product **2-9** based on literature chemical shift values. A silica flash column was run using a 15:1 hexanes:ethyl acetate solvent system to yield pure product **2-9.**

Crude 2-allyl-1-allyloxybenzene was purified via column to yield pure 2-allyl-1-allyloxybenzene (0.743g, theoretical yield 1.948g, 38.1% yield). 2-allyl-1-allyloxybenzene (**2-9**) as a yellow liquid: ^{1}H NMR (400 MHz, $CDCl_3$) δ 7.16 (m, 2H), 6.89 (dt, 1H), 6.82 (d, 1H), 6.03 (m, 2H), 5.41 (dq, 1H), 5.24 (dq, 1H), 5.05 (m, 2H), 4.53 (dt, 2H), 3.41 (d, 2H).

Synthesis of 2,5-dihydro-1-benzoxepin (**2-10**) *via ring closing metathesis:*

2-allyl-1-allyloxybenzene (**2-9**) (0.618g) was dissolved in dry dichloromethane (20mL) and combined with Grubbs first generation catalyst (0.161g, 0.05eq). The solution was purged continuously with nitrogen to ensure that the catalyst had little to no atmospheric moisture exposure. The solution was attached to a reflux condenser fitted with a nitrogen inlet and was refluxed for 2 hours. A crude NMR sample was made via an alumina plug and according to relative NMR integrations a 95% conversion of starting material **2-9** was converted to product **2-10**. A silica flash column was run using a 10:1 hexanes:ethyl acetate solvent system to yield pure product **2-10**.

Crude 2,5-dihydro-1-benzoxepin (**2-10**) was purified via column to yield pure 2,5-dihydro-1-benzoxepin (0.500g, theoretical yield 0.517g, 96.7% yield). 2,5-dihydro-1-benzoxepin (**2-10**) as a yellow solid: ^{1}H NMR (400 MHz, $CDCl_3$) δ 7.19 (m, 1H), 7.09 (d, 1H), 7.03 (m, 2H), 5.85 (dt, 1H), 5.49 (dt, 1H), 4.59 (t, 2H), 3.49 (t, 2H).

Attempted synthesis of 2,5-dibromo-1-benzoxepin (**2-11**) *via* Br_2 *bromination of an alkene:*

Bromine (Br_2) (0.150mL, 0.81eq) was dissolved in a 1:1 solution of chloroform:dichloromethane (15mL) in a vial. **2-10** (0.500g, 1.0eq) was dissolved in the same chloroform:dichloromethane solution (30mL) in a separate 250mL round bottom flask. The bromine solution was pipetted into

the round bottom was flask and the solution was stirred at -78°C for 30 minutes in a dry ice and acetone bath. Solution was filtered through three pipet columns filled with silica to filter off excess bromine solution. Attempted recrystallization with hexanes (8mL) was unsuccessful. GC-MS data and a very impure crude NMR have been obtained for crude **2-11** to this point.

Synthesis of 1,4-dihydro-1,4-epoxynaphthalene (**1-9**) *via Diels Alder with benzyne:*

Furan (9.4 g, 10 mL) was dissolved in 1,2-dimethoxyethane (10 mL) in a 100 mL round bottom flask. This was then set to reflux. In two separate Erlenmeyer flasks, a solution of isoamyl nitrite (4 mL) in DME (10 mL), and a solution of anthranilic acid (**1-8**) (2.74 g) in DME (10 mL). Each solution was then added in 2 mL portions every 9 minutes. Once additions were complete, the solution was then set to reflux for a further 30 minutes. The reaction was then quenched with sodium hydroxide (0.5 g) in water (25mL). The product was then extracted using light petroleum (3 x 15 mL), washed with water (6 x 15 mL), and dried using magnesium sulfate.

Pure 1,4-dihydro-1,4-epoxynaphthalene (**1-9**) (2.51 g, theoretical yield 2.95 g, 85% yield) was collected as a red/orange solid: ^{1}H NMR (400 MHz, $CDCl_3$) δ 7.25 (m, 2H), 7.03 (t, 2H), 6.97 (m, 2H), 5.71 (m, 2H).

Synthesis of 4,5-benzoxepin (**1-5**) *using photoreaction:*

1,4-dihydro-1,4-epoxynaphthalene (6.04 g) was dissolved in absolute ethanol (400 mL) in a 500 mL round bottom flask to prepare stock solution. The solution was set to stir while purging with N_2. From the stock solution, 1,4-dihydro-1,4-epoxynaphthalene (**1-9**) was added to two separate phototubes. The phototubes were then fitted with stoppers and again purged with N_2. The

solutions were then subjected to 254 nm light for 24 hours. After the light exposure, the solvent was evaporated and crude 4,5-benzoxepin was collected as a brown/red oil.

Crude 4,5-benzoxepin was purified using a hexanes column and pure 4,5-benzoxepin (**1-5**) (0.13 g, theoretical yield 0.751 g, 17.3% yield) was collected as a yellow solid: ^{1}H NMR (400 MHz, $CDCl_3$) δ 6.90 (m, 2H), 6.63 (m, 2H), 5.64 (d, J=7.52Hz, 2H), 5.01 (d, J=8.20Hz, 2H).

Two-electron oxidation of 4,5-benzoxepin using cerium (IV) ammonium nitrate (CAN):

CAN (1.99 g, 2 eq) was dissolved in acetone (50 mL) in a 250 mL 3-neck flask fitted with a dropper funnel and 2 stoppers. 4,5-benzoxepin (0.262 g, 1 eq) was dissolved in acetone (50 mL) and added to the dropper funnel. The system was set into the dry ice bath (-78^{o}C), purged with N_2, and aluminum foil was used to minimize light exposure. The 4,5-benzoxepin solution was added in 5 mL portions every 2 minutes until all reagent was used. The dropper funnel was then washed with acetone (5 mL) and added to the reaction. The reaction was then set to stir for 1 hour. Excess CAN reagent was gravity filtered and product was condensed via evaporation. Product was assumed to be "fraction 1" (**1-7**) from previous group reactions, but after NMR analysis it seemed to be purely "fraction 2" (**1-10**).

Crude product was purified via a 3:1 hexanes: ether column and pure "fraction 2" (**1-10**) was collected and evaporated to a yellow solid: ^{1}H NMR (400 MHz, $CDCl_3$) δ 7.54 (d, 2H), 7.46 (dt, 2H), 7.39 (d, 2H), 7.29 (dt, 2H), 7.01 (d, 2H), 6.36 (d, 2H), 6.25 (d, 2H), 5.79 (d, 2H).

Synthesis of 5-bromo-2-dihydro-1-benzoxepin (**2-12a**) *and 2-bromo-5-dihydro-1-benzoxepin* (**2-12b**) *via photochemical NBS bromination:*

2,5-dihydro-1-benzoxepin (**2-10**) (2.07 g, 1.0 eq) was dissolved in carbon tetrachloride (25 mL) and combined with N-bromosuccinimide (3.034 g, 1.2 eq) in a 250mL round bottom flask. Separately, azobisisobutyronitrile (AIBN) (0.351g, 0.15eq) was dissolved in carbon tetrachloride (10 mL) and then added to the reaction flask. The solution was subjected to a visible light/ heat lamp while refluxing under a nitrogen atmosphere for eight hours. Carbon tetrachloride was evaporated, and the solution was re-dissolved in dichloromethane (35 mL) for washes. The organic layer was washed with sodium bicarbonate (10% w/v) (3 x 25 mL), brine (3 x 25 mL), and water (4 x 25 mL). A silica flash column was run using a 3:1 hexanes: diethyl ether solvent system. NMR data confirmed that there was a bromination at both the allylic position as well as the benzylic position, affording a dibrominated compound (**2-12c**) making this synthetic route to 2,3-benzoxepin very difficult to continue.

Synthesis of 2,3-benzoxepin (**2-7**) *via Diels Alder reaction with pyridazine N-oxide:*

Pyridazine N-oxide (**2-13**) (0.518 g) was dissolved in DME (10 mL) in a 100 mL 3-neck flask and fitted with a condenser. Separate solutions of anthranilic acid (**1-8**) (0.712 g) and isoamyl nitrite (1.1 mL) were each individually dissolved in DME (10 mL) and placed into dropper funnels. While refluxing each solution was dropped into the 3-neck flask with portions (3mL) every 10 minutes. Once each reagent was completely used, the dropper funnels were each washed with DME (5mL) and drained into the reaction flask. The reaction was then refluxed for a further 45 minutes. The reaction was quenched with sodium hydroxide (0.555 g) in water

(25mL). The product was then extracted using petroleum ether (3 x 25 mL), followed by washes with brine (3 x 20 mL) and water (3 x 25 mL), and finally dried using sodium sulfate. This was followed by several hours on a high vacuum to remove excess benzene.

Pure 2,3-benzoxepin (**2-7**) (0.222 g, theoretical yield 0.865 g, 25.67% yield) was collected as an orange red solid: ^{1}H NMR (400 MHz, $CDCl_3$) δ 7.31 (t, 1H), 7.28 (d, 1H), 7.09 (t, 1H), 6.95 (d, 1H), 6.69 (d, 1H), 6.25 (d, 1H), 6.06 (dd, 1H), 5.49 (t, 1H).

Two electron oxidation of 2,3-benzoxepin using cerium (IV) ammonium nitrate (CAN):

CAN (0.304 g, 2.0 eq) was dissolved in acetone (20 mL) in a 100 mL 3-neck flask fitted with a dropper funnel and 2 stoppers. 2,3-benzoxepin (0.040 g, 1.0 eq) was dissolved in acetone (15 mL) and added to the dropper funnel. The system was set into the dry ice bath (-78^{o}C), purged with N_2, and aluminum foil was used to minimize light exposure. The 2,3-benzoxepin solution was added in portions (5mL) every 2 minutes until all reagent was used. The dropper funnel was then washed with acetone (5mL) and added to the reaction. The reaction was then set to stir for 20 hours. After evaporation of solvent, a brown product had been collected.

To this point only a crude NMR (in Appendix) has been run, and further analysis is necessary to determine the product of this reaction.

Epoxidation of 2,3-benzoxepin using mCPBA:

2,3-benzoxepin (0.053 g, 1.0 eq) was dissolved in DCM (15 mL) in a 100 mL round bottom flask sitting in an ice bath. *m*CPBA (0.077 g, 1.2 eq) was measured in a scintillation vial and dissolved

in DCM (5 mL). While the solution was stirring, the *m*CPBA solution was pipetted into the reaction flask. The reaction was then set to stir for 22 hours. The crude mixture was then gravity filtered into a separatory funnel. With DCM as the organic layer the product was washed with sodium bisulfate (2 x 25 mL), sodium bicarbonate (2 x 50 mL), and finally brine (2 x 25 mL). DCM was then evaporated, and product turned from a yellow solution to an orange solid.

Crude orange solid was purified via 3:1 hexanes:ethyl acetate column and methanol flush to yield more polar product as a yellow pure solid (0.010g, 16.98% yield). ^{1}H NMR (500 MHz, $CDCl_3$) δ 7.37 (m, 1H), 7.29 (d, 1H), 7.15 (m, 1H), 6.85 (t, 1H), 6.40 (s, 1H), 6.03 (d, 1H), 5.08 (d, 1H), 4.66 (s, 1H).

Enzymatic reactions using cytochrome P450 isoform 1A2 on 4,5-benzoxepin and 2,3-benzoxepin substrates.:

Enzymatic studies were performed on both substrates, the 2,3-benzoxepin being a new substrate and the 4,5-benzoxepin for comparative studies to previous enzyme reactions. Three sets of each substrate were tested. A 0.5 M buffer (100 μL), 33.65 mM $NADP^+$ (3.72 μL), 88.62 mM glucose-6-phosphate (14.11 μL), 44.2 μM/mL G6P-DH (22.62 μL), 98.4 mM magnesium dichloride (17.77 μL), 1000 pmol/mL isoform 1A2 (25 μL), water (314.78 μL), and either 4,5-benzoxepin (200mM, 3 μL) or 2,3-benzoxepin (200mM, 3 μL) were sequentially added into Eppendorf tubes. The solutions were then placed into a bead bath at a constant 37ºC for 30 minutes. The solutions were then all quenched with acetonitrile (250 μL) and centrifuged for 5 minutes at 13500 rpm. The products were then extracted using DCM (501 μL) as the organic

layer which was collected again centrifuged for 2 minutes at 13500 rpm. The organic extracts were then stored for GCMS analysis at -17^{o}C.

Synthesis of 2,2-dimethyl-1,3-dioxolan-4-one/glycolic acid acetonide (**3-3**):

A suspension of phosphorus pentoxide (20g) in Et_2O (50mL) in a 3-neck flask was cooled to -5^{o}C in a NaCl/ice water bath. Attached to the 3-neck flask was an addition funnel containing glycolic acid (5g) dissolved in acetone (25mL). When P_2O_5 clumped, it was kneaded with a spatula. The solution was decanted into a round bottom flask and evaporated via rotovap into an amber oil of 2,2-dimethyl-1,3-dioxolan-4-one (**3-3**) (1.448g, 18.7% yield). ^{1}H NMR (400 MHz, $CDCl_3$) δ 4.32 (s, 2H), 1.56 (s, 6H).

Synthesis of N-glycolyldiethanolamine (**3-5**):

Combined 2,2-dimethyl-1,3-dioxolan-4-one (1.448g) with diethanolamine (1.312g) and dry DCM (45mL) in a round bottom flask. Solution was stirred at room temperature for 8 hours and evaporated to crude N-glycolyldiethanolamine (1.667g crude). Crude product was dissolved in DCM (5mL) and ran through a silica flash column (4:1 methanol:ethyl acetate) to obtain pure N-glycolyldiethanolamine (**3-5**) (1.414g, 69.5% yield) after evaporation of solvent via reduced pressure. ^{1}H NMR (400 MHz, DMSO-d6) δ 4.85 (br. s, 1H), 4.76 (br. s, 1H), 4.35 (br. s, 1H), 4.12 (s, 2H), 3.50 (m, 4H), 3.36 (t, 2H), 3.27 (t, 2H).

Attempted synthesis of 1-methyl-4-silatranone (**3-9**):

N-glycolyldiethanolamine (0.100g) was combined with triethoxymethylsilane (0.109g, 0.122mL) and dissolved in tetrahydrofuran-d8 (2.1mL, 3 ampules) in a 50 mL round bottom flask fitted with a reflux condenser, magnetic stir bar, and N_2 inlet. Solution was stirred at room temperature for 72 hours followed by heating at 40°C for 72 hours, and finally was refluxed (66°C) for 1 addition week. Crude reaction solution was immediately analyzed for NMR and produced no reaction.

Attempted synthesis of 1-methyl-4-silatranone (**3-9**):

Triethoxymethylsilane (0.109g, 0.122mL) was combined with N-glycolyldiethanolamine (0.100g, 1eq.) neat in a 100mL round bottom flask and attached to a rotary evaporator. Crude white solid resulted from reduced pressure and was dissolved in a 1:1 mix of $CDCl_3$ and CD_3OD for NMR analysis. ^{1}H NMR (400 MHz, $CDCl_3$, CD_3OD) δ 4.31 (s, 2H), 3.90 (m, 4H), 3.71 (m, 9H), 3.25 (m, 4H), 3.00 (m, 9H), -0.15 (s, 2H).

Attempted synthesis of 1-propyl-4-silatranone (**3-7**):

1,1-dichlorosilacyclobutane (0.0865g, 0.0727mL) was combined with N-glycolyldiethanolamine (0.100g, 1eq.) neat in a 100mL round bottom flask and attached to a rotary evaporator. Fuming of HCl byproduct was observed. Crude white solid resulted from reduced pressure and was dissolved in a 1:1 mix of $CDCl_3$ and CD_3OD for NMR analysis. Only crude NMR was run for this sample as it contained a lot of oligomeric material and was difficult to characterize/purify.

Synthesis of 2-Hydroxy-N,N-Bis(2-hydroxyethyl)acetamide/N-glycolyldiethanolamine (**3-5**)[79]:

This compound was synthesized according to the procedure of Daryaee et al[79] with an improved procedure[80] for synthesis of the acetonide starting material. Glycolic acid acetonide (0.145 g) was dissolved in dichloromethane (DCM) (5 mL) with dissolved diethanolamine (0.2 g) and reacted for 1 hour at room temperature. The product **3-5** was a clear yellow oil that was purified using column chromatography (silica gel, methanol: ethyl acetate, 4:3). ^{1}H NMR (400 MHz, $CDCl_3$) δ 3.32-3.34 (2H, XX' of AA'XX'), 3.60-3.62 (2H, XX' of AA'XX'), 3.77-3.80 (2H, AA' of AA'XX'), 3.93-3.96 (2H, AA' of AA'XX'), 4.27 (2H, s). ^{13}C NMR (100 MHz, $CDCl_3$) δ 31.15, 42.79, 50.57, 60.36, 61.15, 200.04. IR (neat): 3246, 2872, 1590, 1063, 844 cm^{-1}. IR (CH_3CN): 3623, 1631, 1037, 832 cm^{-1}.

Synthesis of N,N-Bis(2-hydroxyethyl)acetamide (**4-1**)[76]:

Diethanolamine (12.1 g, 115 mmol) was added to a round bottom flask followed by acetic anhydride (11.2 mL, 115 mmol) and THF (10 mL). The mixture was refluxed for 1 hour, then cooled to room temperature and concentrated. A small portion of the mixture was dissolved in $CDCl_3$ then treated with a few powdered granules of KOH and stirred for 10 minutes to neutralize acetic acid. Sodium sulfate was added and the mixture filtered through a glass wool plug to afford pure **4-1** (39% yield). ^{1}H NMR (400 MHz, $CDCl_3$) δ 2.16 (3H, s), 3.48-3.50 (2H, XX' of AA'XX'), 3.52-3.54 (2H, XX' of AA'XX'), 3.77-3.79 (2H, AA' of AA'XX'), 3.80-3.82 (2H, AA' of AA'XX'). ^{13}C NMR (100 MHz, $CDCl_3$) δ 22.29, 50.62, 53.39, 60.77, 61.41, 173.31. IR (neat): 3347, 2934, 1606, 1037 cm^{-1}. IR (CH_3CN): 3092, 1639, 1037 cm^{-1}.

Synthesis of N,N-Diethyl-2-hydroxyacetamide (**4-3**)[80]:

This compound had been prepared earlier and characterized by Andreas *et al*.[15] *N,N*-Diethyl-2-bromoacetamide (0.182 mL, 1.3 mmol) was added to a round bottom flask with a magnetic stir bar. 1 M NaOH (10 mL) was added to the flask and stirred at room temperature for 30 hours. The mixture was extracted with ethyl acetate (3 x 25 mL). The combined organic layers were washed with water and brine, dried, and concentrated under reduced pressure to afford **4-3** (51 mg, 31% yield). ^{1}H NMR (400 MHz, $CDCl_3$) δ 1.16 (3H, t, J=7.2 Hz), 1.19 (3H, t, J=7.2 Hz), 3.17 (2H, q, J=7.2 Hz), 3.45 (2H, q, J = 7.2 Hz), 4.15 (2H, s). ^{13}C NMR (100 MHz, $CDCl_3$) δ 13.08, 14.05, 40.17, 40.66, 59.87, 170.77. IR (neat): 3407, 2975, 1633, 1076 cm^{-1}. IR (CH_3CN): 3092, 1647, 1081, 1037 cm^{-1}.

Synthesis of N,N-Bis[2-(acetyloxy)ethyl]acetamide (**4-4**)[76]:

Diethanolamine (11.13 g, 95 mmol), was placed in a round bottom flask with THF (25 mL) and a magnetic stir bar. The flask was cooled to 0^{o}C and acetic anhydride (10.3 mL, 98 mmol) was added dropwise by pipet. The mixture was then refluxed at 90^{o}C for 1 hour and 15 minutes. The reaction was stirred for another 4 hours at room temperature, then concentrated under reduced pressure. The resulting oil was dissolved in ethyl acetate and washed with 1M HCl, 1M NaOH, and brine, dried and concentrated to give **4-4** (4% yield). ^{1}H NMR (400 MHz, $CDCl_3$) δ 2.06 (3H, s), 2.08 (3H, s), 2.15 (3H, s), 3.60-3.65 (4H, XX' of AA'XX'), 4.20-4.23 (4H, AA' of AA'XX'). ^{13}C NMR (100 MHz, $CDCl_3$) δ 20.58, 20.69, 21.30, 45.15, 48.06, 61.60, 62.04, 170.47, 170.63, 171.02. IR (neat): 2959, 1734, 1638, 1234, 1034 cm^{-1}. IR (CH_3CN): 1739, 1643, 1234, 1037 cm^{-1}.

Synthesis of imine trinitrile (**5-3**):

Combined acetaldehyde (17mL), toluene (30mL), K_2CO_3 (2.5g), and Na_2SO_4 into a 250mL Schlenk flask. Fitted Schlenk flask with a septum and purged with N_2 atmosphere. The flask was placed in an ice bath and cyclohexylamine (40mL) was syringe loaded into the flask slowly. Once additions were completed, solution was allowed to stir for 30 minutes. Syringed amber liquid/ top organic layer into a glass pressure reactor with acrylonitrile (50mL). Sealed pressure reactor with a greased cap and heated glass pressure reactor in an oil bath behind a blast shield for 4 hours at 170°C. Solution turned dark black. Reaction was depressurized and cooled to 0°C slowly and Et_2O (100mL) was used to precipitate into a yellow crude solid and was vacuum filtered into crude imine trinitrile (22.4g, 51% yield). ^{1}H NMR (500 MHz, $CDCl_3$) δ 7.43 (s, 1H), 3.08 (m, 1 H), 2.34 (t, J=7.94Hz, 6H), 1.93 (t, J=7.94Hz, 6H), 1.78-1.30 (m, 10H). ^{13}C NMR (125 MHz, $CDCl_3$) δ 160.30, 119.09, 68.36, 45.78, 36.05, 30.77, 25.44, 24.33, 11.88.

Synthesis of aldehyde trinitrile (**5-4**):

Imine trinitrile (22.4g) was placed into a 250mL round bottom flask and was combined with H_2O (130mL) and concentrated HCl (5mL). Solid does not dissolve leaving a suspension. A reflux condenser and N_2 inlet were attached to the flask and was refluxed for 30 minutes. Cooled solution slightly and hot vacuum filter off black impurities. Placed the filtrate in an ice bath to precipitate aldehyde as a yellow solid. Vacuum filtered to isolate solid product as a yellow powder (9.8g, 95% yield). ^{1}H NMR (500 MHz, DMSO-d6) δ 9.44 (s, 1H), 2.44 (t, J=8.09Hz, 6H), 1.86 (t, J=8.09Hz, 6H). ^{13}C NMR (125 MHz, DMSO-d6) δ 203.31, 122.86, 52.06, 28.48, 14.23.

Synthesis of alcohol trinitrile (**5-5**):

Aldehyde (9.8g) was dissolved in methanol (50mL) in a 250mL round bottom flask with a magnetic stir bar in an ice bath. $NaBH_4$ (1.82g, 1eq.) was added to the solution and was allowed to stir overnight at 0°C to room temperature. Solution becomes homogeneous as it reacts. Quenched reaction with H_2O (50mL). 3M HCl was added to the solution until pH=1. Methanol was rotovapped off to yield product floating on remaining H_2O. The aqueous solution was extracted with dichloromethane (3 x 75mL) and organic extracts were dried with Na_2SO_4. Dichloromethane was evaporated via rotovap and high vacuum to yield alcohol trinitrile as an orange oil (9.7g, 99% yield). ^{1}H NMR (500 MHz, $CDCl_3$) δ 3.55 (s, 2H), 2.42 (t, J=7.94Hz, 6H), 1.87 (br. s, 1H), 1.77 (t, J=7.94Hz, 6H). ^{13}C NMR (125 MHz, $CDCl_3$) δ 120.11, 65.98, 40.23, 29.87, 13.09.

Synthesis of TBS protected alcohol trinitrile (**5-6**):

Alcohol trinitrile (9.70g), DMAP (5.77g, 1eq.), DIPEA (8.08mL, 1eq.), and dichloromethane (50mL) were combined in a 500mL round bottom flask with a magnetic stir bar. TBS-OTf (11.94mL, 1.1eq.) was added slowly to the flask and fuming was observed. A condenser with N_2 inlet was quickly attached and the solution was refluxed for 48 hours. Solution was transferred to separatory funnel and was washed with 1M HCl (3 x 25mL), 15% NaOH (2 x 10mL), brine (2 x 25mL), and H_2O (1 x 25mL). The organic layer was dried with Na_2SO_4. Dichloromethane was evaporated via rotovap and high vacuum to yield a white solid TBS protected alcohol trinitrile (5.95g, 70% yield). ^{1}H NMR (500 MHz, $CDCl_3$) δ 3.38 (s, 2H), 2.35 (t, J=7.63Hz, 6H), 1.73 (t,

J=8.24Hz, 6H), 0.90 (s, 9H), 0.08 (s, 6H). ^{13}C NMR (125 MHz, $CDCl_3$) δ 117.67, 65.81, 39.40, 30.20, 26.57, 20.83, 12.65, -4.34.

Synthesis of TBS protected alcohol triamine (**5-7**):

TBS protected alcohol trinitrile (0.502g, 1eq.) was dissolved in a 250mL Erlenmeyer flask in methanol (95mL) under gentle heating 40°C while stirring. Raney nickel (0.723g, 5.30eq) was added to the solution. Solution was removed from heat and placed in an ice bath. Separately, a solution of 8M NaOH (15mL) and $NaBH_4$ (0.598g, excess) was prepared in a 100mL beaker. 8M NaOH/$NaBH_4$ solution was added into the Raney nickel/TBS protected alcohol trinitrile solution in portions every 10 min over the course of 1 hour to maintain a reaction temperature of 60°C. Solution effervesces upon addition. Once all $NaBH_4$/NaOH was added, methanol (5mL) was used to rinse the 100mL beaker to complete the transfer. Reaction solution was removed from the ice bath once bubbling ceased and was heated in a warm water bath at 40°C for 72 hours to ensure all nitrile groups were reduced. Upon completion, solution was transferred to a round bottom flask and methanol was evaporated via rotovap. H_2O (30mL) was added to the round bottom flask. Solution was extracted with dichloromethane (3 x 50mL) and the organic extract was dried with Na_2SO_4. Dichloromethane was evaporated via rotovap and high vacuum to yield TBS protected alcohol triamine (0.450g, 86% conversion via NMR) as a yellow oil. ^{1}H NMR (500 MHz, $CDCl_3$) δ 3.26 (s, 2H), 2.64 (t, J=7.01Hz, 6H), 1.33 (m, 7H, NH, CH_2), 1.18 (m, 7H, NH, CH_2), 0.86 (s, 9H), 0.00 (s, 6H). ^{13}C NMR (125 MHz, $CDCl_3$) δ 67.11, 45.00, 39.26, 32.97, 28.09, 25.84, 13.14, -5.68.

LIST OF REFERENCES

1. Vogel, E.; Günther, H. Benzene Oxide-Oxepin Valence Tautomerism. *Angew. Chem. Int. Ed. Engl*. **1967**, 6, 385–401.

2. Davies, S.G.; Whitham, G.H. Benzene Oxide-Oxepin Oxidation to Muconaldehyde. *J. Chem. Soc. Perkin Trans*. **1977**, 1, 1346–1347.

3. Witz, G.; Latriano, L.; Goldstein, B.D. Metabolism and Toxicity of trans, trans-Muconaldehyde, an Open-Ring Microsomal Metabolite of Benzene. *Environ. Health Persp*. **1989**, 82, 19–22.

4. Snyder, R.;Witz, G.; and Goldstein, B.D. The Toxicology of Benzene. *Environ. Health Persp*. **1993**, 100, 293–306.

5. Snyder, R.; Hedli, C.C. An Overview of Benzene Metabolism. *Environ. Health Persp*. **1996**, 104, 1165–1171.

6. Snyder, R. Benzene's Toxicity: A Consolidated Short Review of Human and Animal Studies by H.A. Khan. *Hum. Exp. Toxicol*. **2007**, 26, 687–696.

7. Lovern, M.R.; Turner, M.J.; Meyer, M.; Kedderis, G.L.; Bechtold,W.E.; Schlosser, P.M. Identification of Benzene Oxide as a Product of Benzene Metabolism by Mouse, Rat, and Human Liver Microsomes. *Carcinogenesis*. **1997**, 18, 1695–1700.

8. Henderson, A.P.; Barnes, M.L.; Bleasdale, C.; Cameron, R.; Clegg, W.; Heath, S.L.; Lindstrom, A.B.; Rappaport, S.M.;Waidyanatha, S.;Watson,W.P.; et al. Reactions of Benzene Oxide with Thiols including Glutathione. *Chem. Res. Toxicol*. **2005**, 18, 265–270.

9. Monks, T.J.; Butterworth, M.; Lau, S.S. The Fate of Benzene Oxide. *Chem. Biol. Interact*. **2010**, 184, 201–206.

10. Zarth, A.T.; Murphy, S.E.; Hecht, S.S. Benzene Oxide is a Substrate for Glutathione S-Transferases. *Chem. Biol. Interact*. **2015**, 242, 390–395.

11. Weisel, C.P. Benzene Exposure: An Overview of Monitoring Methods and Their Findings. *Chem. Biol. Interact*. **2010**, 184, 58–66.

12. Tomida, I.; Nakajima, M.Z. The Chemistry of 3,5-Cyclohexadiene-1,2-diol VI. Metabolism of the Glycols and Muconic Dialdehyde. *Physiol. Chem*. **1960**, 318, 171–178.

13. Goldstein, B.D.; Witz, G.; Javid, J.; Amaruso, M.A.; Rossman, T.; Wolder, B. Muconaldehyde, a Potential Toxic Metabolite of Benzene Metabolism. *Adv. Exp. Med. Biol*. **1982**, 136 Pt A, 331–339.

14. Latriano, L.; Goldstein, B.D.;Witz, G. Formation of Muconaldehyde, an Open-Ring Metabolite of Benzene, in Mouse Liver Microsomes: An Additional Pathway for Toxic Metabolism. *Proc. Natl. Acad. Sci*. USA **1986**, 83, 8356–8360.

15. Grotz, V.L.; Ji, S.C.; Kline, S.A.; Goldstein, B.D.;Witz, G.Metabolismof Benzene and trans, trans-Muconaldehyde in the Isolated Perfused Rat Liver. *Toxicol. Lett*. **1994**, 70, 281–290.

16. Amin, D.P.; Witz, G. DNA-Protein Crosslink and DNA Strand Break Formation in HL-60 Cells Treated with trans, trans-Muconaldehyde, Hydroquinone, and Their Mixture. *Int. J. Toxicol*. **2001**, 20, 69–80.

17. Rivedal, E.; Witz, G.; Leithe, E. Gap Unction Intercellular Communication and Benzene Toxicity. *Chem. Biol. Interact*. **2010**, 184, 229–232.

18. Nakajima, T.; Wang, R.-S.; Elovaara, E.; Park, S.S.; Gelboin, H.V.; Hietanen, E.; Vainio, H. Monoclonal Antibody-Directed Characterization of Cytochrome P450 Isozymes Responsible for Toluene Metabolism in Rat Liver. *Biochem. Pharmacol*. **1991**, 41, 395–404.

19. Zhang, Z.H.; Goldstein, B.D.;Witz, G. Iron-Stimulated Ring-Opening of Benzene in a Mouse Liver Microsomal System: Mechanistic Studies and Formation of a New Metabolite. *Biochem. Pharmacol*. **1995**, 50, 1607–1617.

20. Klotz, B.; Volkamer, R.; Hurley, M.D.; Anderson, M.P.S.; Nielsen, O.J.; Barnes, I.; Imamura, T.; Wirtz, K.; Becker, K.H.; Platt, U.; et al. OH-Initiated Oxidation of Benzene. Part II. Influence of Elevated NOx Concentrations. *Phys. Chem. Chem. Phys*. **2002**, 4, 4399–4411.

21. Golding, B.T.; Kennedy, G.; Watson, W.P. Simple Synthesis of Isomers of Muconaldehyde and 2-Methylmuconaldehyde. *Tetrahedron Lett*. **1988**, 29, 5991–5994.

22. Golding, B.T.; Bleasdale, C.; MacGregor, J.O.; Nieschalk, J.; Pearce, K.; Watson,W.P. Chemistry of Muconaldehyde of Possible Relevance to the Toxicology of Benzene. *Environ. Health Perspect*. **1996**, 104, 1201–1209.

23. Greenberg, A.; Bock,C.W.; George,P.;Glusker, J.P. Energetics of the Metabolic Production of (E,E)-Muconaldehyde from Benzene via the Intermediates 2,3-Epoxyoxepin and (Z,Z)- and (E,Z)-Muconaldehyde: Ab Initio Molecular Orbital Calculations. *Chem. Res. Toxicol*. **1993**, 6, 701–710.

24. Rosner, P.; Wol_, C.; Tochtermann, W. Syntheses of Medium and Large Rings. III. Reactions of _,_' Hexano-Bridged Oxepins. *Chem. Ber*. **1982**, 115, 1162–1169.

25. Morgan, J.P.; Greenberg, A. Insights into the Formation and Isomerization of the Benzene Metabolite Muconaldehyde and Related Molecules: Comparison of Computational and Experimental Studies of Simple, Benzo-Annelated, and Bridged 2,3-Epoxyoxepins. *J. Org. Chem*. **2010**, 75, 4761–4768.

26. Greenberg, A.; Ozari, A.; Carlin, C.M. Reactions of 2,7-Dimethyloxepin with Dimethyldioxirane and Methyl(trifluoromethyl)dioxirane: Ring Opening and Probable Observation of the Intermediate "2,3-Epoxyoxepin". *Struct. Chem*. **1998**, 9, 223–236.

27. Bleasdale, C.; Cameron, R.; Edwards, C.; Golding, B.T. Dimethyldioxirane Converts Benzene Oxide/Oxepin into (Z,Z)-Muconaldehyde and sym-Oxepin Oxide: Modeling the Metabolism of Benzene and its Photooxidation Degradation. *Chem. Res. Toxicol*. **1997**, 10, 1314–1318.

28. Nauduri, D.; Greenberg, A. Direct Observation by 1H-NMR of 4,5-Benzoxepin-2,3-oxide and its Surprisingly Rapid Ring-Opening Rearrangement to 1H-2-Benzopyran-1-carboxaldehyde. *Tetrahedron Lett*. **2004**, 45, 4789–4793.

29. Golding, B.T.; Barnes, M.L.; Bleasdale, C.; Henderson, A.P.; Jiang, D.; Li, X.; Mutlu, E.; Petty, H.J.; Sadeghi, M.M. Modeling the formation and reactions of benzene metabolites. *Chem. Biol. Interact*. **2010**, 184, 196–200.

30. Morgan, J.P.; Greenberg, A. Curtin-Hammett Principle: Application to Benzene Oxide-Oxepin Tautomers. *Struct. Chem*. **2013**, 24, 1945–1956.

31. Greenberg, A.; Bock, C.W.; George, P.; Glusker, J.P. Mechanism of Metabolic Ring-Opening of Benzene and its Relation to Mammalian PAH Metabolism. *Polycycl. Aromat. Compd*. **1994**, 7, 123–128.

32. Boyd, D.R.; Sharma, N.D. The Changing Face of Arene Oxide-Oxepine Chemistry. *Chem. Soc. Rev*. **1996**, 25, 289–296.

33. Spartan 14, 1.1.0; Wavefunction, Inc.: Irvine, CA, USA, 2014.

34. Suzuki, J.; Watanabe, T.; Suzuki, S. Formation of Mutagens by Photochemical Reaction of 2-Naphthol in Aqueous Nitrile Solution. *Chem. Pharm. Bull*. **1988**, 36, 2204–2211.

35. Hauser, F.M.; Baghdanov, V.M. A New Procedure for Regiospecific Syntheses of Benzopyran-1-ones. *J. Org. Chem*. **1988**, 53, 4676–4681.

36. Thazana, N.; Worayuthakarn, R.; Kradanrat, P.; Hohn, E.; Young, L.; Ruchirawat, S. Copper(I)-Mediated and Microwave-AssistedCaryl-Carboxylic Coupling: Synthesis of Benzopyranones and Isolamellarin Alkaloids. *J. Org. Chem*. **2007**, 72, 9379–9382.

37. Cariou, M.; Carlier, R.; Simonet, J. Enamines and Enediamines: Synthesis and Anodic Oxidation. Application to the Formation of Novel Heterocycles. *Bull. Soc. Chim. France* **1986**, 67, 81–792.

38. Fukuyama, K.; Fujita, H.; Tokushima, S.; Tsukihara, T.; Katsube, Y.; Motoyama, T. Crystal and Molecular Structures of the Adduct Fluoreno[9,1-bc]pyrylium-3-olate with Methyl Cinnamate and the Dimer of Fluoreno[9,1-bc]-pyrylium-3-olate. *Bull. Chem. Soc. Jpn*. **1986**, 59, 255–258.

39. Cambie, R.C.; Joblin, K.N.; Preston, A.F. Chemistry of the Podocarpaceae. XLIII. Utilization of the 8_,13-epoxylabd-14-ene and Related Compounds for the Preparation of Ambergris-Type Compounds. *Aust. J. Chem*. **1972**, 25, 1767–1778.

40. Tochtermann,W.; Rösner, P. Eine Möglichkeit zur Ringerweiterung des Cyclooctins: Synthese und Reaktionenvon 3,6-Hexano-oxepin-4,5-dicarbonsäure-diethylester. *Tetrahedron Lett*. **1980**, 21, 4905–4908.

41. Stok, J.E.; Chow, S.; Krenske, E.H.; Soto, C.F.; Matyas, C.; Poirier, R.A.; Williams, C.M.; De Voss, J.J. Direct Observation of an Oxepin from a Bacterial Cytochrome P450-Catalyzed Oxidation. *Chem. Eur. J*. **2016**, 22, 4408–4412.

42. Zeigler, G.R. Mechanisms of Photochemical Reactions in Solution. LVII. Photorearrangement of 1,4-Epoxy-1,4-dihydronaphthalene to Benzo[f]oxepin. *J. Am. Chem. Soc*. **1969**, 91, 446.

43. Paquette, L.A. and Barrett, J.H. 2,7-Dimethyloxepin. *Org. Synth*. **1969**, 49, 62.

44. Rabideau, Peter W. and Burkholder, E. Metal-ammonia reduction and reductive alkylation of polycyclic aromatic compounds: nature of the anionic intermediates. *J. Org Chem*. **1978**, *43*, 4283-4288.

45. Cho, T.H.; Rose, R.L.; and Hodgson, E. In vitro metabolism of naphthalene by human liver microsomal cytochrome P450 enzymes. *Drug Metabolism and Disposition*. **2006**, 34, 176-183.

46. Klotz, B.; Barnes, I.; Becker, K.H.; and Golding, B.T. Atmospheric chemistry of benzene oxide/oxepin. *J. Chem. Soc., Faraday Trans*., **1997**, 93(8), 1507-1516.

47. Snyder, R.; Witz, G.; and Goldstein, B.D. The toxicology of benzene. Environmental Health Perspectives. **1993**, 100, 293-306.

48. Weaver-Guevara, H.M.; Fitzgerald, R.W.; Cote, N.A.; and Greenberg, A. Cytochrome P450 can epoxidize an oxepin to a reactive 2,3-epoxyoxepin intermediate: potential insights into metabolic ring-opening of benzene. *Molecules*. **2020**, 25, 4542.

49. Li, S-R.; Chen, H-M.; Chen, L-Y.; Tsai, J-C.; Chen, P-Y.; Hsu, S. C-N.; and Wang, E-C. Synthesis of 1-benzoxepin-5-ones (ols) from salicylaldehydes via ring-closing metathesis. *ARKIVOC*. **2008**, 2, 172-182.

50. Yamaguchi, S.; Tsuchida, N.; Miyazawa, M.; and Hirai, Y. Synthesis of Two Naturally Occurring 3-Methyl-2,5-dihydro-1-benzoxepin Carboxylic Acids. *J. Org. Chem.* **2005**, *70*, 7505-7511.

51. Das, S.K. and Panda, G. Stereoselective approach to aminocyclopentitols from Garner aldehydes. *RSC Adv.*, **2013**, 3, 9916–9923.

52. Morgan, J. P.; Weaver-Guevara, H.M.; Fitzgerald, R.W.; Dunlap-Smith, A.; and Greenberg, A. Ab initio computational study of 1-methyl-4-silatranone and attempts at its conventional synthesis. *Struct. Chem*. **2017**, 28, 327.

53. Morgan, J.P. and Greenberg, A. Novel bridgehead bicyclic lactams: (a) Molecules predicted to have O-protonated and N-protonated tautomers of comparable stability; (b)

hyperstable lactams and their O-protonated tautomers. *J. Chem. Thermodynamics*. **2014**, 73, 206-212.

54. Morgan, J.P. and Greenberg, A. N-protonated and O-protonated tautomers of 1-azabicyclo[3.3.1]nonan-2-one: observation of individual 13C-NMR carbonyl peaks and comparisons with protonated tautomers of planar and other distorted lactams. *J. Phys. Org. Chem.* **2012**, 25, 1422-1428.

55. Weaver-Guevara, H.M.; Fitzgerald, R.W.; and Greenberg, A. Rotational barriers in five related amides. *Can. J. Chem.* **2017**, 95, 271-277.

56. Frye, C.L.; Vogel, G.E.; and Hall, J.A. Triptych-Siloxazolidines: pentacoördinate bridgehead silanes resulting from transanular interaction of nitrogen and silicon. *J. Am. Chem. Soc.* **1961**, 83, 4, 996–997.

57. Greenberg, A.; Plant, C.; and Venanzi, C.A. Ab initio molecular orbital study of 1-methylsilatrane and model compounds. *Journal of Molecular Structure (Theochem)*. **1991**, 234, 291-301.

58. Dunlap-Smith A. Computational chemistry of silatranes. Testing the limits of modern Density Functional Theory. Dissertation for the Bachelor of Science in Chemistry, **2016**, University of New Hampshire, Durham, NH.

59. Morgan, J.P. Two studies in bio-organic chemistry and toxicology. Doctoral Dissertation, **2014**, University of New Hampshire, Durham, New Hampshire.

60. Puri, J.K.; Singh, R.; and Chahal, V.K. Silatranes: a review on their synthesis, structure, reactivity and applications. *Chem. Soc. Rev*. **2011**, 40, 1791–1840.

61. Gordon, M.S.; Carroll, M.T.; Jensen, J.H.; Davis, L.P., Burggraf, L.W.; and Guidry, R.M. Nature of the SI-N Bond in Silatranes. *Organometallics*. **1991**, 10, 2657-2660.

62. Chandrasekaran, A.; Day, R.O.; and Holmes, R.R. A New Class of Silatranes: Structure and Dynamic NMR Behavior. *J. Am. Chem. Soc*. **2000**, 122, 1066-1072.

63. Baret, T.P.; Imbert, D.; Pierre, J.-L.; and Serratrice, G. Partition Coefficients (Free Ligands and their Iron(Ill) Complexes) and Lipophilic Behavior of New Abiotic Chelators. Correlation to Biological Activity. *Bioorganic & Medicinal Chemistry Letters*. **1999**, 9, 3035-3040.

64. Hermes-Lima, M.; Ponka, P.; and Schulman, H.M. The iron chelator pyridoxal isonicotinoyl hydrazone (PIH) and its analogues prevent damage to 2-deoxyribose mediated by ferric iron plus ascorbate. *Biochimica et Biophysica Acta*. **2000**, 1523, 154-160.

65. Caris, C.; Baret, P.; Beguin, C.; Serratrice, G.; Pierre, J.-L.; and Laulherel, J.-P. Metabolization of iron by plant cells using O-Trensox, a high-affinity abiotic iron-chelating agent. *Biochem. J*. **1995**, 312, 879-885.

66. Imbert, D.; Thomas, F.; Baret, P.; Serratrice, G.; Gaude, D.; Pierre, J.-L.; and Laulhe`re, J.-P. Synthesis and iron(III) complexing ability of CacCAM, a new analog of enterobactin possessing a free carboxylic anchor arm. Comparative studies with TRENCAM. *New J. Chem*. **2000**, 24, 281-288.

67. d'Hardemare, A.M.; Torelli, S.; Serratrice, G.; and Pierre, J.-L. Design of iron chelators: syntheses and iron (III) complexing abilities of tripodal tris-bidentate ligands. *BioMetals*. **2006**, 19, 349–366.

68. Baret, P.; Beaujolais, V.; Be´guin, C.; Gaude, D.; Pierre, J.-L.; and Serratrice, G. Towards New Iron(III) Chelators: Synthesis and Complexing Ability of a Water-Soluble Tripodal Ligand Based on 2,29-Dihydroxybiphenyl Subunits. *Eur. J. Inorg. Chem*. **1998**, 613-619.

69. Pierre, J.-L.; Baret, P.; and Serratrice, G. Hydroxyquinolines as Iron Chelators. *Current Medicinal Chemistry*. **2003**, 10, 1077-1084.

70. Moniz, T.; Dias da Silva, D.; Carmo, H.; de Castro, B.; Bastos, M.L.; Rangel, M. Insights on the relationship between structure vs. toxicological activity of antibacterial rhodamine-labelled 3-hydroxy-4-pyridinone iron(III) chelators in HepG2 cells. *Interdiscip Toxicol*. **2018**, 11, 3, 189-199.

71. Kennedy, D. P.; DiPasquale, A. G.; Rheingold, A. L.; and Planalp, R. P. Ni(II)-Mediated Synthesis of the Novel Tripodal Aminopyridyl Ligand Tamepyr: Coordination Geometry and Rigidity of Complexes with the Divalent 3d Metals Fe – Zn and with In(III). *Polyhedron*. **2007**, 26, 197.

72. Abbate, V.; Reelfs, O.; Hider, Robert C.; Pourzand, C. Design of novel fluorescent mitochondria-targeted peptides with iron-selective sensing activity. *Biochem. J.* **2015,** 469, 3, 357.

73. Zhao, K.; Zhao, G. M.; Wu, D.; Soong, Y.; Birk, A. V.; Schiller, P. W.; Szeto, H. H. Cell-permeable peptide antioxidants targeted to inner mitochondrial membrane inhibit mitochondrial swelling, oxidative cell death, and reperfusion injury. *J. Biol. Chem*. **2004**, 279, 33, 34682-34690.

74. Berezowska, I.; Chung, N. N.; Lemieux, C.; Zelent, B.; Szeto, H. H.; Schiller, P. W. Highly potent fluorescent analogues of the opioid peptide [Dmt1]DALDA. *Peptides* **2003**, 24, 8, 1195-1200.

75. Dixon, S.J. Lemberg, K.M. Lamprecht, M.R.; Skouta, R.; Zaitsev, E.M.; Gleason, C.E.; Patel, D.N.; Bauer, A.J.; Cantley, A.M.; Yang, W.S.; Barclay Morrison, B.; and Stockwell, B.R. Ferroptosis: an iron-dependent form of nonapoptotic cell death. *Cell*. **2012,** 149, 5, 1060-1072.

76. Aitken, R.A.; Smith, M.H.; and Wilson, H.S. Variable temperature ^{1}H and ^{13}C NMR study of restricted rotation in N,N-bis(2-hydroxyethyl)acetamide. *J. Mol. Struct*. **2016**, 1113, 171.

77. Amman, C.; Meier, P.; Merbach, A. E. A simple multinuclear NMR thermometer. *J. Magn. Reson*. **1982**, 46, 319-321.

78. Boyoko, V. I.; Rodik, R. V.; Severenchuk, I. N.; Voitenko, Z. V.; Kalchenko, V. I. A Novel Method for the Synthesis of 2,2-Dimethyl-1,3-dioxolan-4-one, and Its Reactions with Secondary Amines. *Synthesis*. **2007**, 14, 2095-2096.

79. Daryaee, F.; Kobarfard, F.; Khalaj, A.; Farnia, P. Synthesis and evaluation of in vitro anti-tuberculosis activity of N-substituted glycolamides. *Eur. J. Med. Chem.* **2009**, 44, 289-295.

80. Crank, G.; Khan, H. R. Formation of Thioamide Derivatives from Reactions of Isothiocyanates with Oxazol-2-amines. *Aust. J. Chem*. **1985**, *38*, 447-458.

81. Reich, H. J. WINDNMR: Dynamic NMR Spectra for Windows. *J. Chem. Educ*. **1995**, 72, 1086.

82. Lv, H.; Shang, P. The significance, trafficking and determination of labile iron in cytosol, mitochondria and lysosomes. *Metallomics*. **2018**, 10, 7, 899-916.

83. Wisnovsky, S.; Lei, E. K.; Jean, S. R.; Kelley, S. O., Mitochondrial Chemical Biology: New Probes Elucidate the Secrets of the Powerhouse of the Cell. *Cell Chem. Biol*. **2016**, 23, 8, 917-927.

84. Childers, M. L.; Cho, J.; Regino, C. A. S.; Brechbiel, M. W.; DiPasquale, A. G.; Rheingold, A. L.; Torti, S. V.; Torti, F. M.; Planalp, R. P. Influence of ligand structure on Fe(II) spin-state and redox rate in cytotoxic tripodal chelators. *J. Inorg. Biochem*. **2008**, 102, 1, 150-156.

APPENDIX

^{1}H NMR (400 MHz, $CDCl_3$) δ 7.10 (m, 4H), 5.91 (t, 2H), 3.40 (d, 4H).

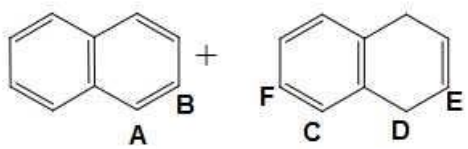

1-1

1-2

II

^{1}H NMR (400 MHz, $CDCl_3$) δ 7.14 (m, 2H), 7.04 (m, 2H), 3.48 (m, 2H), 3.31 (d, J=16.16Hz, 2H), 3.17 (d, J=13.84Hz, 2H).

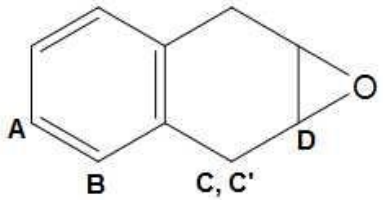

1-3

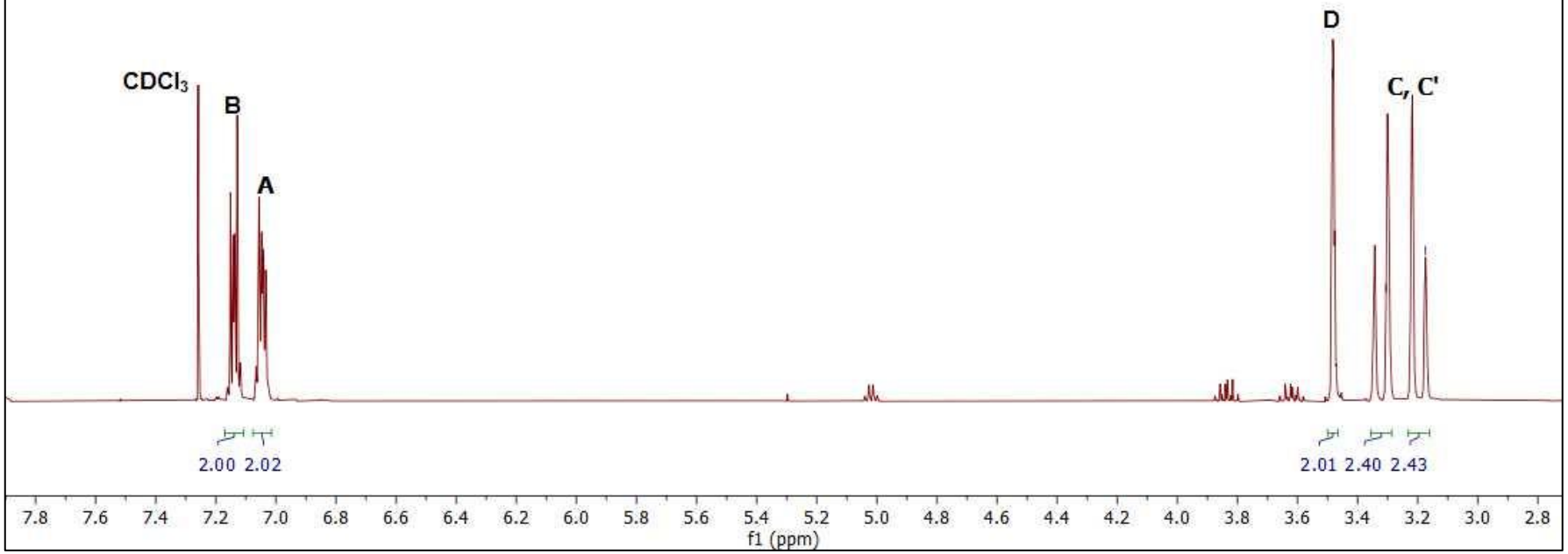

III

^{1}H NMR (400 MHz, $CDCl_3$) δ 8.08 (dd, 1H), 7.68 (dt, 1H), 7.53 (dt, 1H), 7.25 (dd, 1H), 5.54 (d, 1H), 3.78 (t, 1H), 3.65 (t, 1H), 3.29 (d, 2H).

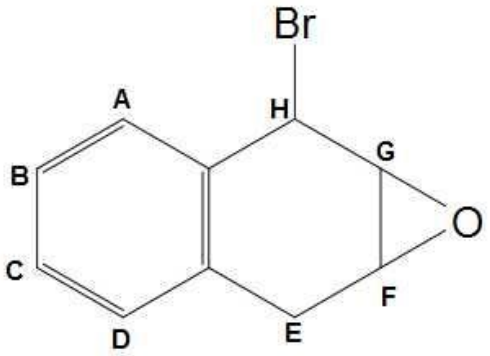

1-4

IV

^{1}H NMR (400 MHz, $CDCl_3$) δ 6.90 (m, 2H), 6.63 (m, 2H), 5.66 (d, J=7.52Hz, 2H), 5.05 (d, J=8.20Hz, 2H).

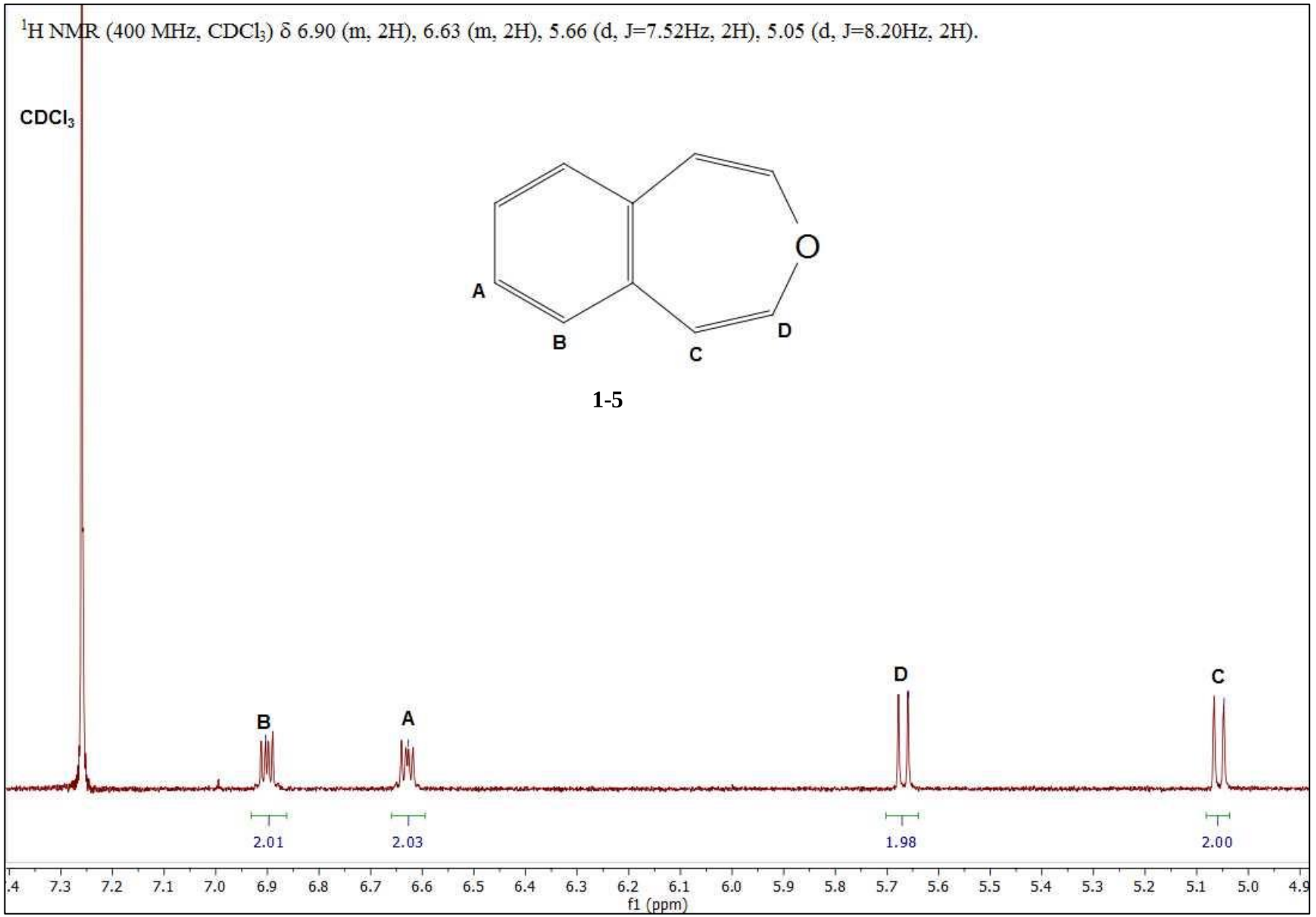

1-5

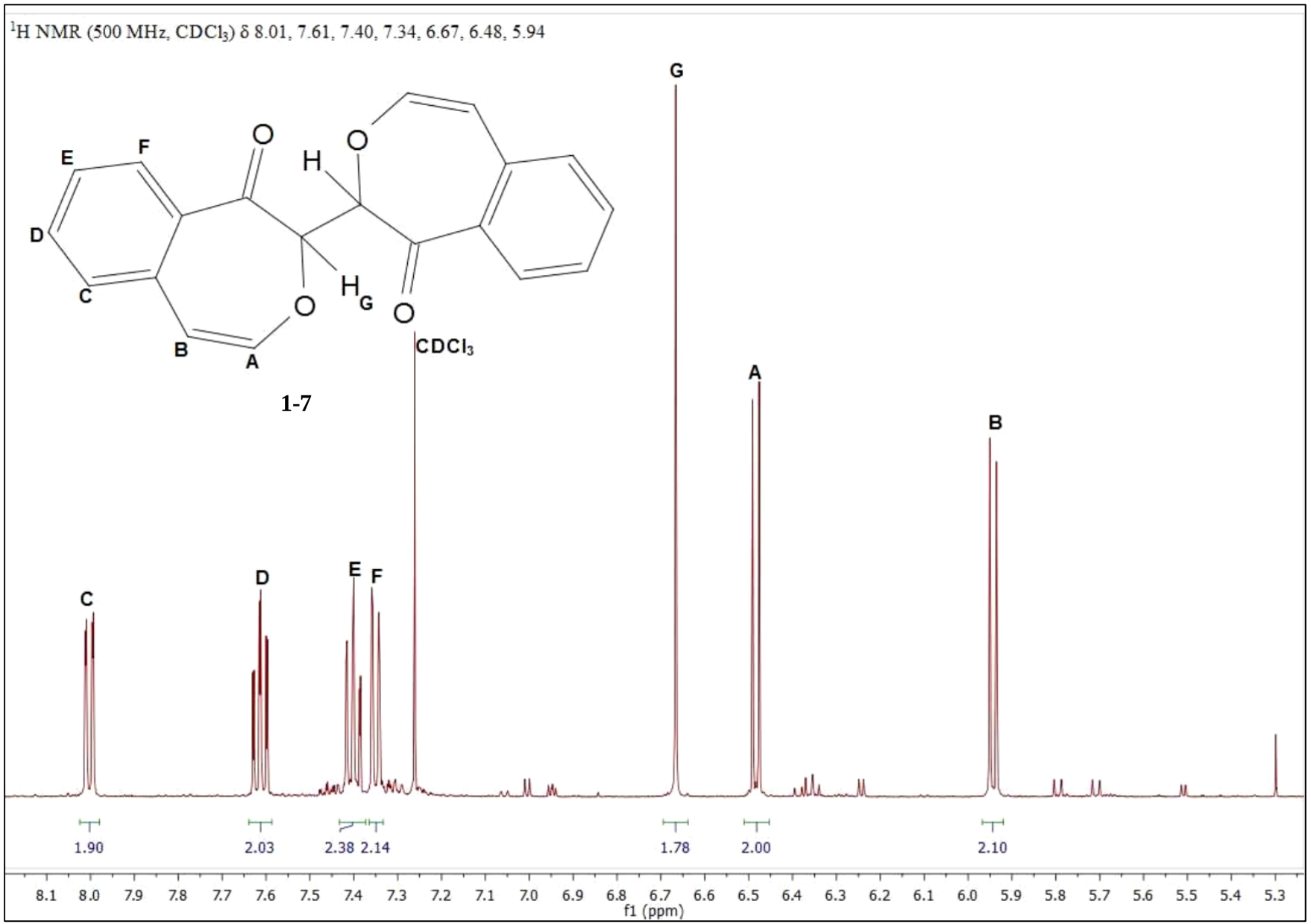
^{1}H NMR (500 MHz, $CDCl_3$) δ 8.01, 7.61, 7.40, 7.34, 6.67, 6.48, 5.94
G
A
B
C
D
E
F
$CDCl_3$
1.90
2.03
2.38
2.14
1.78
2.00
2.10
f1 (ppm)

1-7

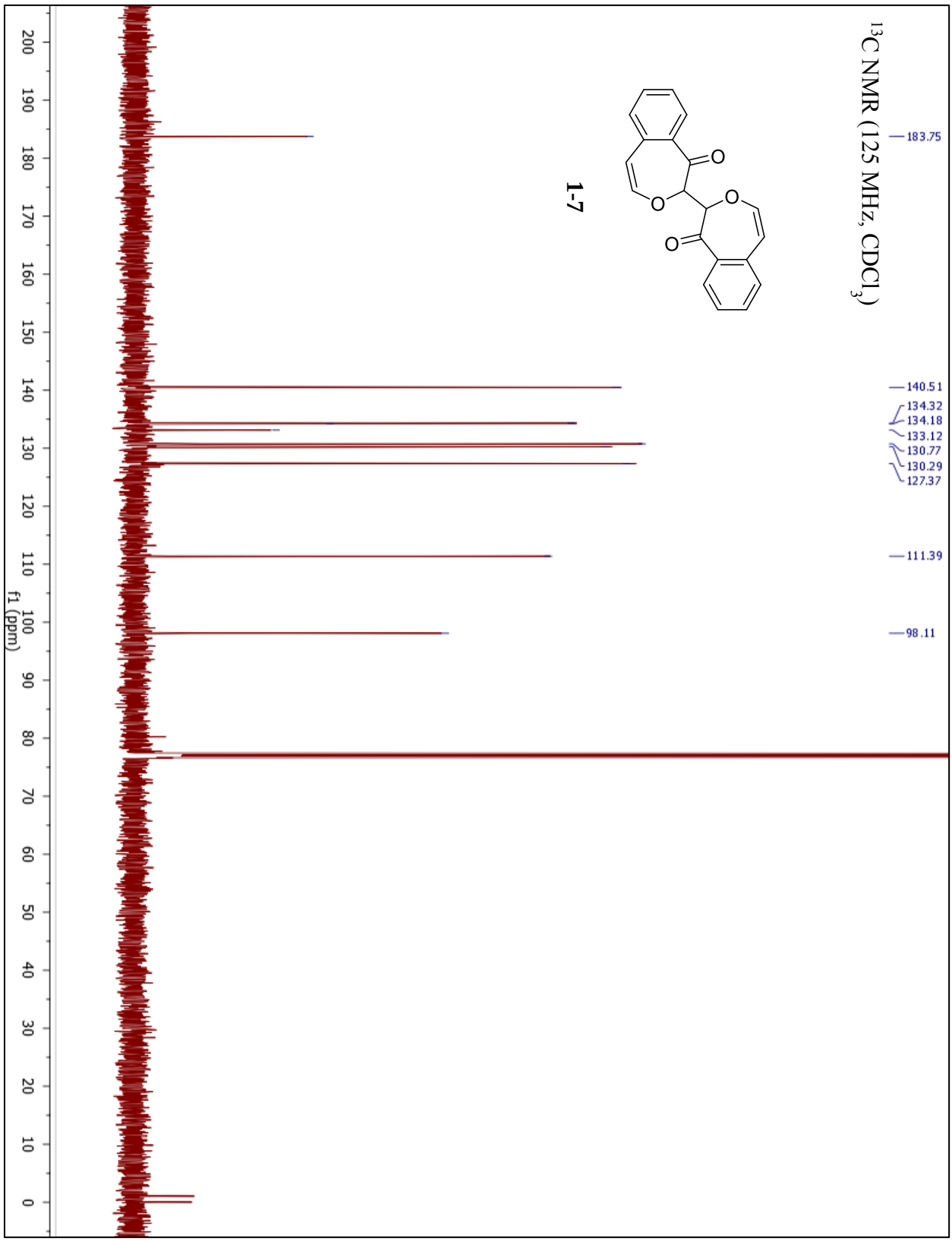
^{13}C NMR (125 MHz, CDCl$_3$)
183.75
140.51
134.32
134.18
133.12
130.77
130.29
127.37
111.39
98.11
1-7
O
O
O
O
f1 (ppm)
200
190
180
170
160
150
140
130
120
110
100
90
80
70
60
50
40
30
20
10
0

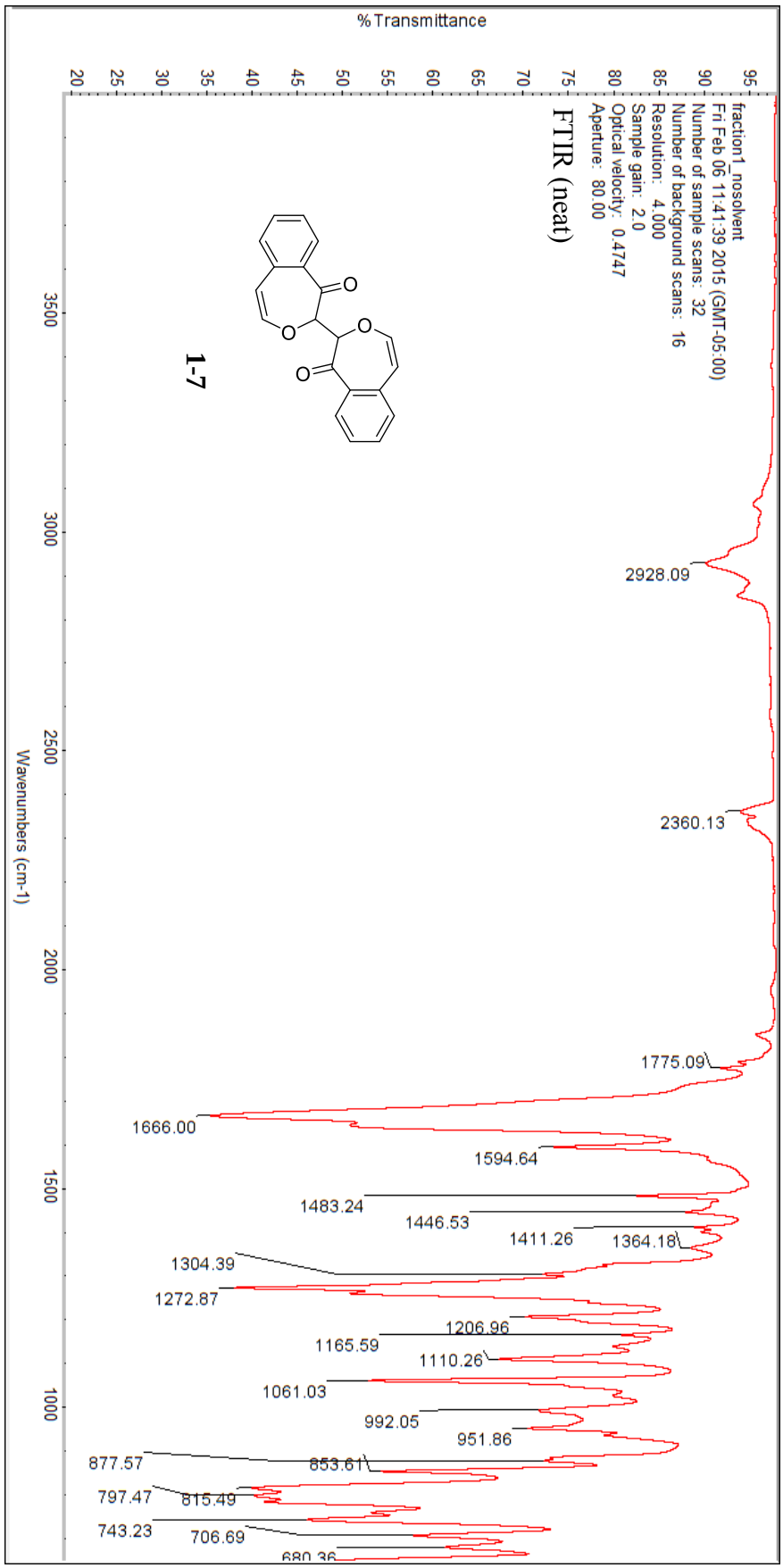
% Transmittance
Wavenumbers (cm-1)
FTIR (neat)
fraction1_nosolvent
Fri Feb 06 11:41:39 2015 (GMT-05:00)
Number of sample scans: 32
Number of background scans: 16
Resolution: 4.000
Sample gain: 2.0
Optical velocity: 0.4747
Aperture: 80.00
1-7
2928.09
2360.13
1775.09
1666.00
1594.64
1483.24
1446.53
1411.26
1364.18
1304.39
1272.87
1206.96
1165.59
1110.26
1061.03
992.05
951.86
877.57
853.61
797.47
815.49
743.23
706.69
680.36

COSY (500 MHz, $CDCl_3$)

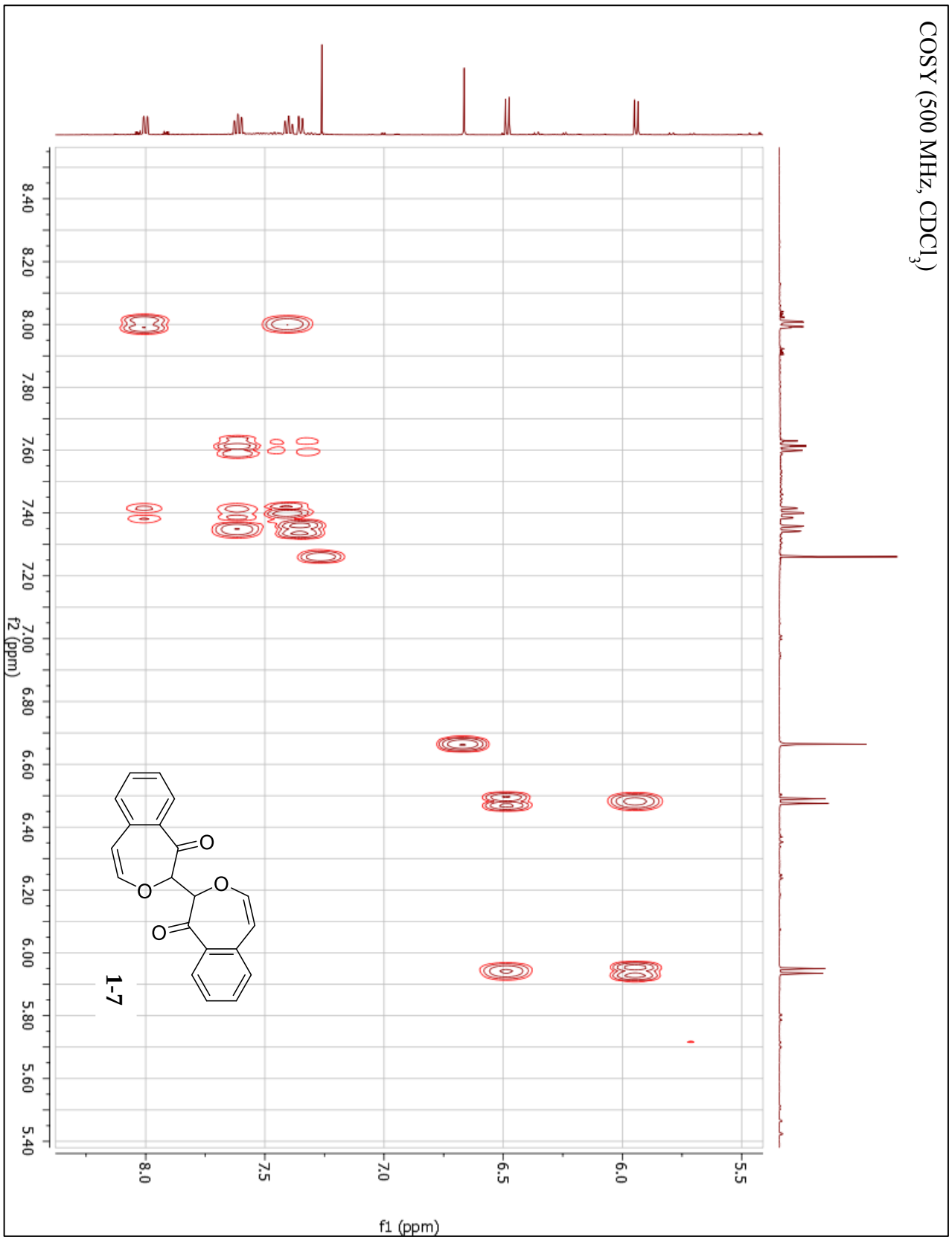

NOESY (500 MHz, $CDCl_3$)

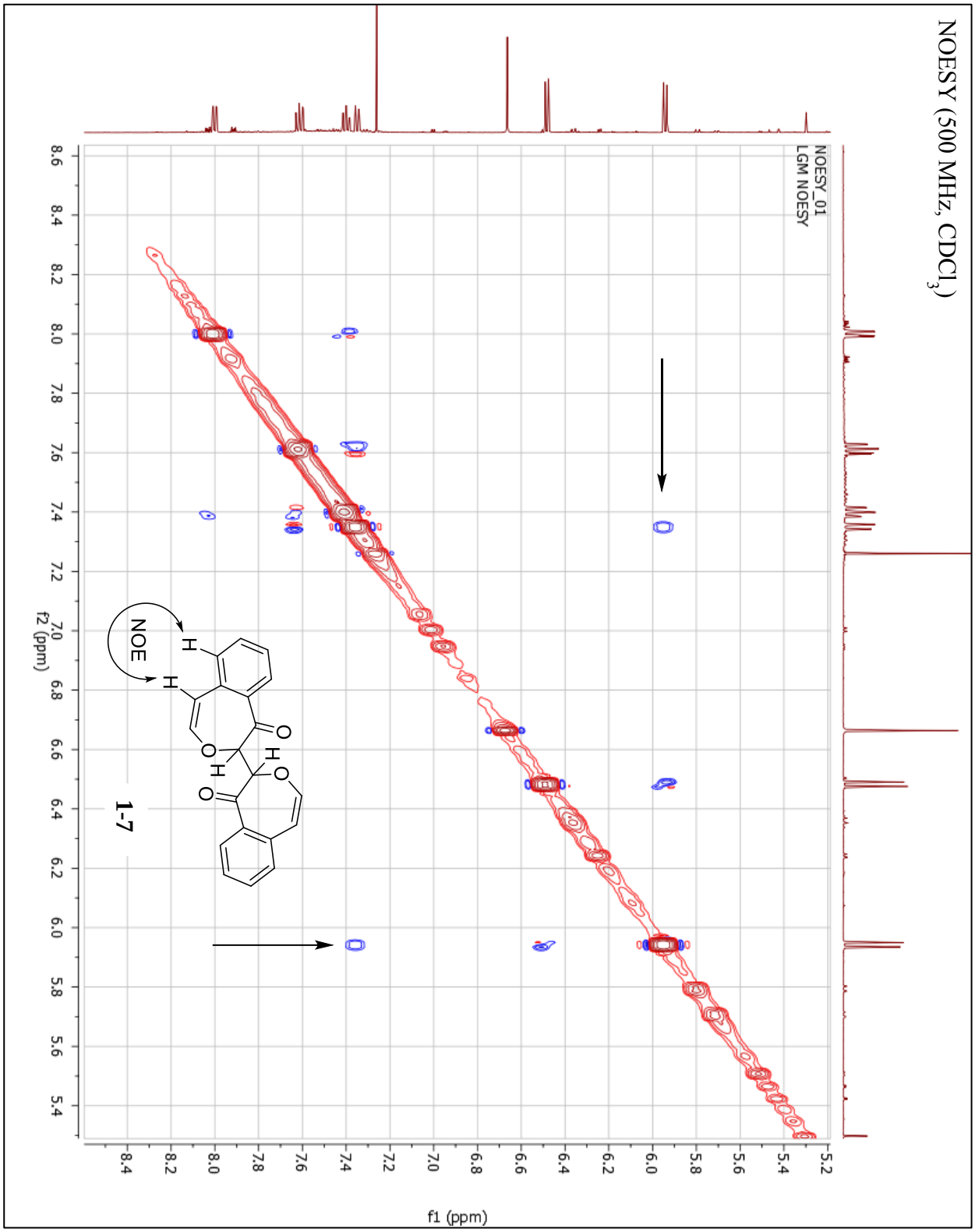

HMQC (500 MHz, $CDCl_3$)

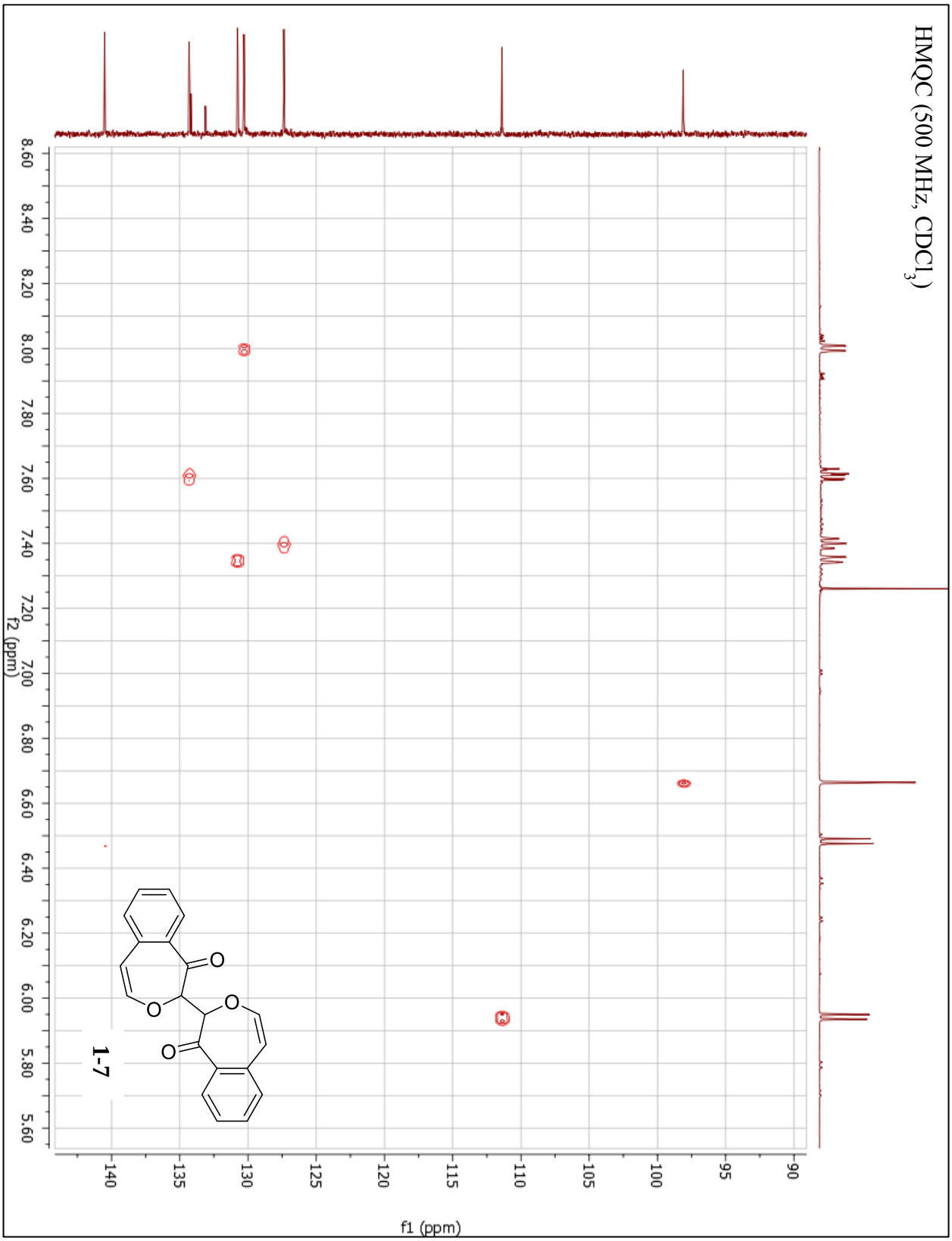

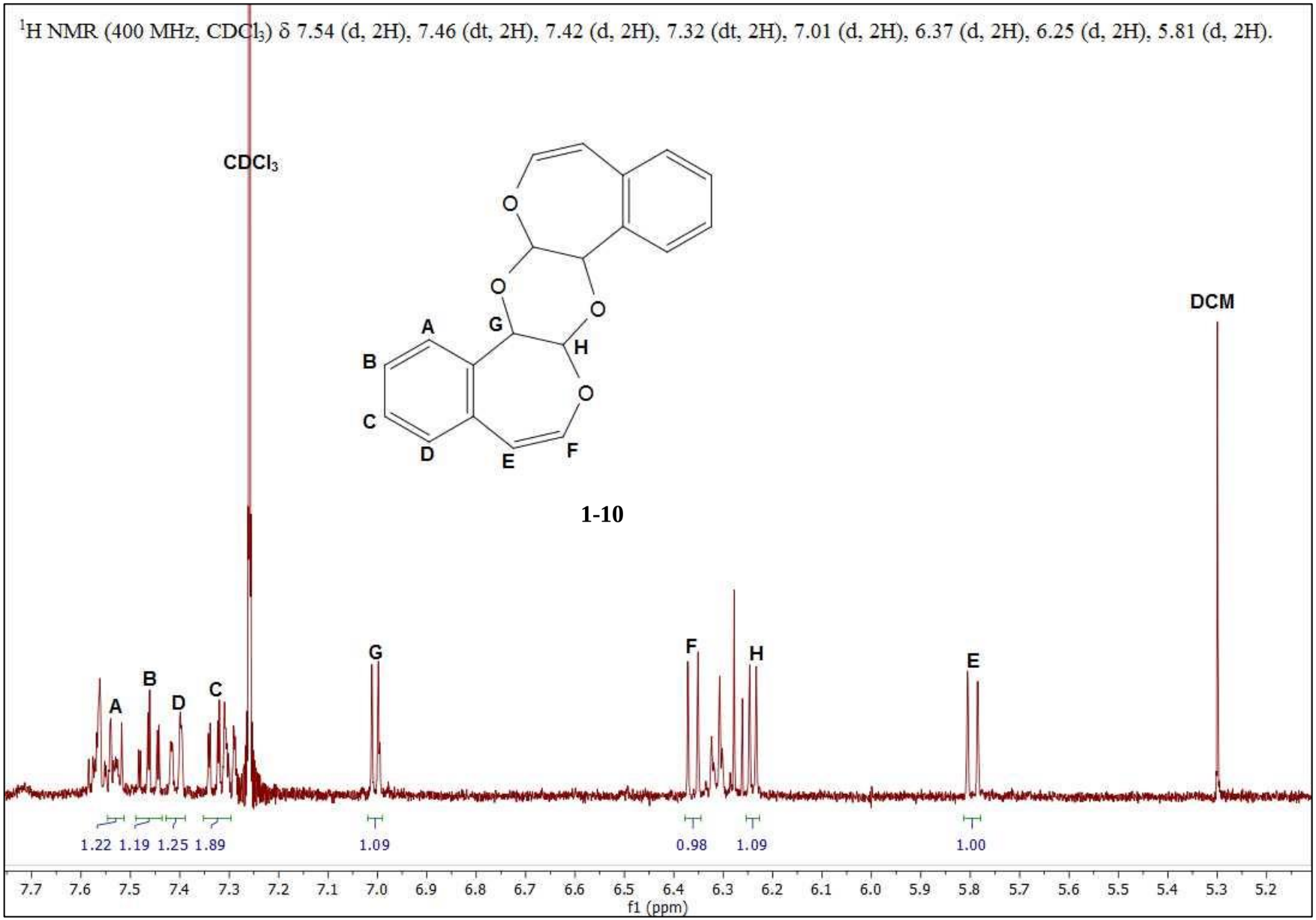
^{1}H NMR (400 MHz, $CDCl_3$) δ 7.54 (d, 2H), 7.46 (dt, 2H), 7.42 (d, 2H), 7.32 (dt, 2H), 7.01 (d, 2H), 6.37 (d, 2H), 6.25 (d, 2H), 5.81 (d, 2H).
CDCl3
DCM
A
B
C
D
E
F
G
H
1.22 1.19 1.25 1.89
1.09
0.98
1.09
1.00
f1 (ppm)

1-10

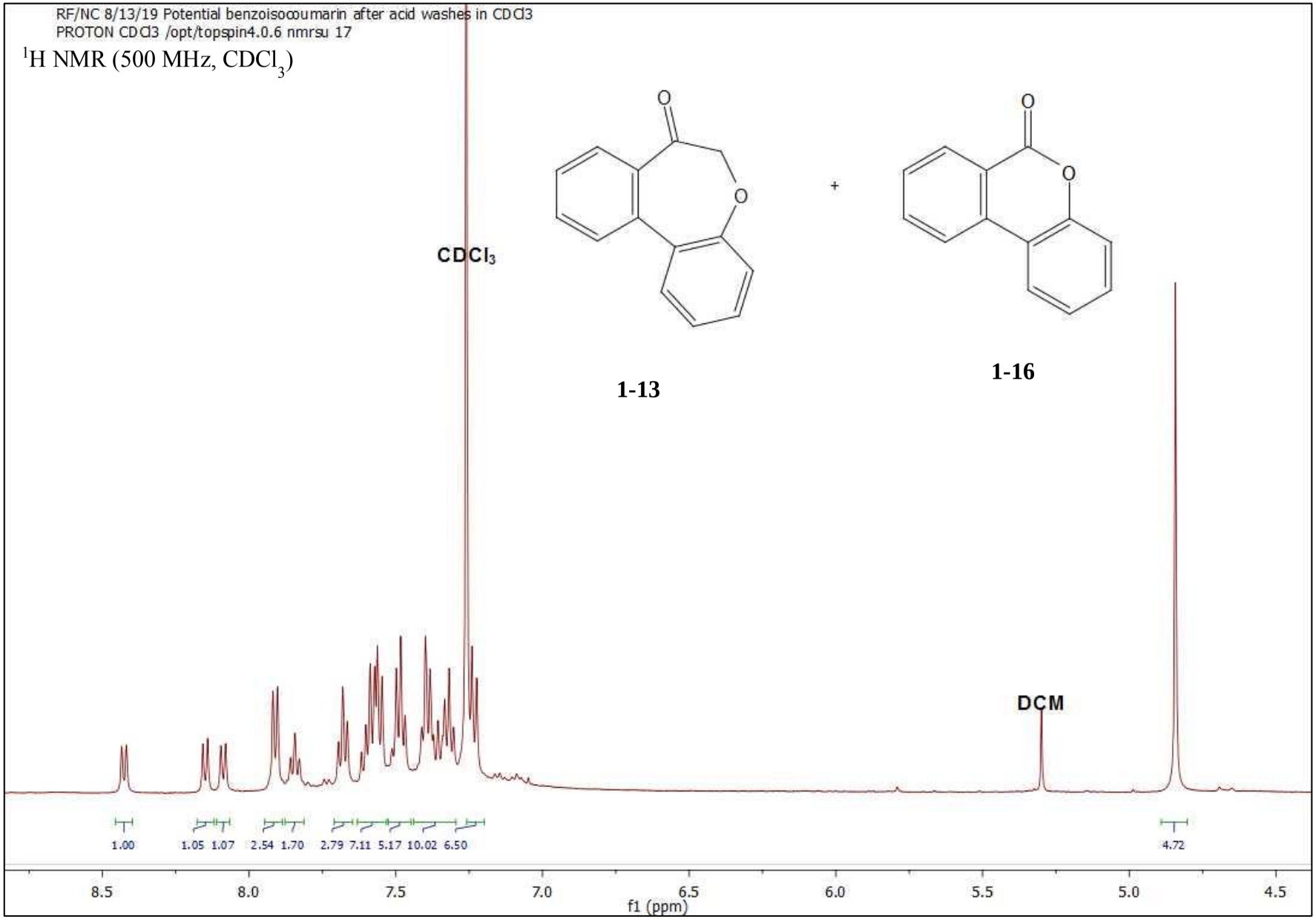
RF/NC 8/13/19 Potential benzoisocoumarin after acid washes in CDCl3
PROTON CDCl3 /opt/topspin4.0.6 nmrsu 17
^{1}H NMR (500 MHz, $CDCl_3$)
$CDCl_3$
1-13
1-16
DCM
1.00
1.05 1.07
2.54 1.70
2.79 7.11 5.17 10.02 6.50
4.72
8.5
8.0
7.5
7.0
6.5
6.0
5.5
5.0
4.5
f1 (ppm)

^{1}H NMR (400 MHz, $CDCl_3$) δ 7.16 (m, 2H), 6.89 (dt, 1H), 6.82 (d, 1H), 6.03 (m, 2H), 5.41 (dq, 1H), 5.24 (dq, 1H), 5.05 (m, 2H), 4.53 (dt, 2H), 3.41 (d, 2H).

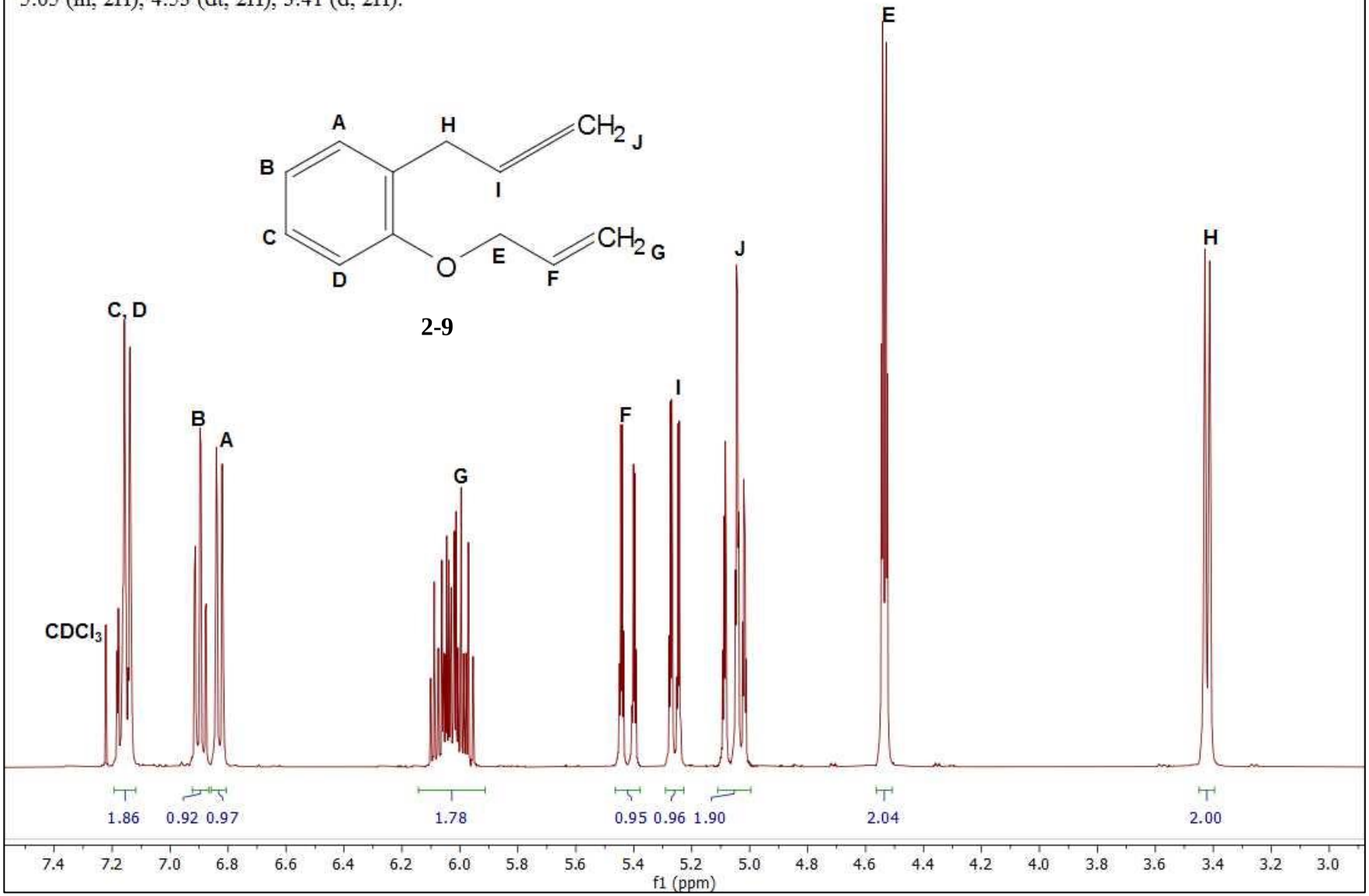

2-9

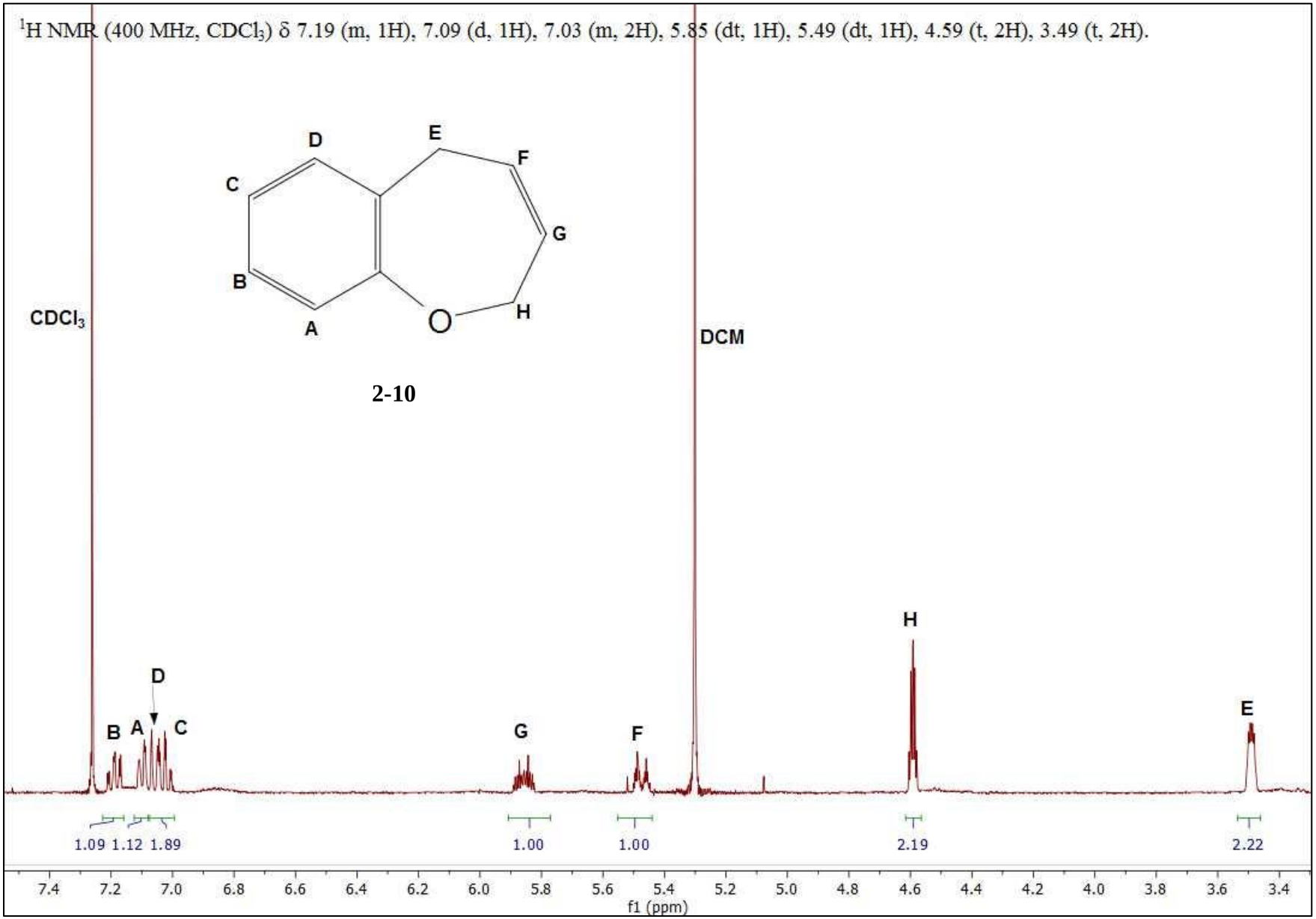
^{1}H NMR (400 MHz, $CDCl_3$) δ 7.19 (m, 1H), 7.09 (d, 1H), 7.03 (m, 2H), 5.85 (dt, 1H), 5.49 (dt, 1H), 4.59 (t, 2H), 3.49 (t, 2H).
D
E
F
C
G
B
A
O
H
2-10
CDCl3
DCM
H
D
E
B
A
C
G
F
1.09 1.12 1.89
1.00
1.00
2.19
2.22
7.4 7.2 7.0 6.8 6.6 6.4 6.2 6.0 5.8 5.6 5.4 5.2 5.0 4.8 4.6 4.4 4.2 4.0 3.8 3.6 3.4
f1 (ppm)

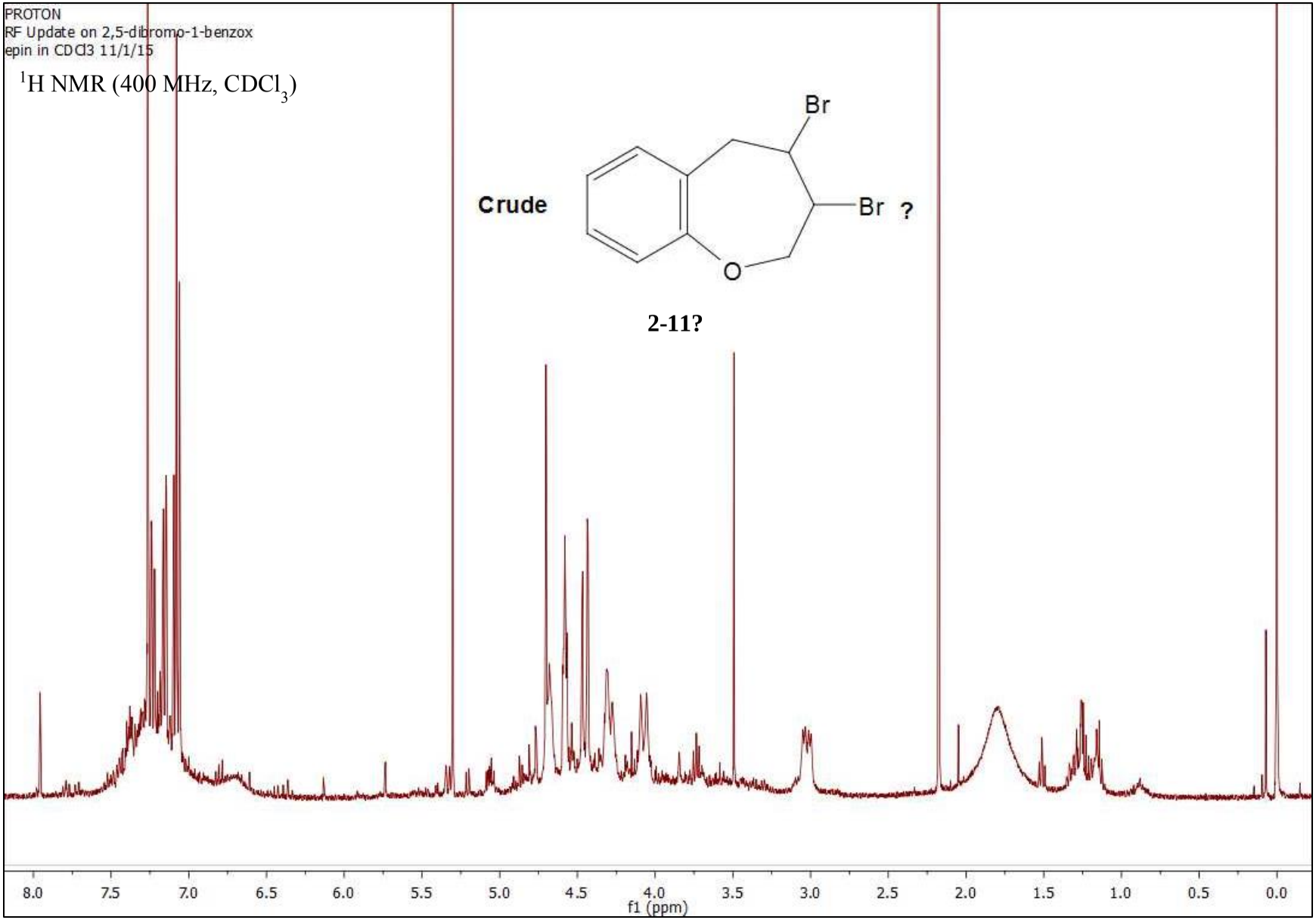
PROTON
RF Update on 2,5-dibromo-1-benzox
epin in CDCl3 11/1/15
^{1}H NMR (400 MHz, $CDCl_3$)
Crude
Br
Br ?
O
2-11?
8.0
7.5
7.0
6.5
6.0
5.5
5.0
4.5
4.0
3.5
3.0
2.5
2.0
1.5
1.0
0.5
0.0
f1 (ppm)

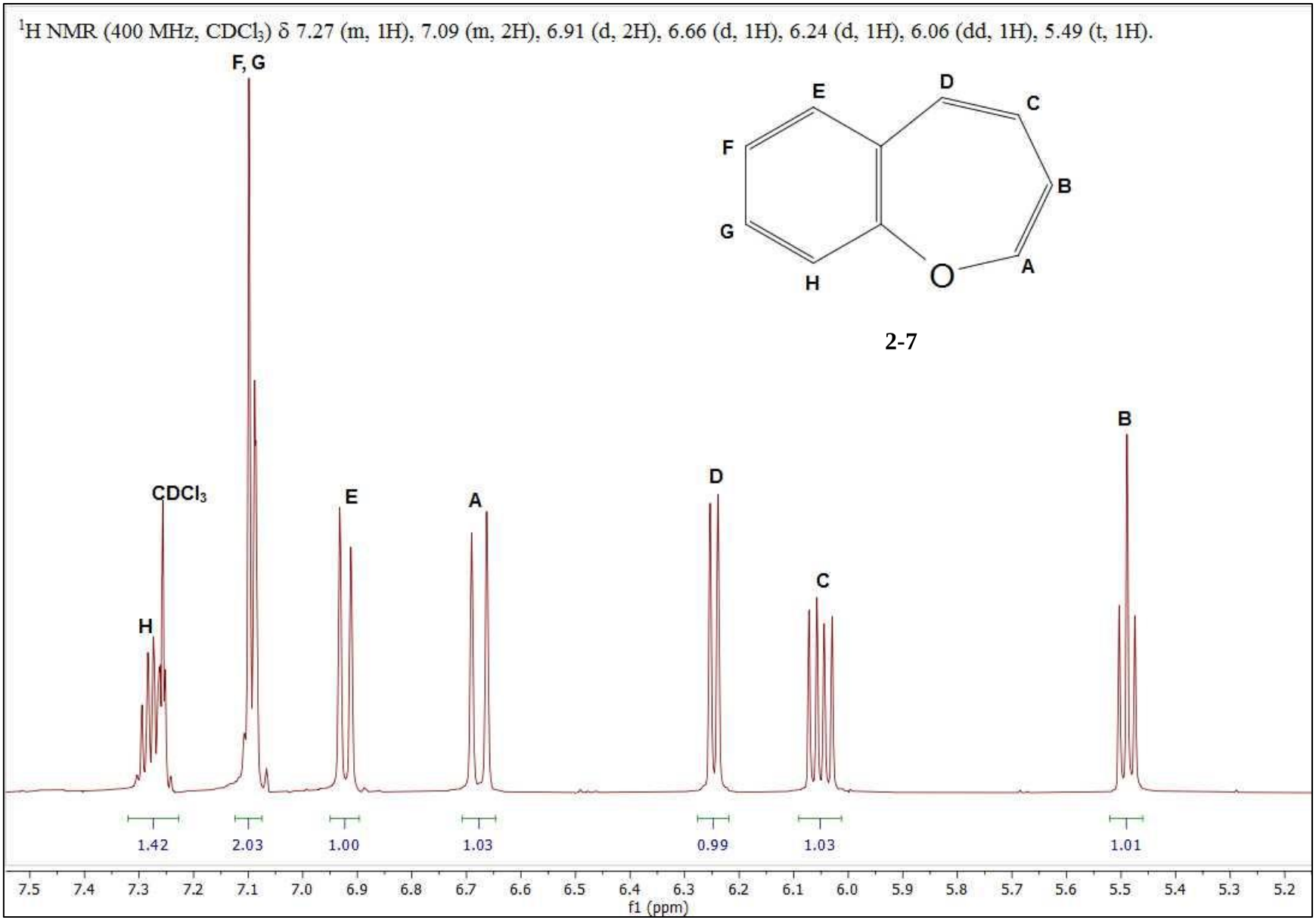
^{1}H NMR (400 MHz, $CDCl_3$) δ 7.27 (m, 1H), 7.09 (m, 2H), 6.91 (d, 2H), 6.66 (d, 1H), 6.24 (d, 1H), 6.06 (dd, 1H), 5.49 (t, 1H).
F, G
CDCl3
H
E
A
D
C
B
E
D
C
F
B
G
A
H
O
2-7
1.42
2.03
1.00
1.03
0.99
1.03
1.01
7.5 7.4 7.3 7.2 7.1 7.0 6.9 6.8 6.7 6.6 6.5 6.4 6.3 6.2 6.1 6.0 5.9 5.8 5.7 5.6 5.5 5.4 5.3 5.2
f1 (ppm)

^{1}H NMR (500 MHz, $CDCl_3$) δ 7.37 (m, 1H), 7.29 (d, 1H), 7.15 (m, 1H), 6.85 (t, 1H), 6.40 (s, 1H), 6.03 (d, 1H), 5.08 (d, 1H), 4.66 (s, 1H).

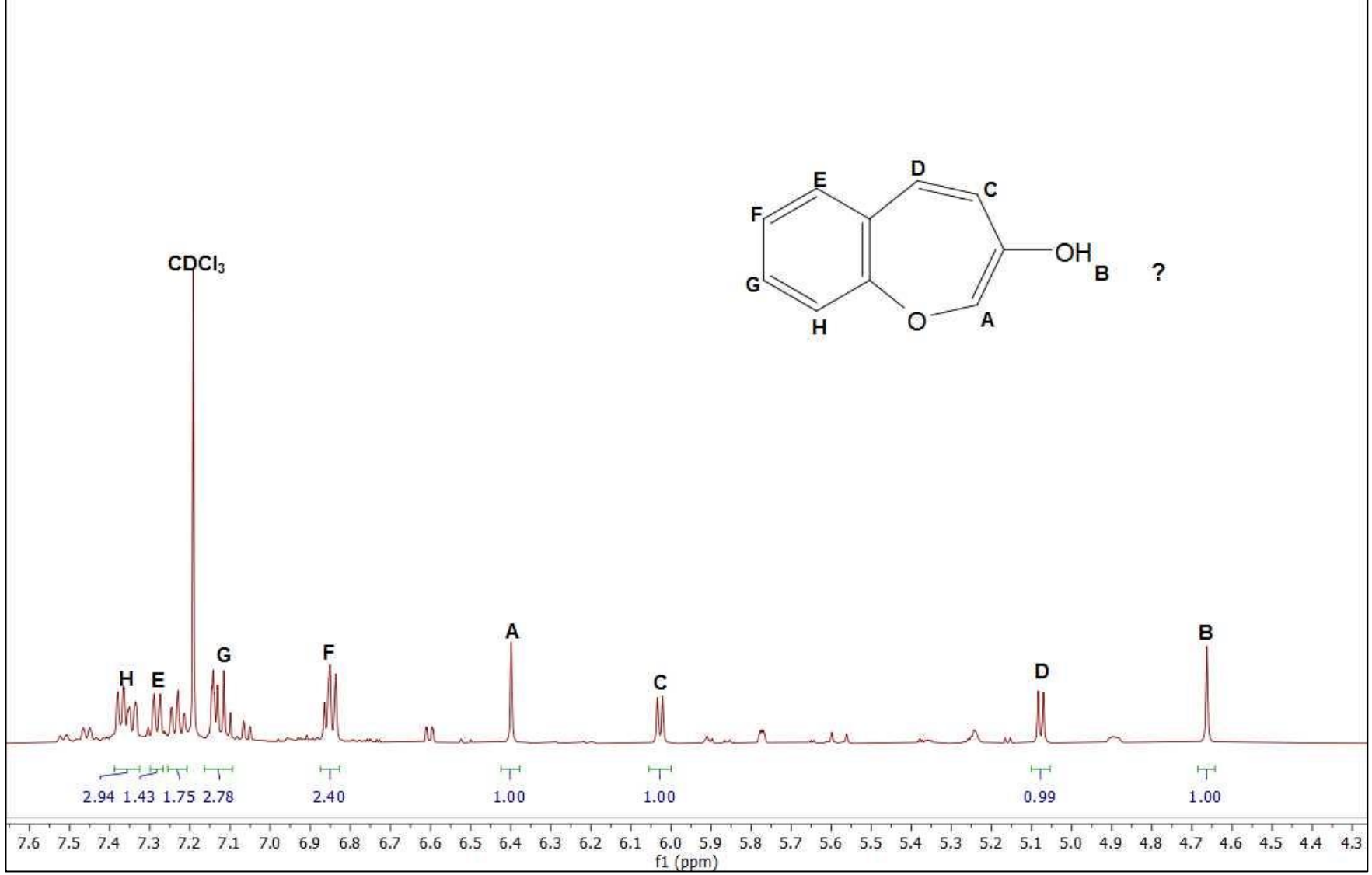

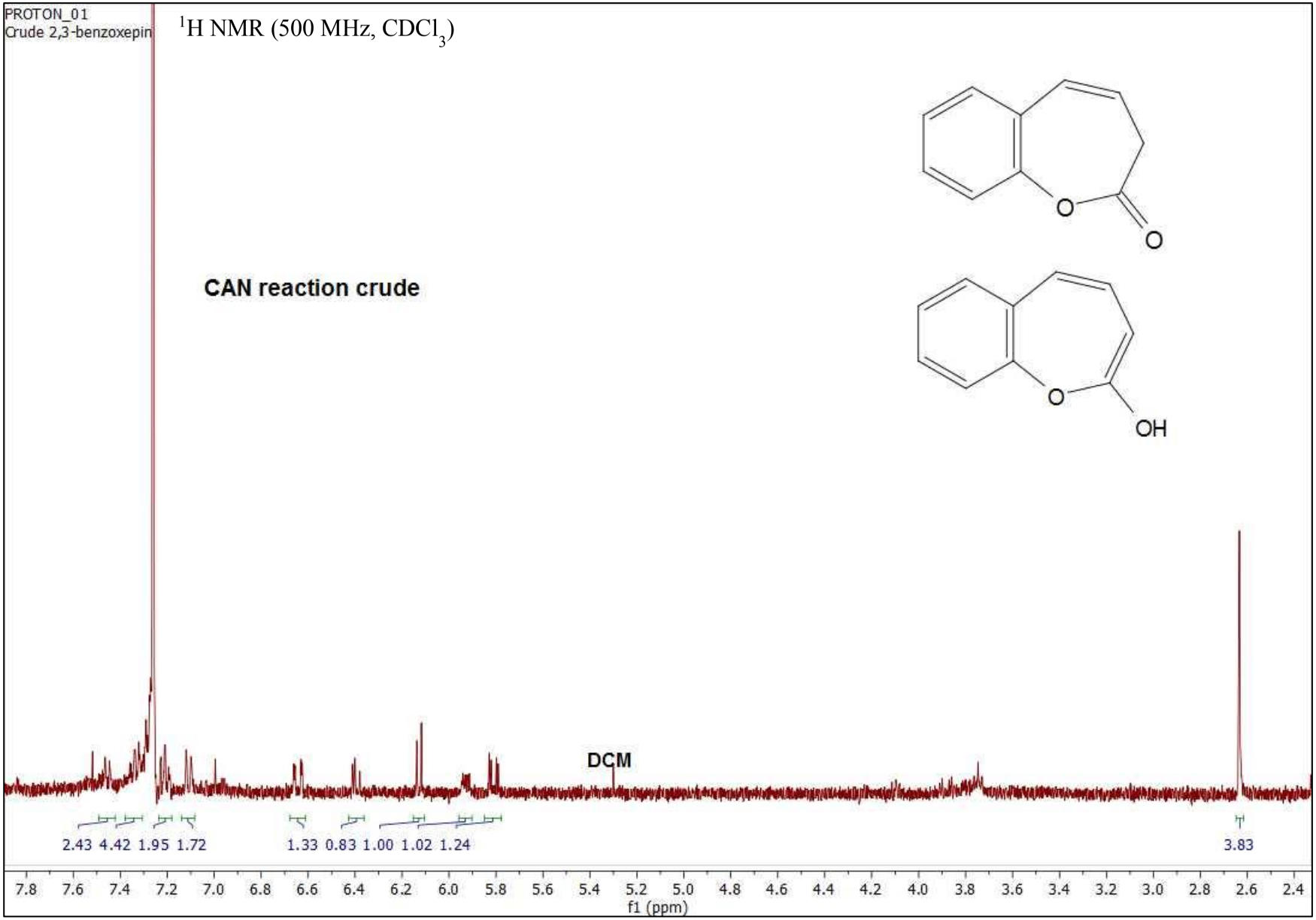
PROTON_01
Crude 2,3-benzoxepin
^{1}H NMR (500 MHz, $CDCl_3$)
CAN reaction crude
O
O
O
OH
DCM
2.43 4.42 1.95 1.72
1.33 0.83 1.00 1.02 1.24
3.83
7.8 7.6 7.4 7.2 7.0 6.8 6.6 6.4 6.2 6.0 5.8 5.6 5.4 5.2 5.0 4.8 4.6 4.4 4.2 4.0 3.8 3.6 3.4 3.2 3.0 2.8 2.6 2.4
f1 (ppm)

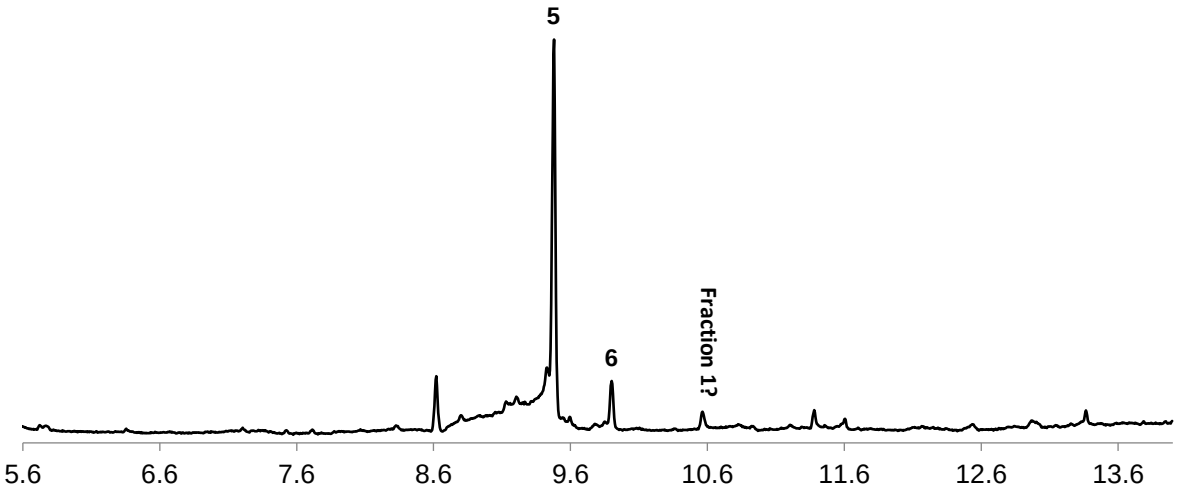

GC/MS of reaction of 4,5-benzoxepin (**1**-**5**) with P450 2E1.

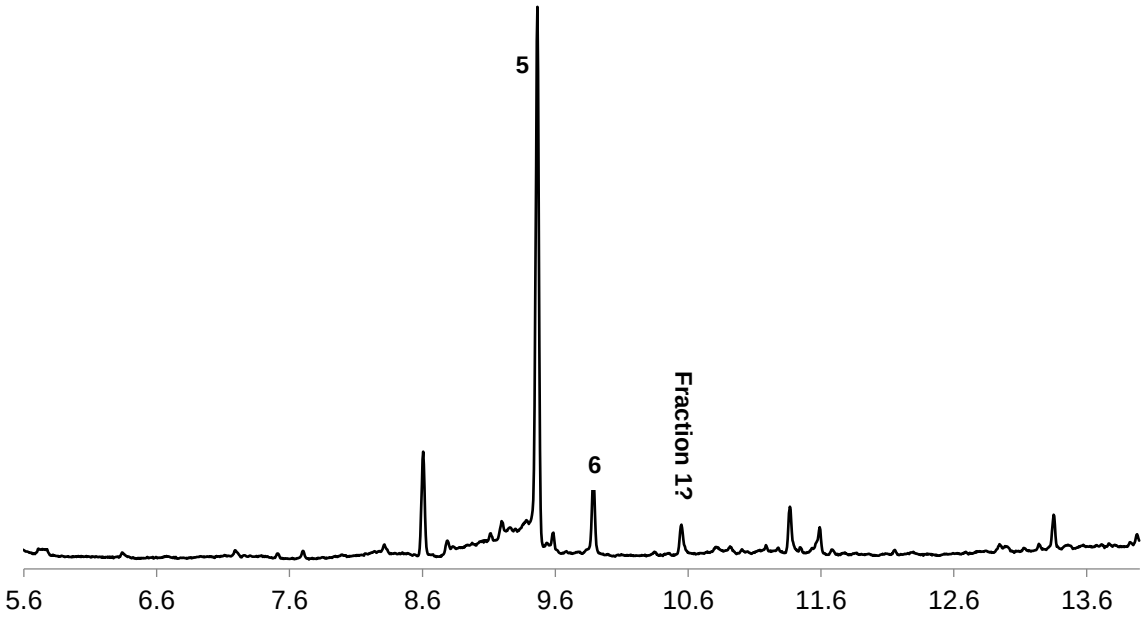

GC/MS of reaction of 4,5-benzoxepin (**1**-**5**) with P450 3A4.

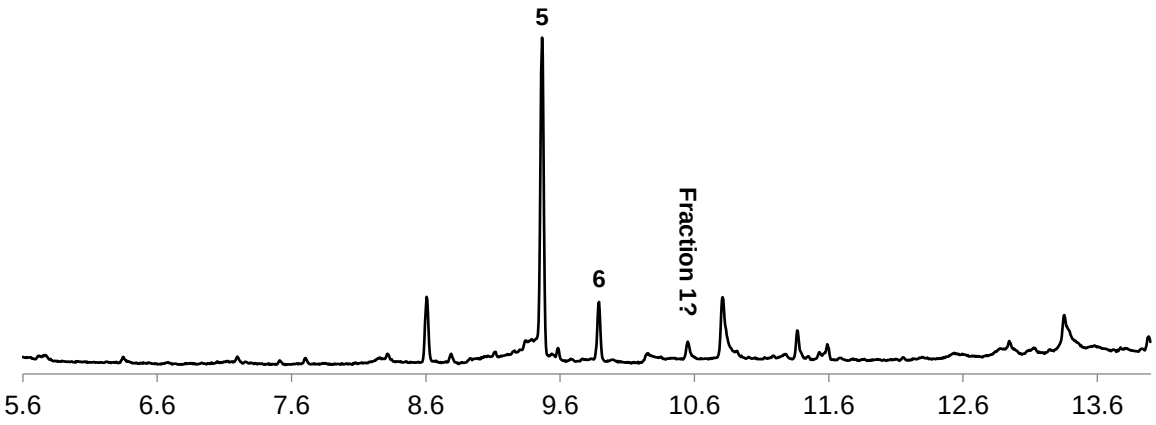

GC/MS reaction of 4,5-benzoxepin (**1**-**5**) with pHLM.

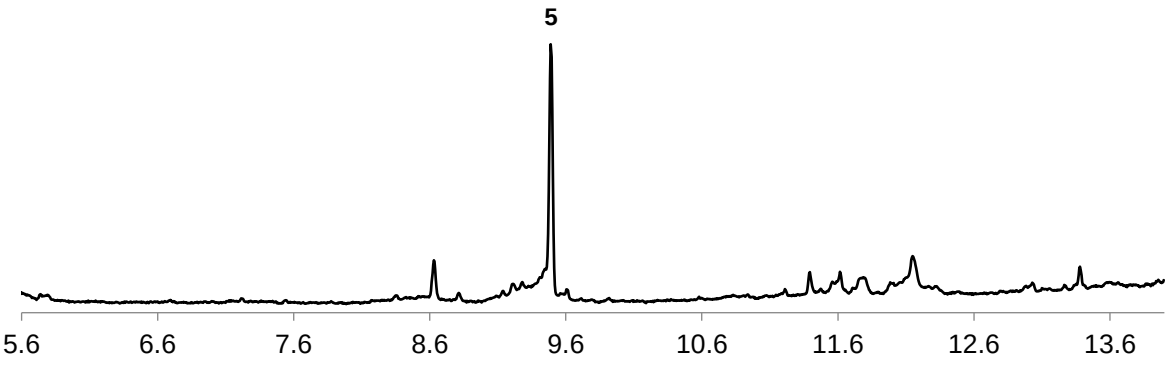

GC/MS of incubation of 4,5-benzoxepin (**1**-**5**) with no enzyme – control experiment.

^{1}H NMR (400 MHz, $CDCl_3$) δ 4.32 (s, 2H), 1.56 (s, 6H).

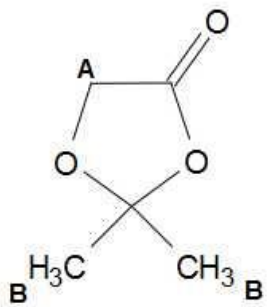

3-3

^{1}H NMR (400 MHz, DMSO) δ 4.85 (br. s, 1H), 4.76 (br. s, 1H), 4.35 (br. s, 1H), 4.12 (s, 2H), 3.50 (m, 4H), 3.36 (t, 2H), 3.27 (t, 2H).

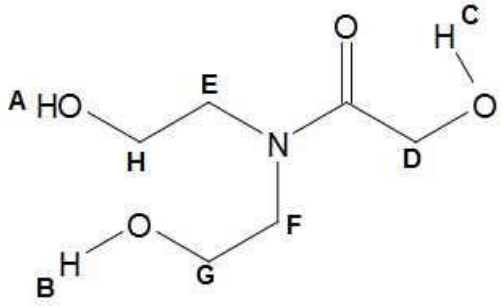

3-5

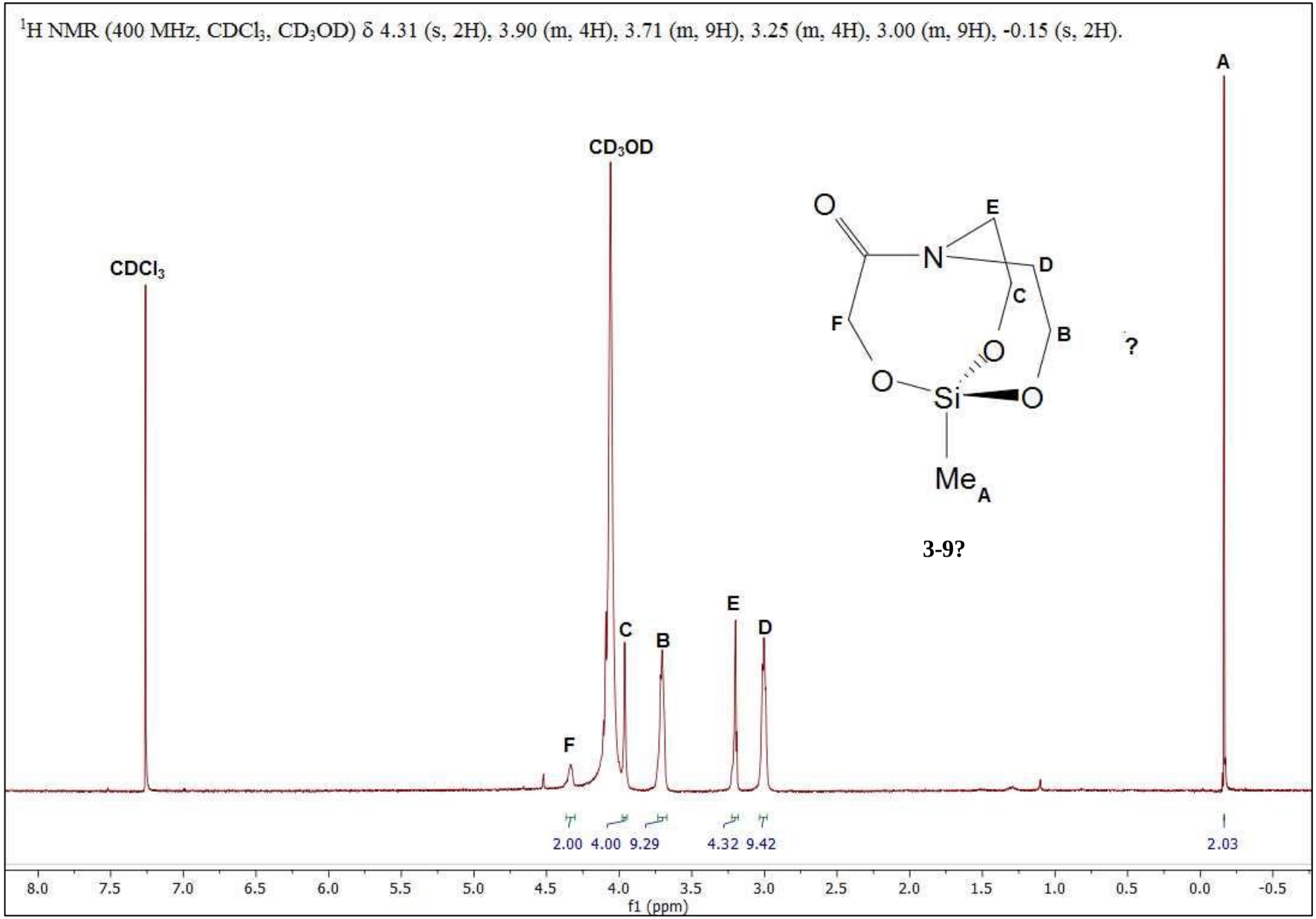
[1]H NMR (400 MHz, CDCl3, CD3OD) δ 4.31 (s, 2H), 3.90 (m, 4H), 3.71 (m, 9H), 3.25 (m, 4H), 3.00 (m, 9H), -0.15 (s, 2H).
CDCl3
CD3OD
A
O
E
N
D
C
F
B
O
O
Si
O
Me
A
?
3-9?
E
D
C
B
F
2.00 4.00 9.29 4.32 9.42 2.03
8.0 7.5 7.0 6.5 6.0 5.5 5.0 4.5 4.0 3.5 3.0 2.5 2.0 1.5 1.0 0.5 0.0 -0.5
f1 (ppm)

COSY (400 MHz, $CDCl_3$)

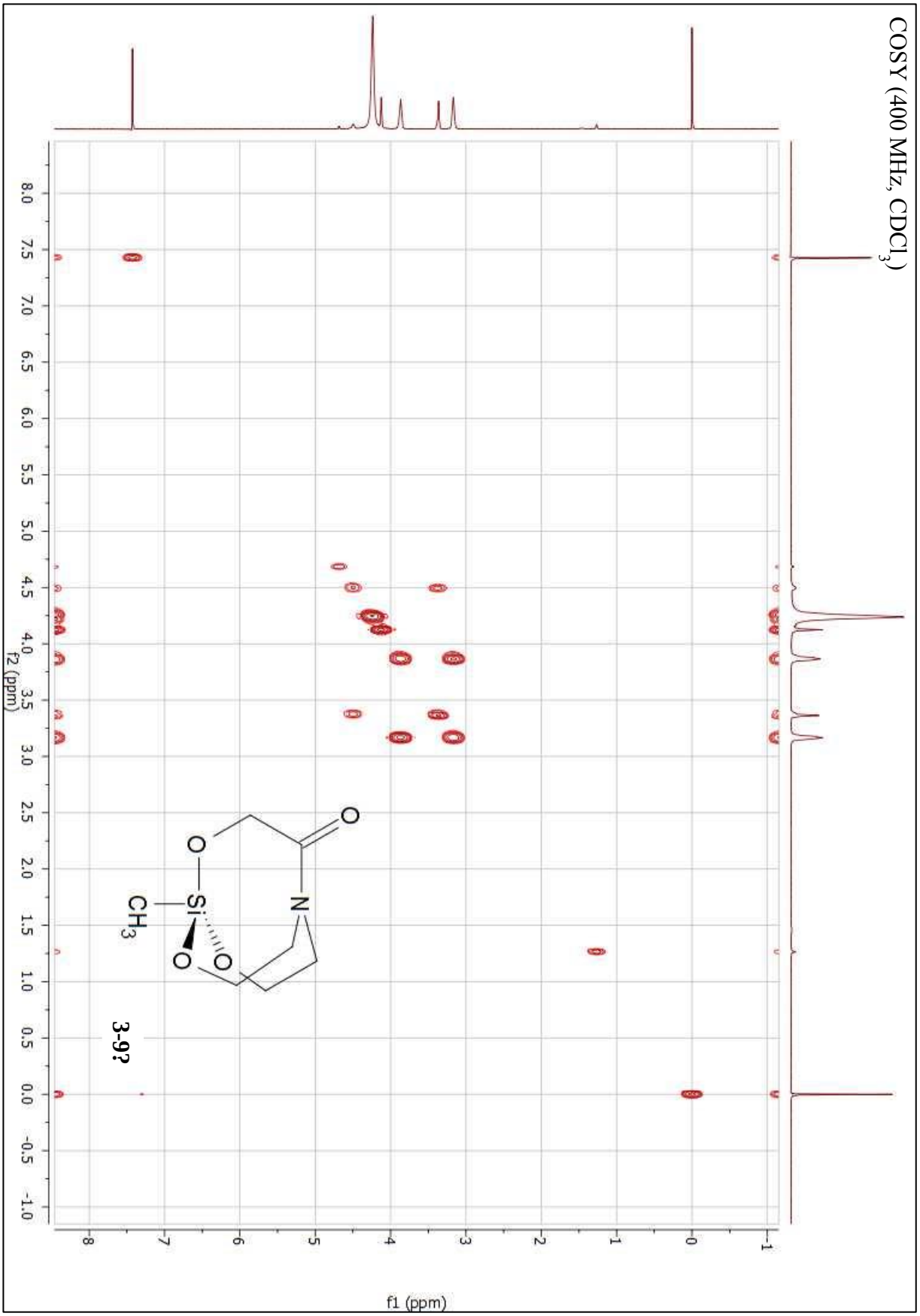

3-9?

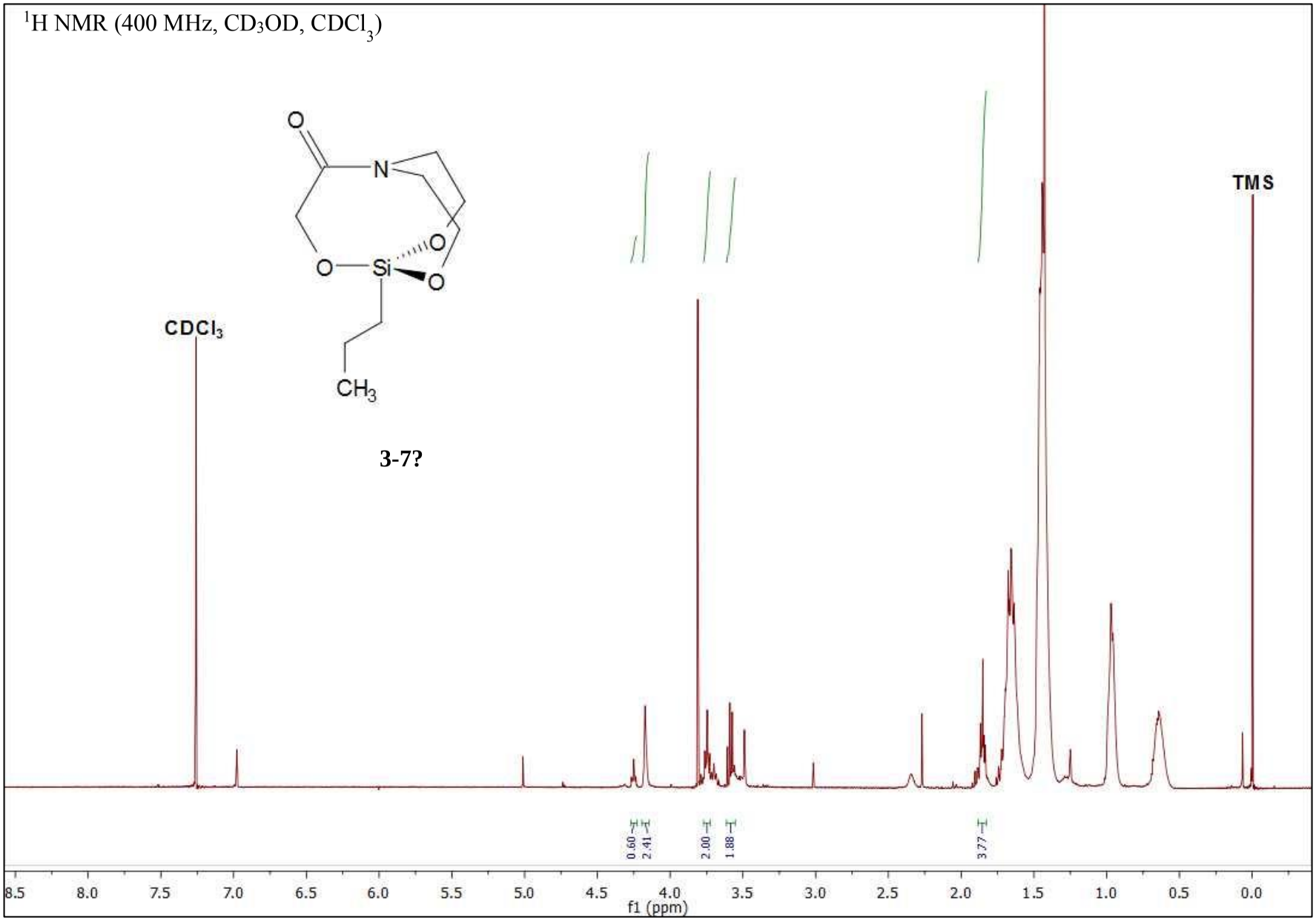
^{1}H NMR (400 MHz, CD_3OD, $CDCl_3$)
O
N
O
O
Si
O
CH_3
3-7?
$CDCl_3$
TMS
0.60
2.41
2.00
1.88
3.77
8.5
8.0
7.5
7.0
6.5
6.0
5.5
5.0
4.5
4.0
3.5
3.0
2.5
2.0
1.5
1.0
0.5
0.0
f1 (ppm)

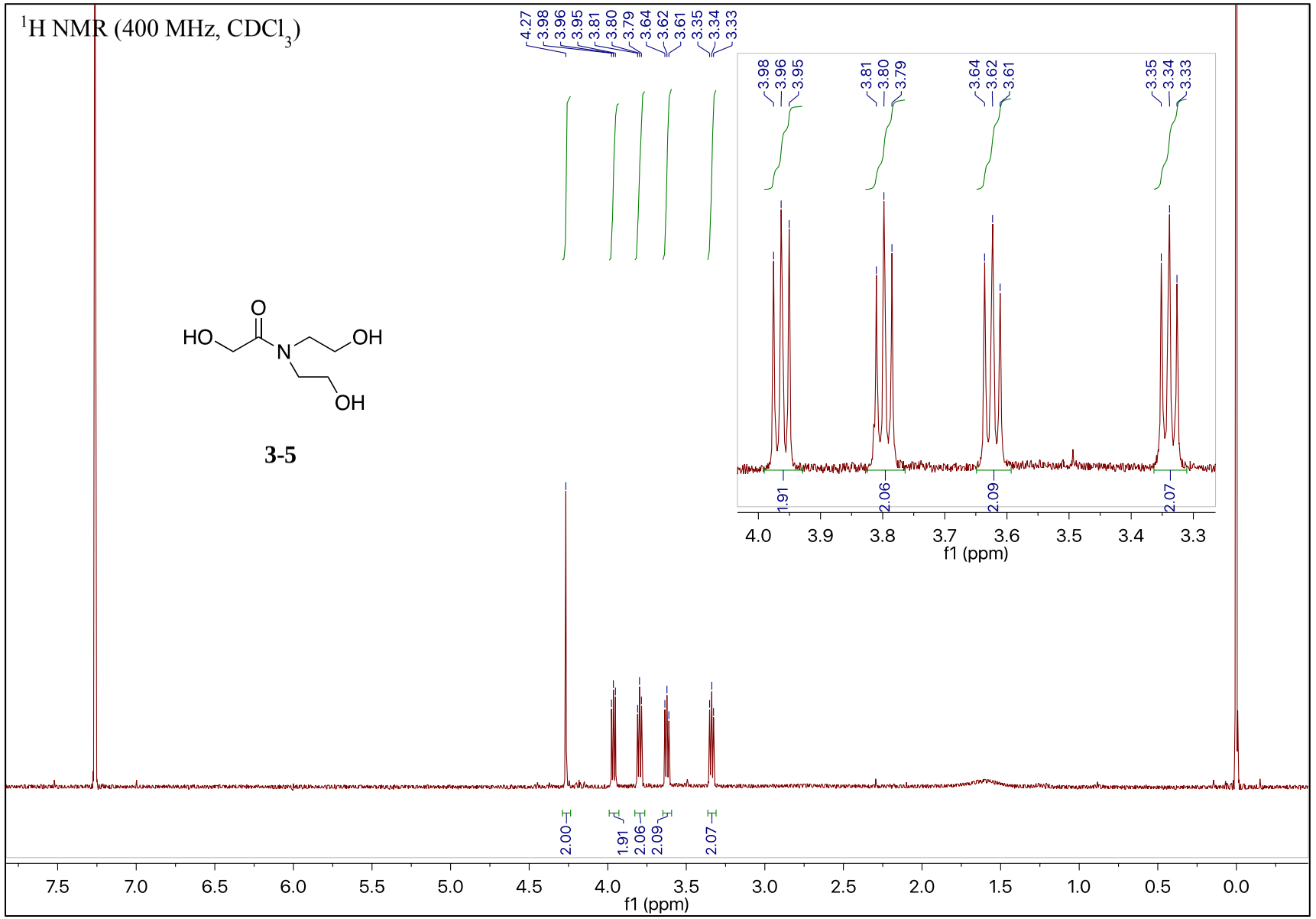
1H NMR (400 MHz, CDCl3)
4.27
3.98
3.96
3.95
3.81
3.80
3.79
3.64
3.62
3.61
3.35
3.34
3.33
HO
O
N
OH
OH
3-5
2.00
1.91
2.06
2.09
2.07
f1 (ppm)

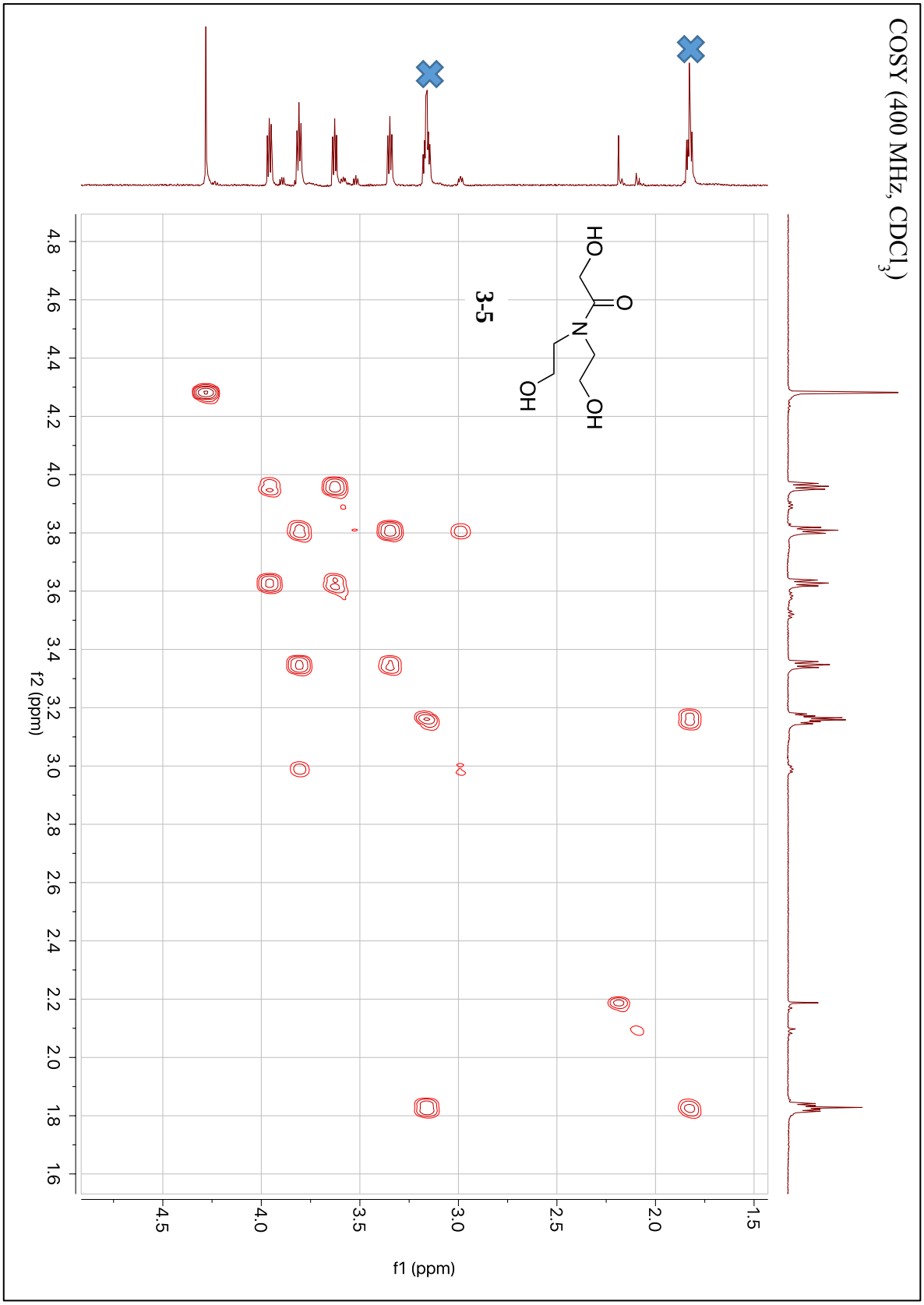
COSY (400 MHz, CDCl3)
3-5
HO
O
N
OH
OH
f1 (ppm)
f2 (ppm)

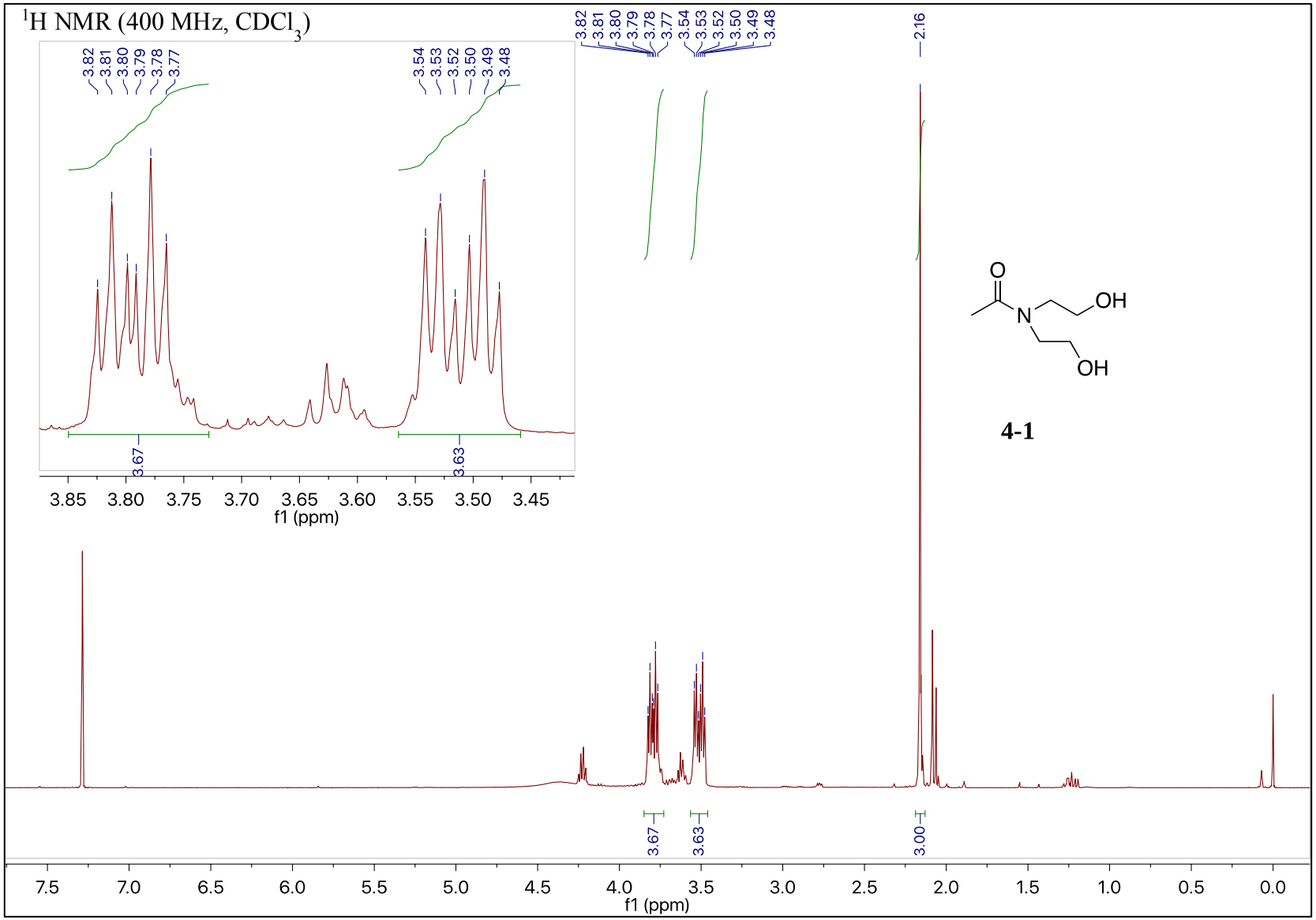
1H NMR (400 MHz, CDCl3)
3.82
3.81
3.80
3.79
3.78
3.77
3.54
3.53
3.52
3.50
3.49
3.48
2.16
3.67
3.63
3.00
f1 (ppm)
O
N
OH
OH
4-1

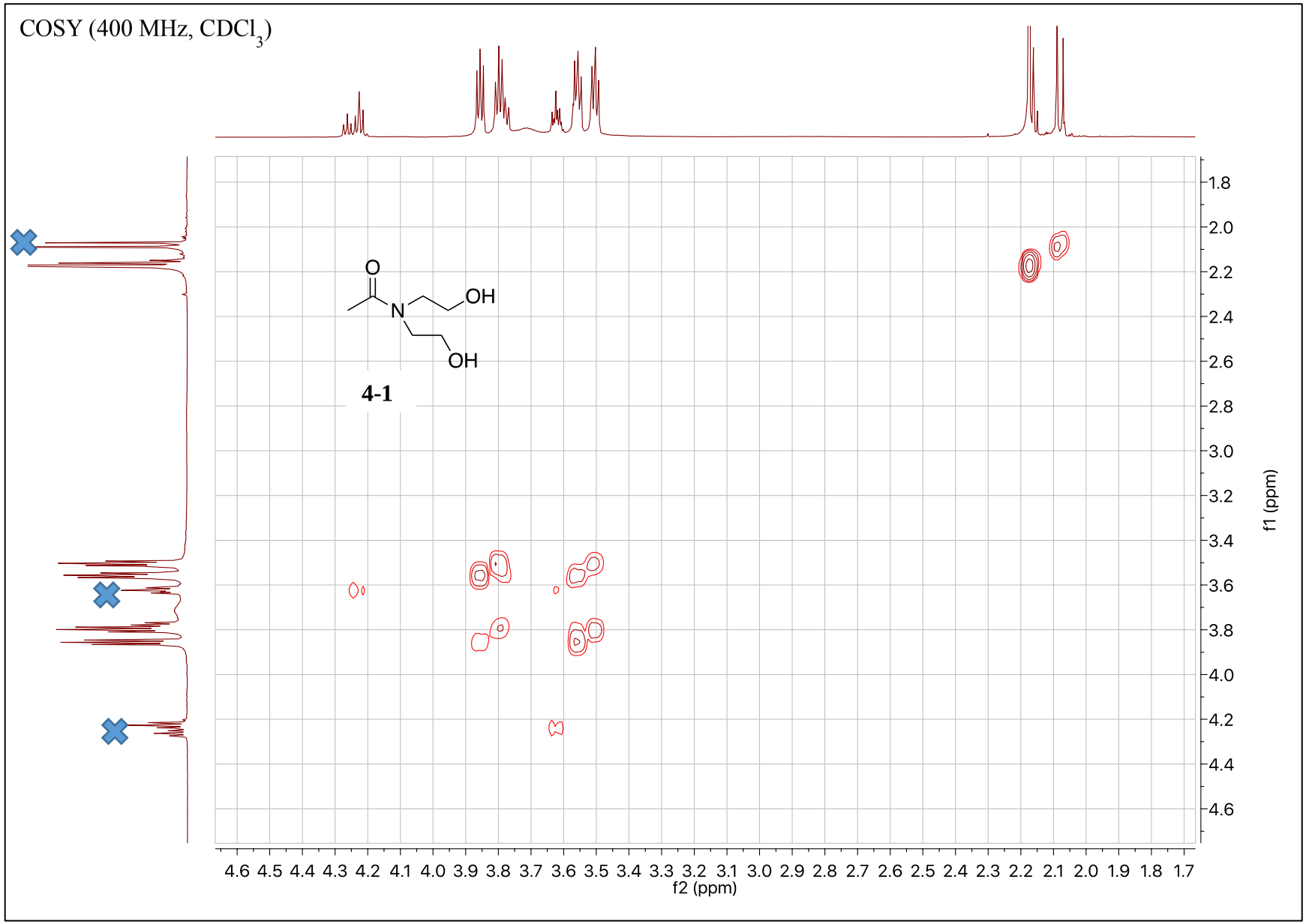
COSY (400 MHz, CDCl3)
O
N
OH
OH
4-1
f2 (ppm)
f1 (ppm)

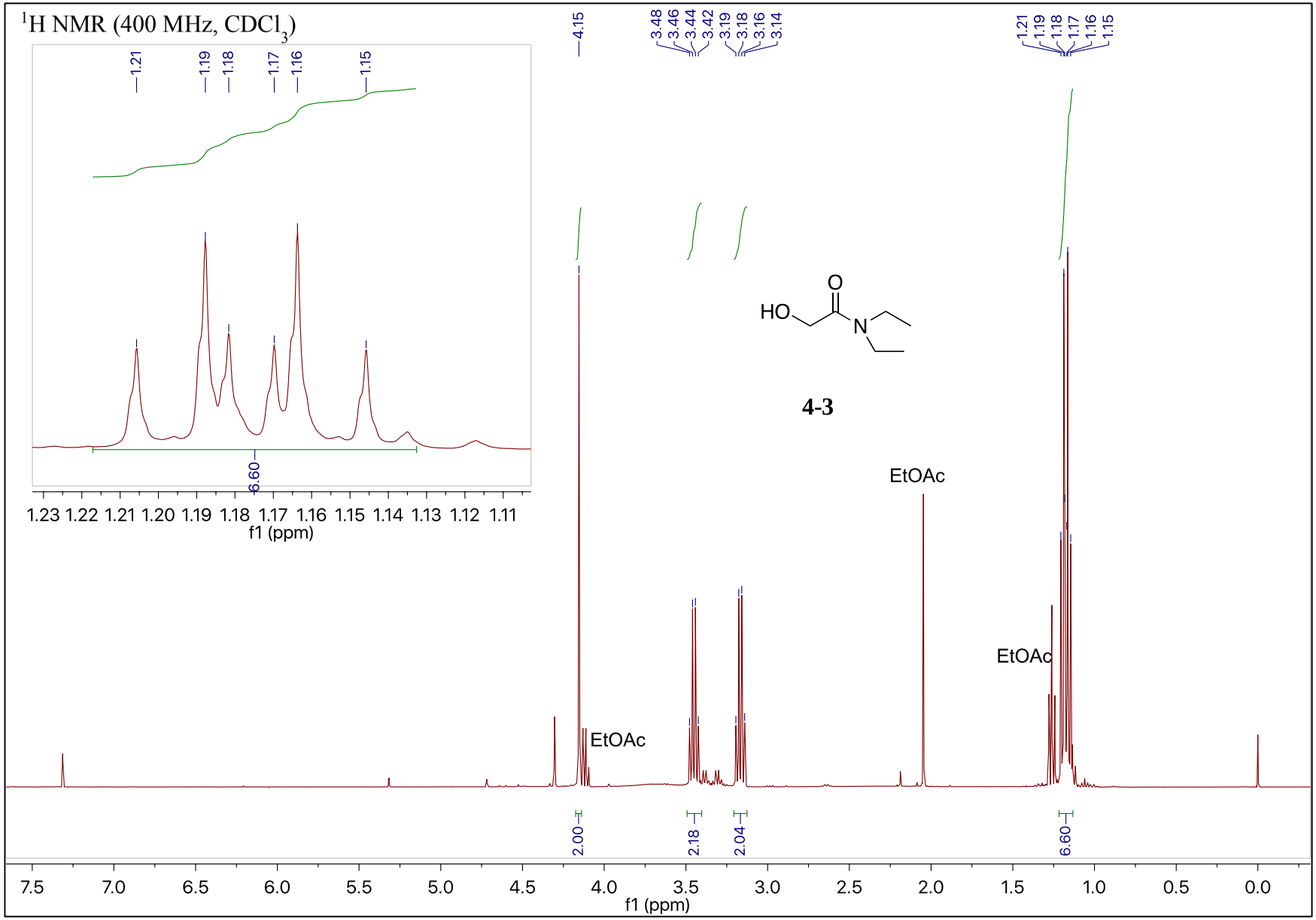
1H NMR (400 MHz, CDCl3)
4.15
3.48
3.46
3.44
3.42
3.19
3.18
3.16
3.14
1.21
1.19
1.18
1.17
1.16
1.15
6.60
1.23 1.22 1.21 1.20 1.19 1.18 1.17 1.16 1.15 1.14 1.13 1.12 1.11
f1 (ppm)
HO
O
N
4-3
EtOAc
EtOAc
EtOAc
2.00
2.18
2.04
6.60
7.5 7.0 6.5 6.0 5.5 5.0 4.5 4.0 3.5 3.0 2.5 2.0 1.5 1.0 0.5 0.0
f1 (ppm)

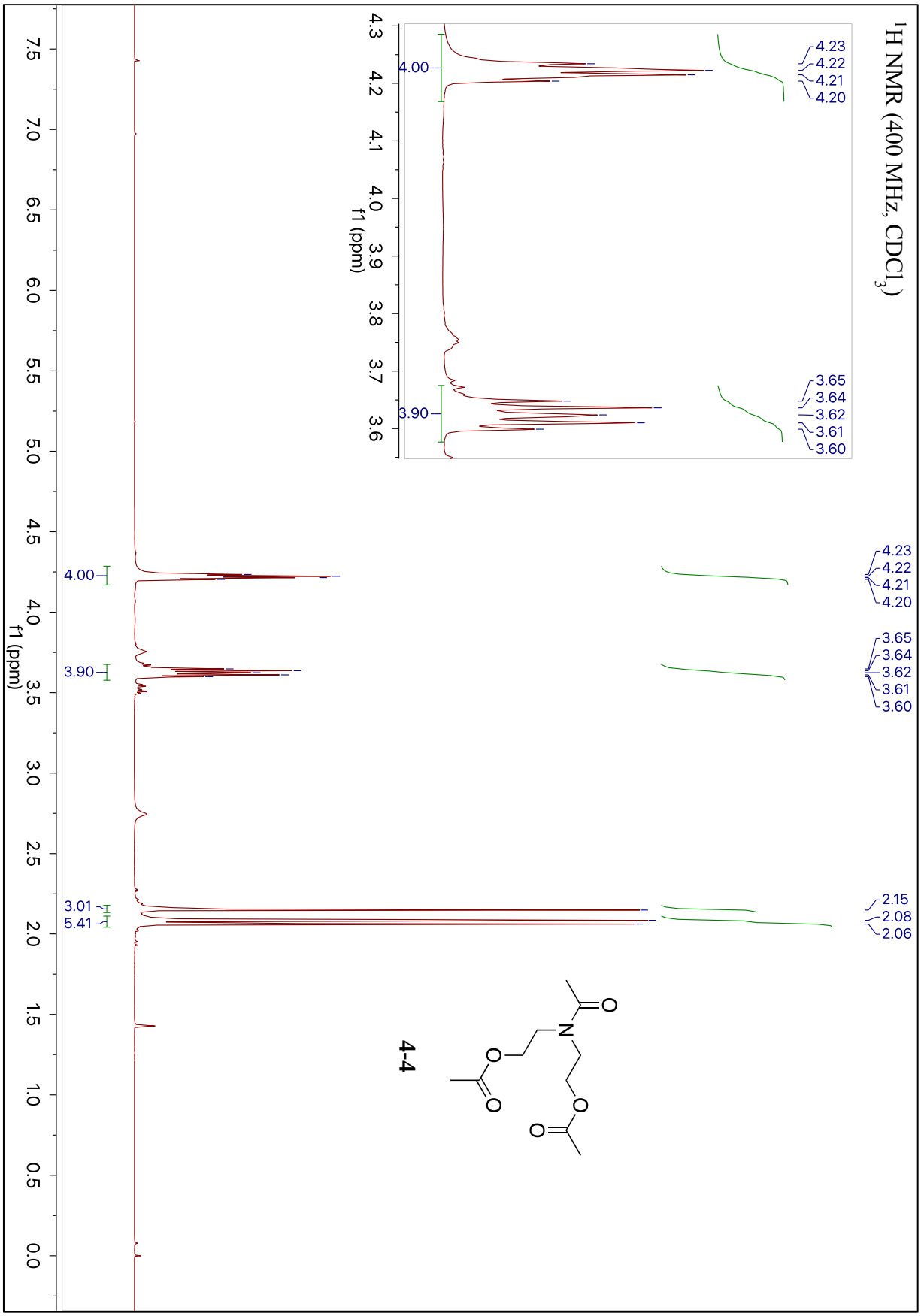
^{1}H NMR (400 MHz, $CDCl_3$)
4.23
4.22
4.21
4.20
3.65
3.64
3.62
3.61
3.60
4.00
3.90
f1 (ppm)
2.15
2.08
2.06
3.01
5.41
4-4

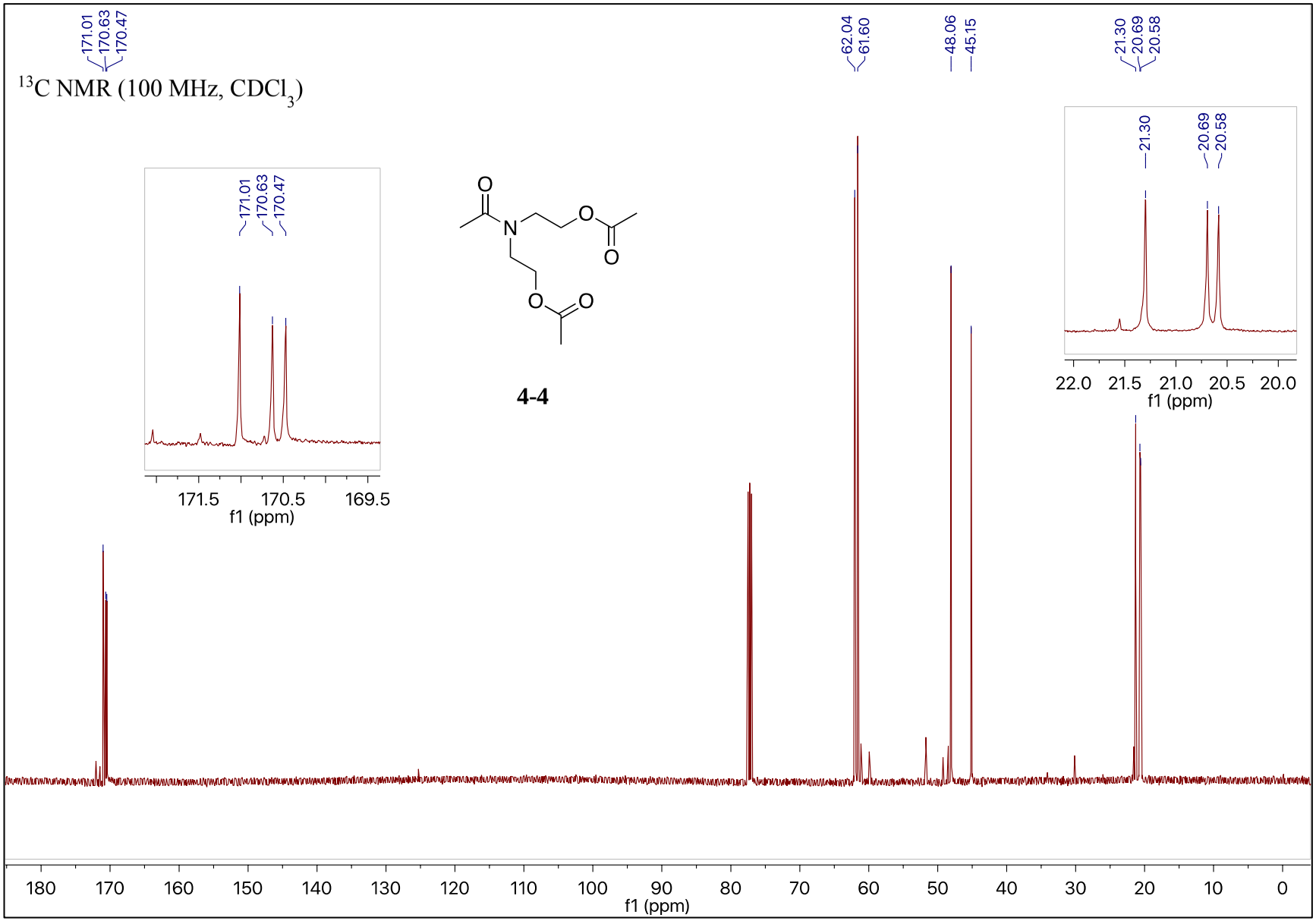
171.01
170.63
170.47
62.04
61.60
48.06
45.15
21.30
20.69
20.58
^{13}C NMR (100 MHz, CDCl$_3$)
4-4
f1 (ppm)

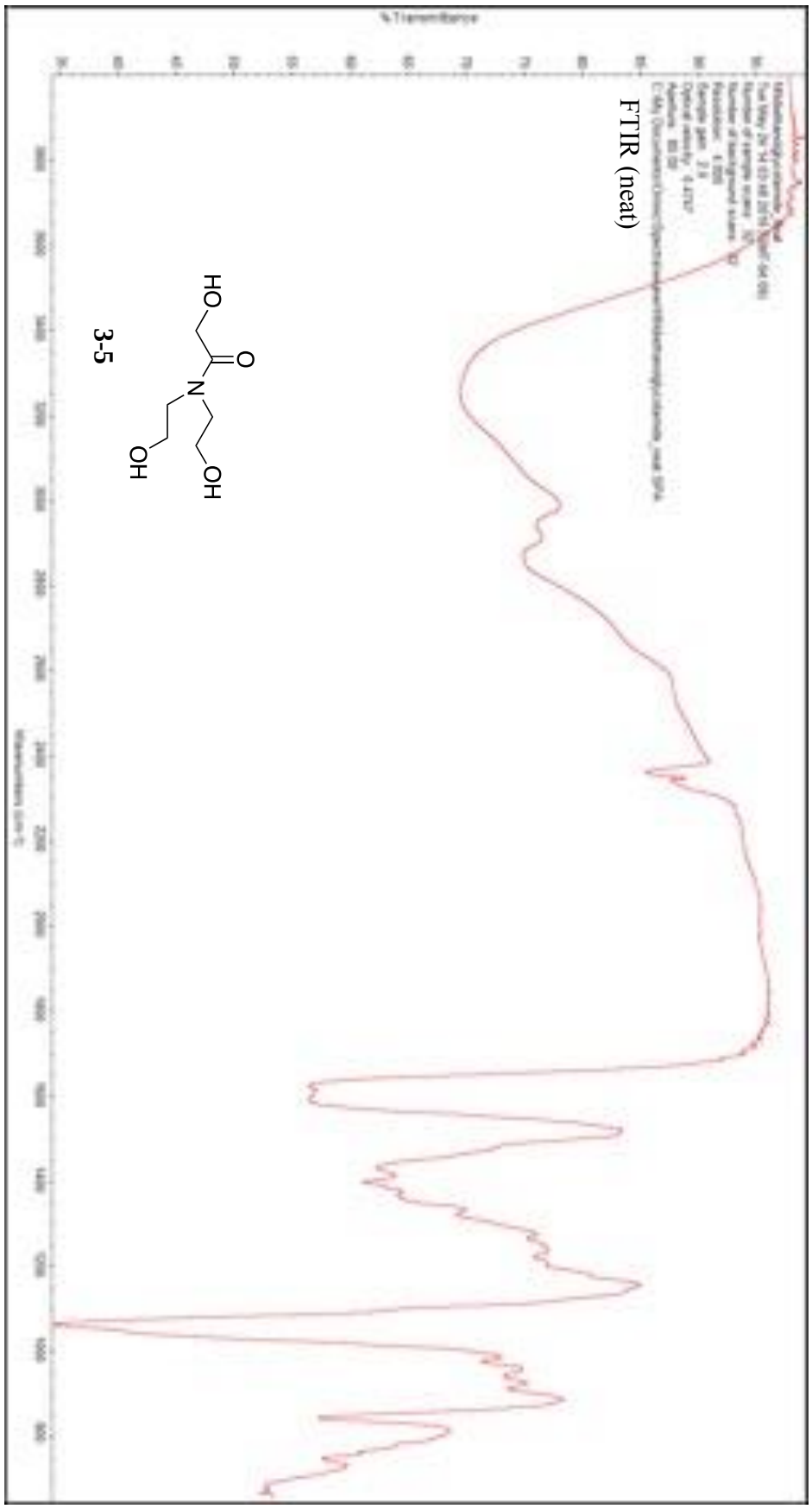
FTIR (neat)
3-5
HO
O
N
OH
OH

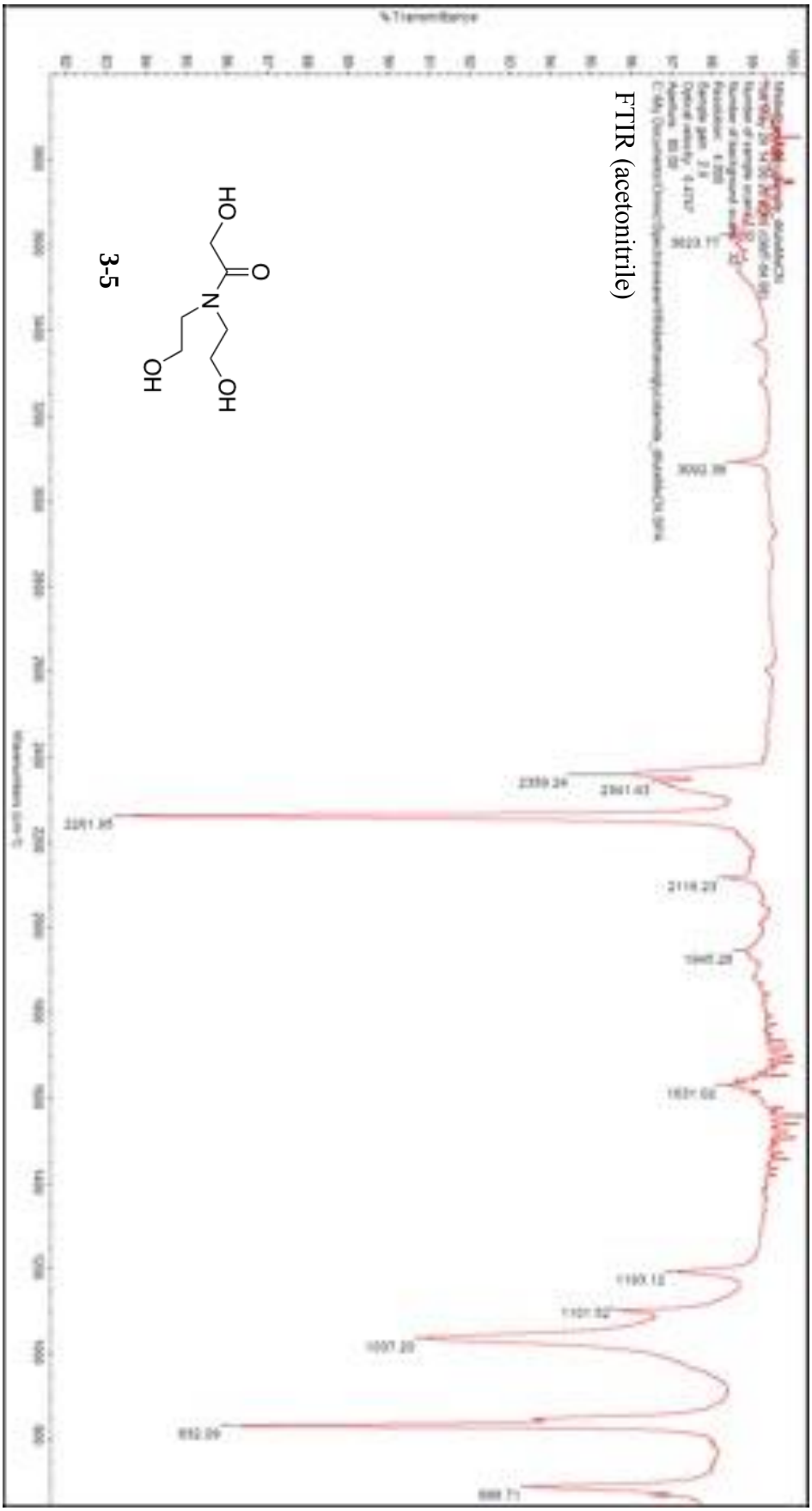
FTIR (acetonitrile)
3-5
HO
O
N
OH
OH
%Transmittance
Wavenumber (cm-1)
3923.77
3002.39
2359.24
2341.63
2251.95
2116.23
1945.28
1631.02
1193.12
1101.92
1037.20
932.09
888.71

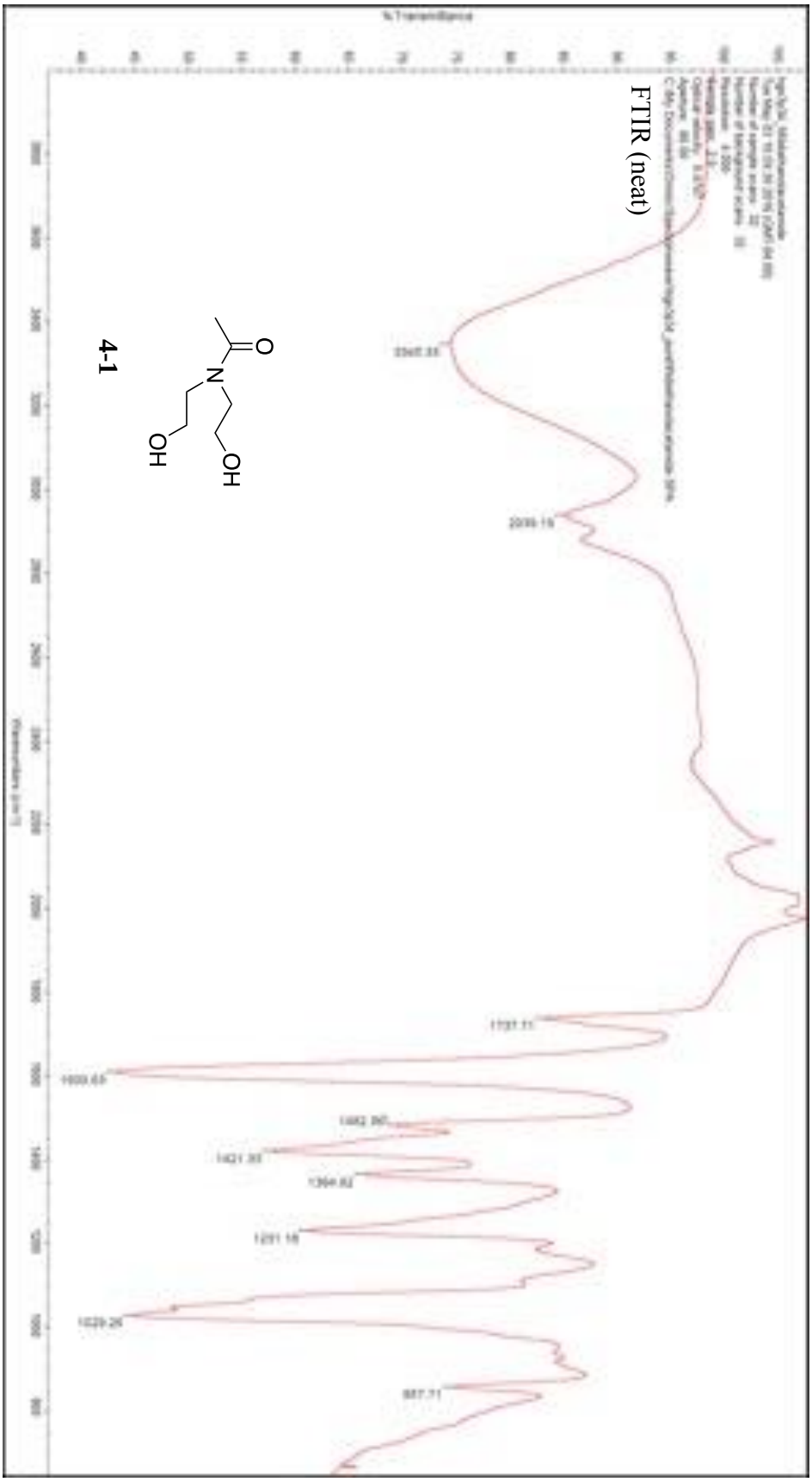
FTIR (neat)
4-1
O
N
OH
OH
3345.33
2939.19
1737.11
1459.63
1402.90
1421.33
1364.82
1251.16
1029.26
857.71

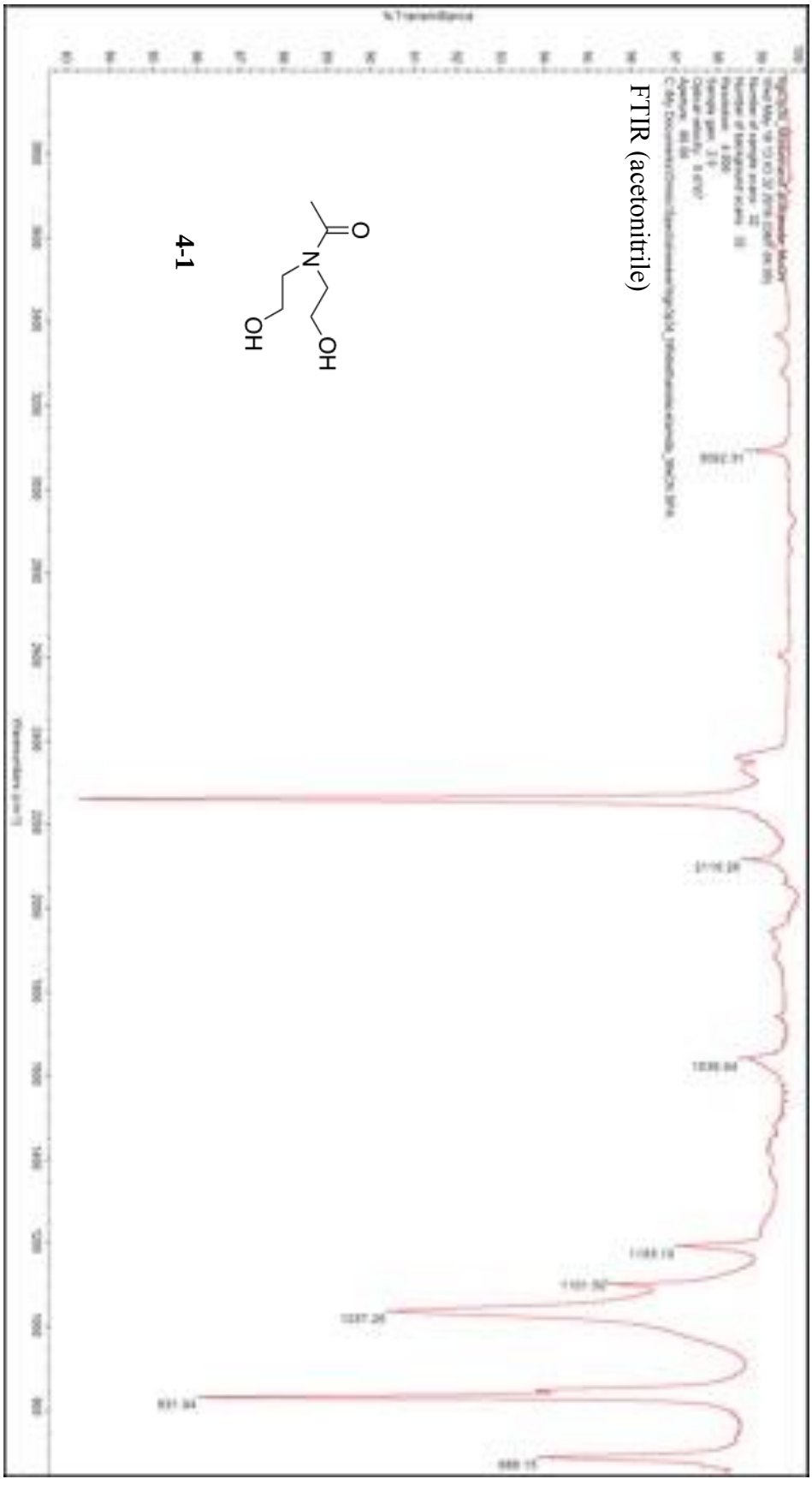
FTIR (acetonitrile)
4-1
OH
N
O
OH

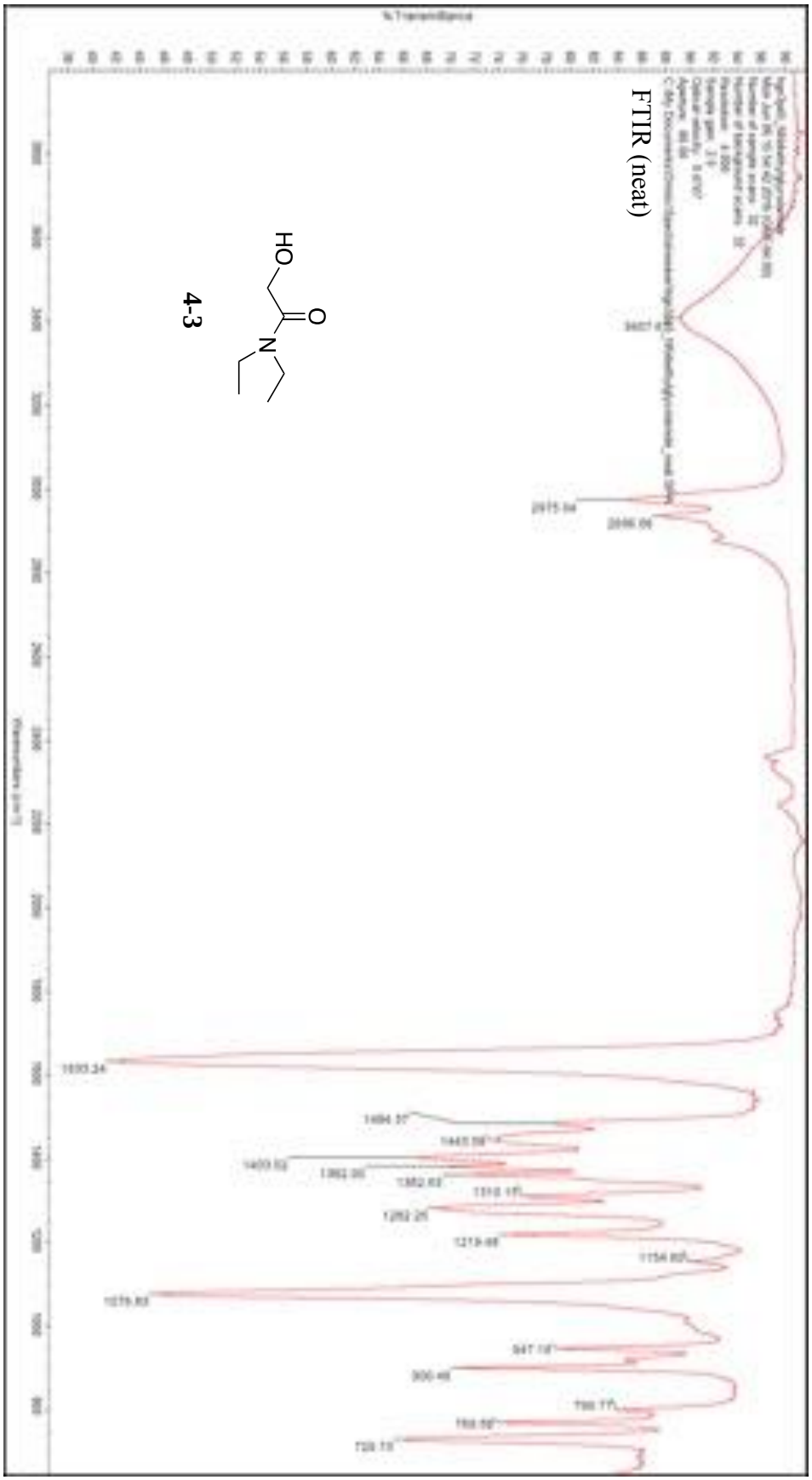
FTIR (neat)
4-3
HO
O
N

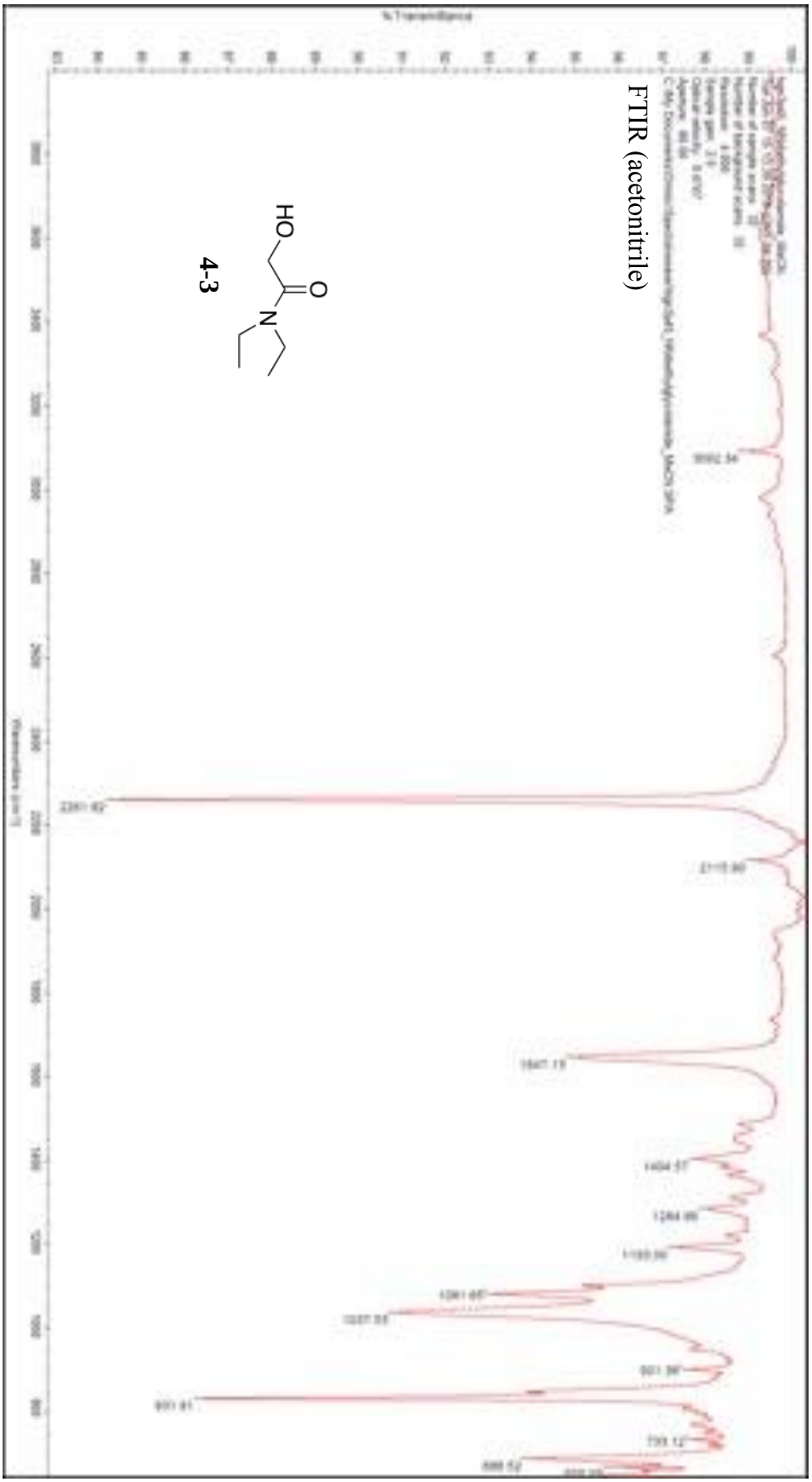

4-3

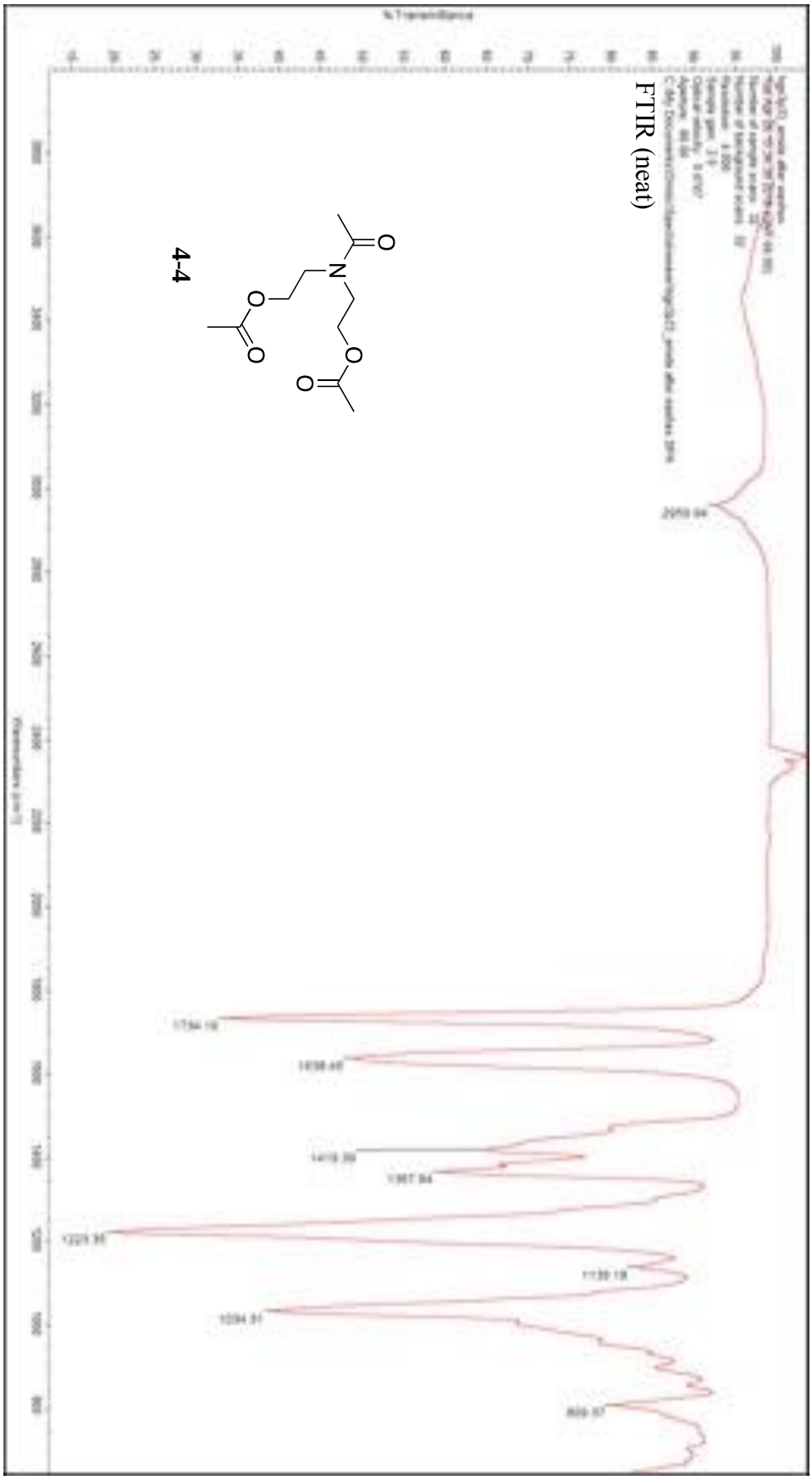
FTIR (neat)
4-4
2959.94
1734.10
1438.48
1413.39
1367.84
1221.35
1139.19
1094.31
809.97

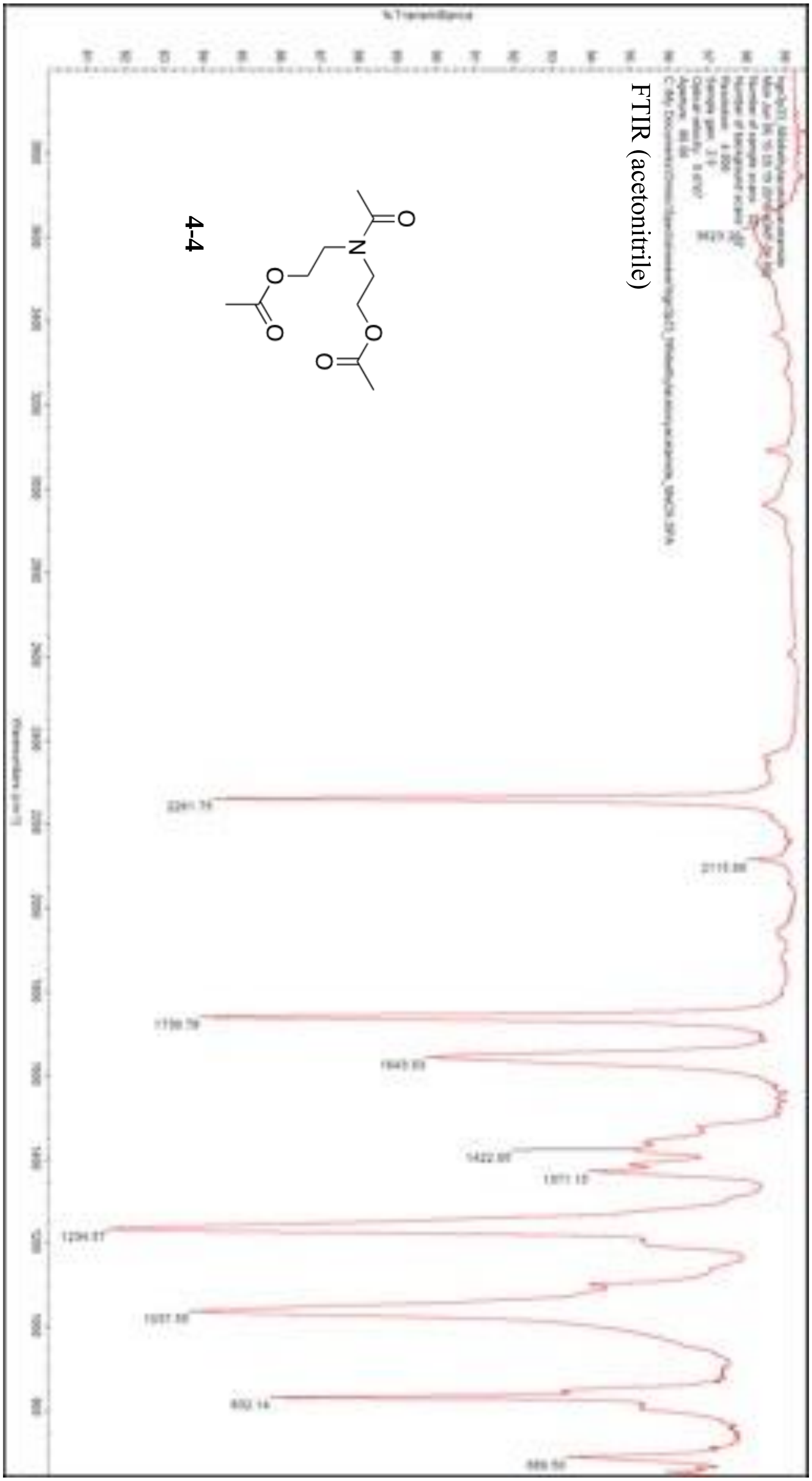
FTIR (acetonitrile)
4-4

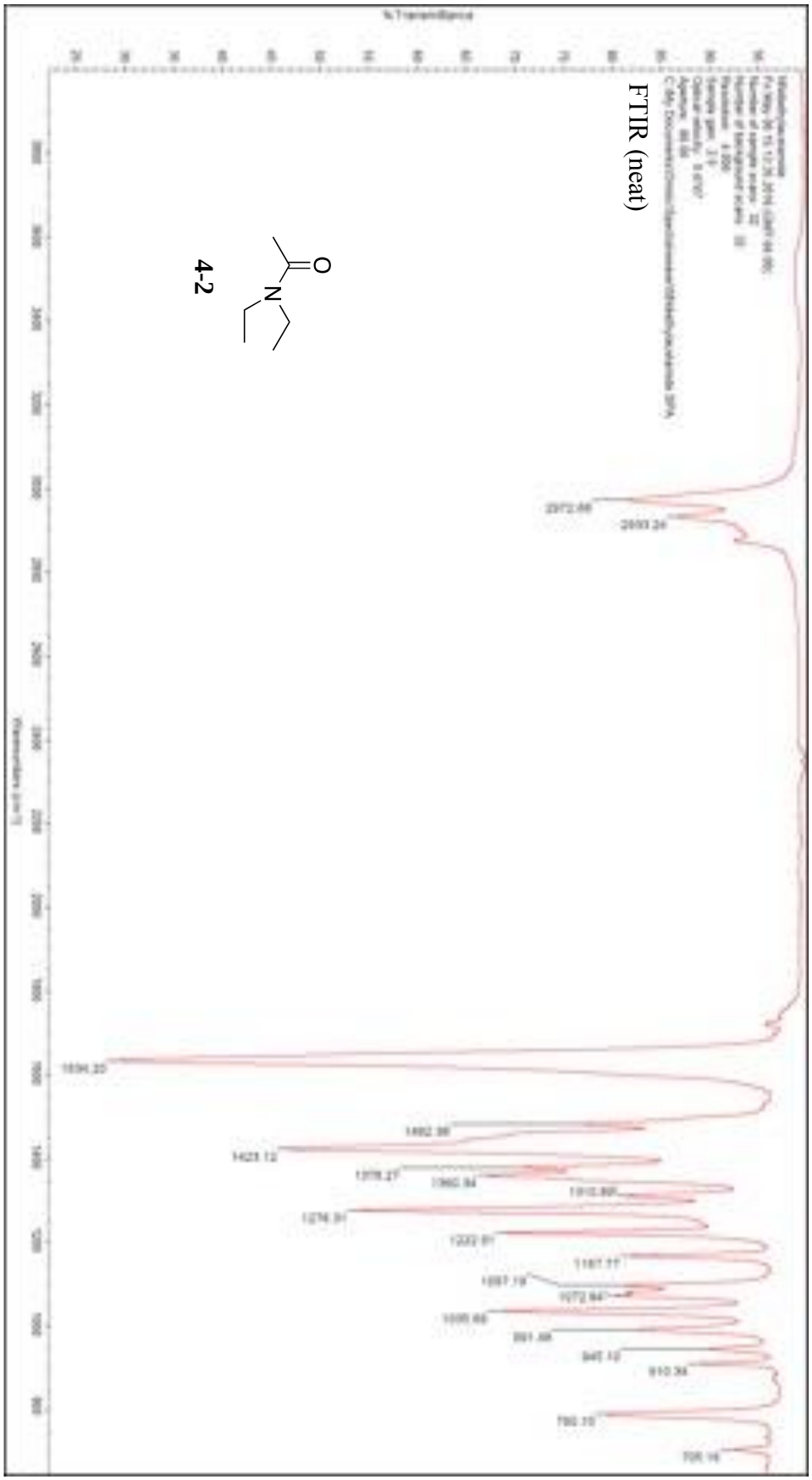
FTIR (neat)
4-2
O
N
2972.69
2933.24
1634.20
1492.38
1423.12
1378.27
1360.84
1310.80
1274.31
1232.91
1187.77
1097.19
1072.84
1035.48
991.08
940.12
910.38
780.10
705.16

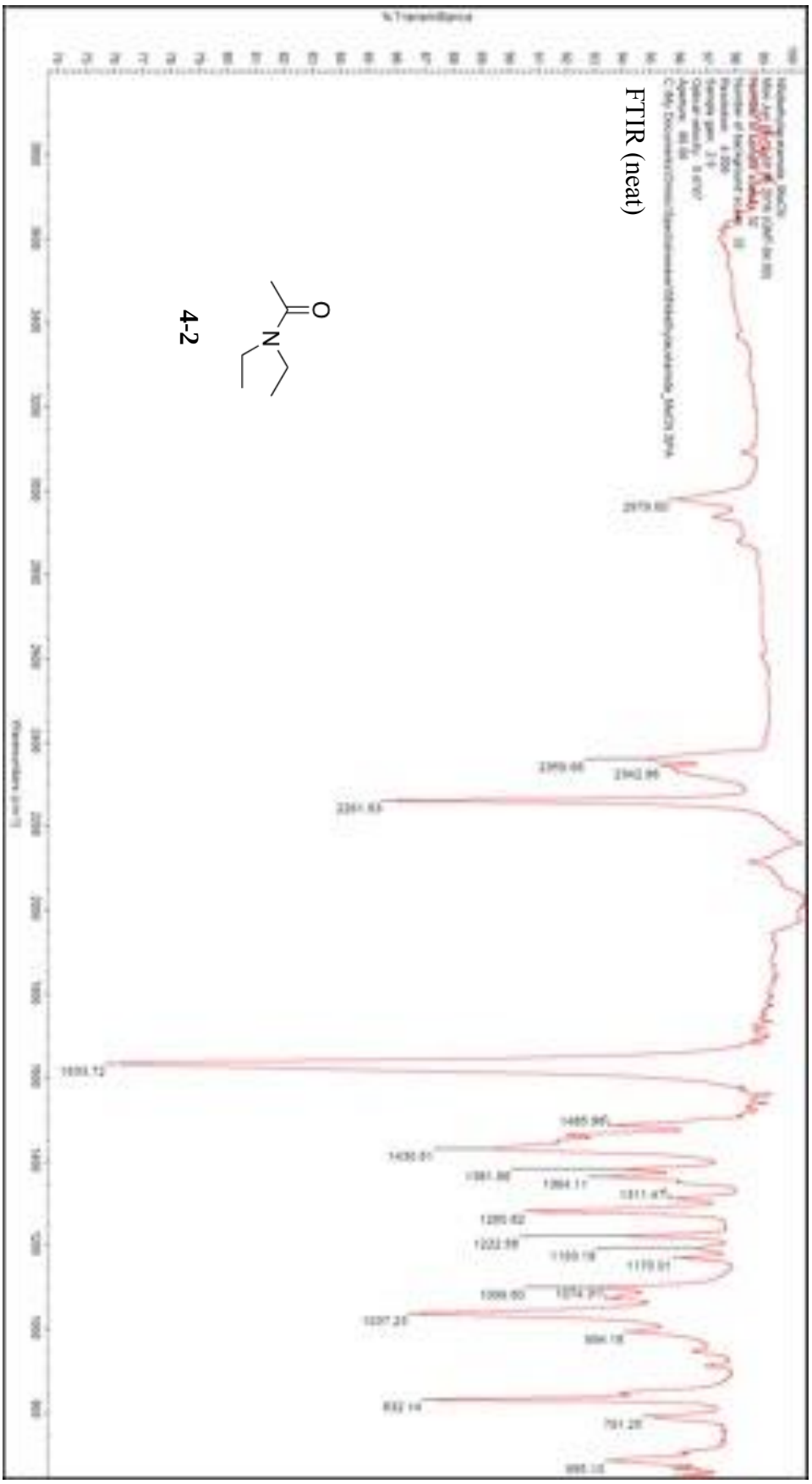
FTIR (neat)
4-2
O
N

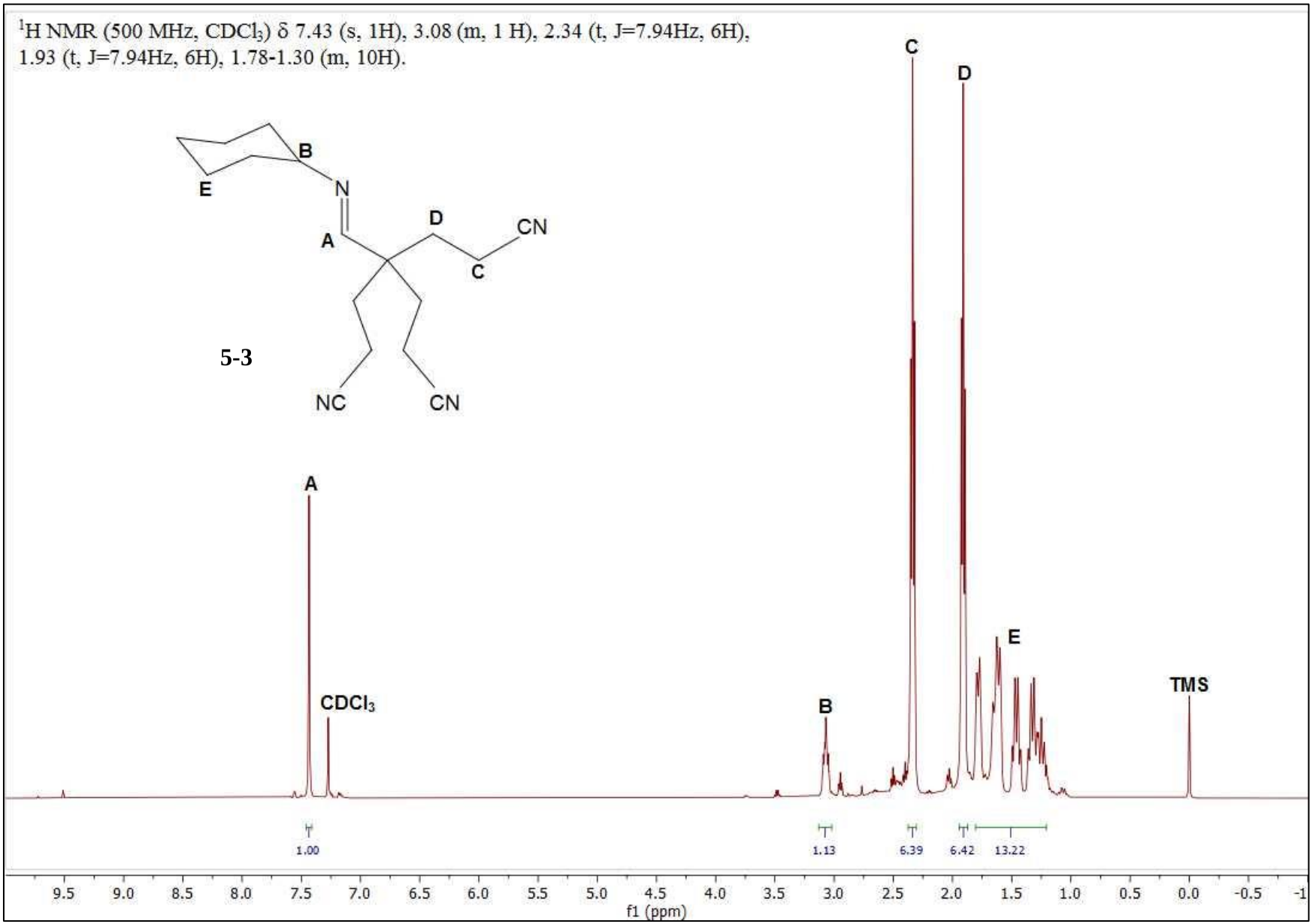
^{1}H NMR (500 MHz, $CDCl_3$) δ 7.43 (s, 1H), 3.08 (m, 1 H), 2.34 (t, J=7.94Hz, 6H), 1.93 (t, J=7.94Hz, 6H), 1.78-1.30 (m, 10H).
B
E
N
A
D
CN
C
NC
CN
5-3
A
CDCl3
B
C
D
E
TMS
1.00
1.13
6.39
6.42
13.22
9.5 9.0 8.5 8.0 7.5 7.0 6.5 6.0 5.5 5.0 4.5 4.0 3.5 3.0 2.5 2.0 1.5 1.0 0.5 0.0 -0.5 -1
f1 (ppm)

^{13}C NMR (125 MHz, $CDCl_3$) δ 160.30, 119.09, 68.36, 45.78, 36.05, 30.77, 25.44, 24.33, 11.88.

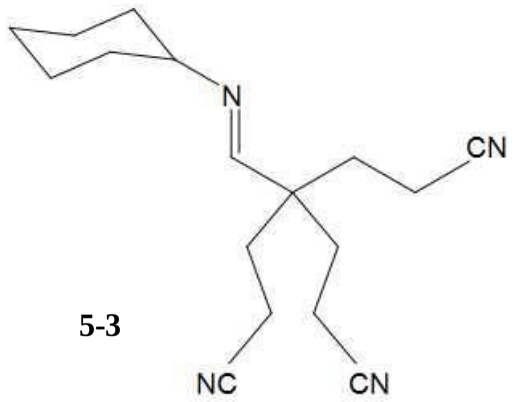

5-3

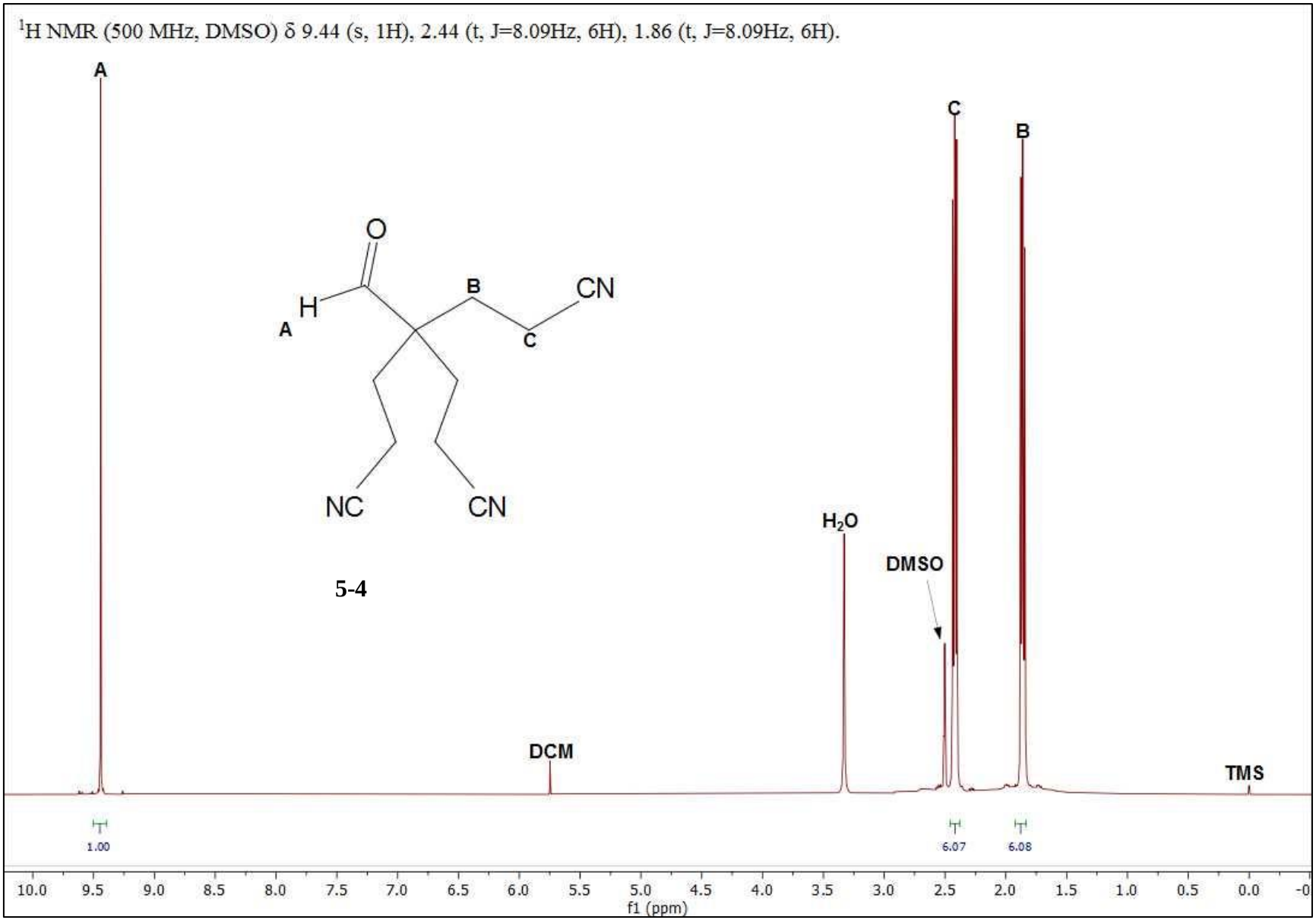
[1]H NMR (500 MHz, DMSO) δ 9.44 (s, 1H), 2.44 (t, J=8.09Hz, 6H), 1.86 (t, J=8.09Hz, 6H).
A
C
B
O
H
A
B
CN
C
NC
CN
5-4
H2O
DMSO
DCM
TMS
1.00
6.07
6.08
10.0 9.5 9.0 8.5 8.0 7.5 7.0 6.5 6.0 5.5 5.0 4.5 4.0 3.5 3.0 2.5 2.0 1.5 1.0 0.5 0.0
f1 (ppm)

^{13}C NMR (125 MHz, DMSO) δ 206.05, 122.28, 50.86, 30.06, 12.52.

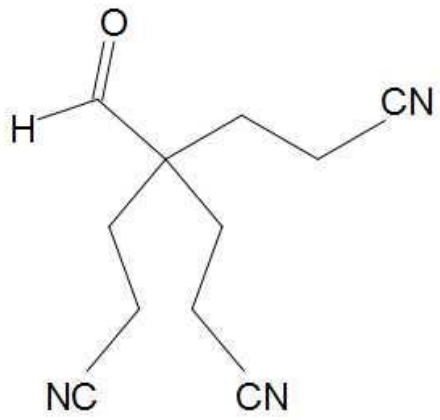

5-4

^{1}H NMR (500 MHz, $CDCl_3$) δ 3.55 (s, 2H), 2.42 (t, J=7.94Hz, 6H), 1.87 (br. s, 1H), 1.77 (t, J=7.94Hz, 6H).

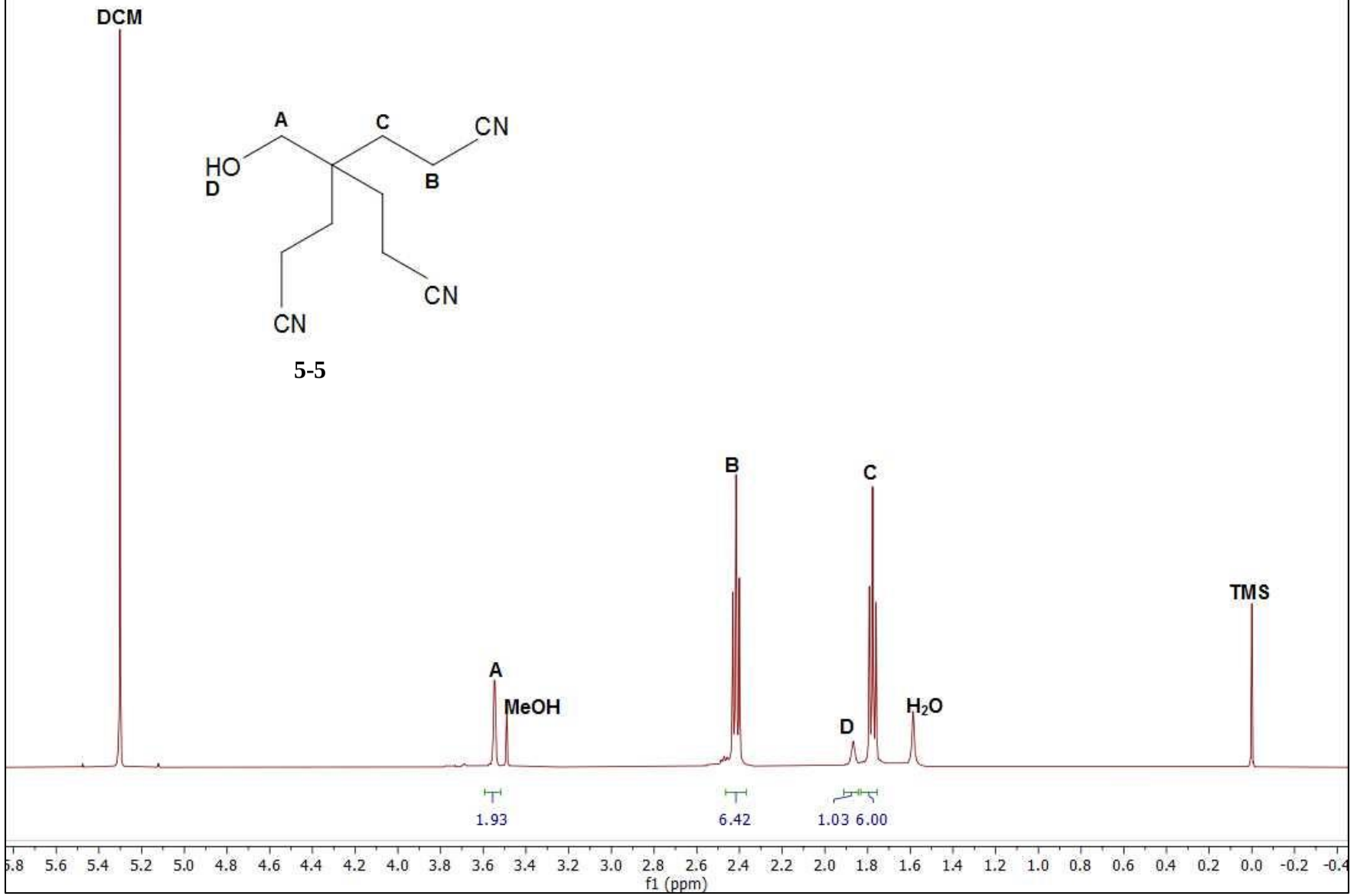

5-5

L

^{13}C NMR (125 MHz, $CDCl_3$) δ 120.11, 65.98, 40.23, 29.87, 13.09.

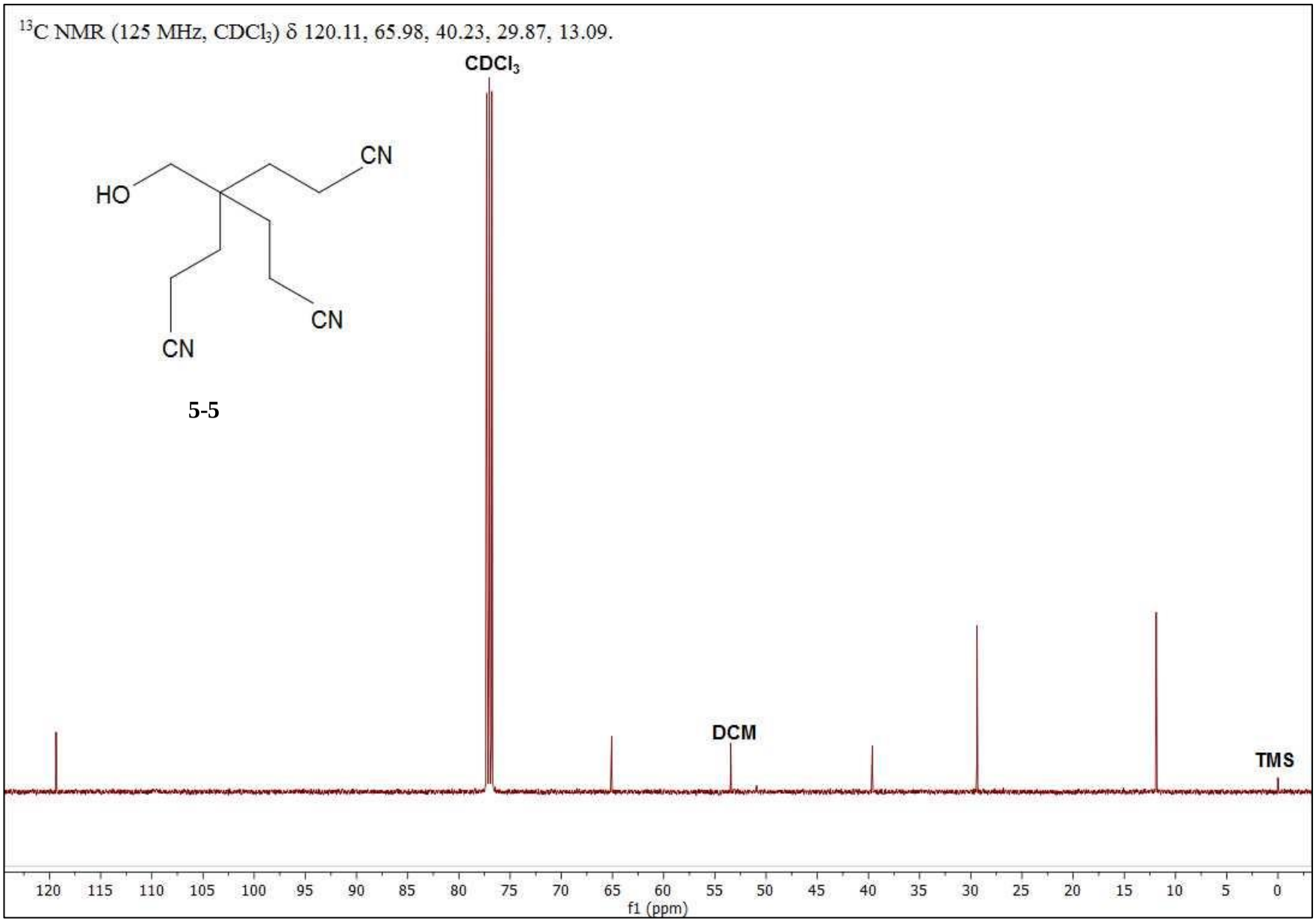

5-5

^{1}H NMR (500 MHz, $CDCl_3$) δ 3.38 (s, 2H), 2.35 (t, J=7.63Hz, 6H), 1.73 (t, J=8.24Hz, 6H), 0.90 (s, 9H), 0.08 (s, 6H).

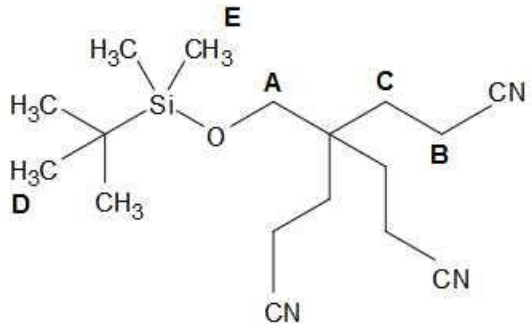

5-6

^{13}C NMR (125 MHz, $CDCl_3$) δ 117.67, 65.81, 39.40, 30.20, 26.57, 20.83, 12.65, -4.34.

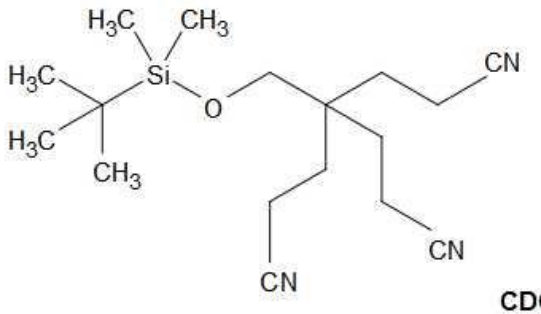

5-6

^{1}H NMR (500 MHz, $CDCl_3$) δ 3.26 (s, 2H), 2.64 (t, J=7.01Hz, 6H), 1.33 (m, 7H), 1.18 (m, 7H), 0.86 (s, 9H), 0.00 (s, 6H).

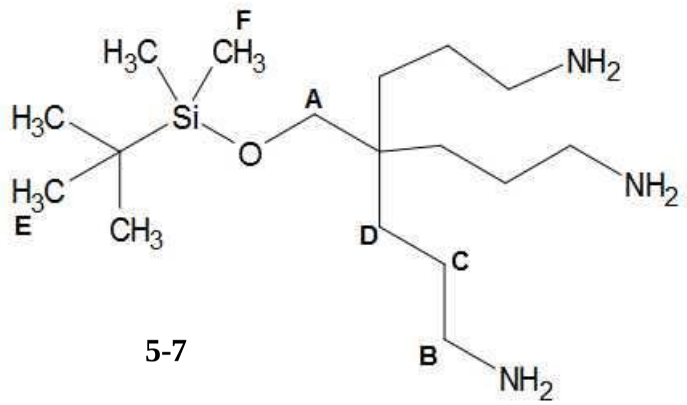

5-7

86.45% conversion

^{13}C NMR (125 MHz, $CDCl_3$) δ 67.11, 45.00, 39.26, 32.97, 28.09, 25.84, 13.14, -5.68.

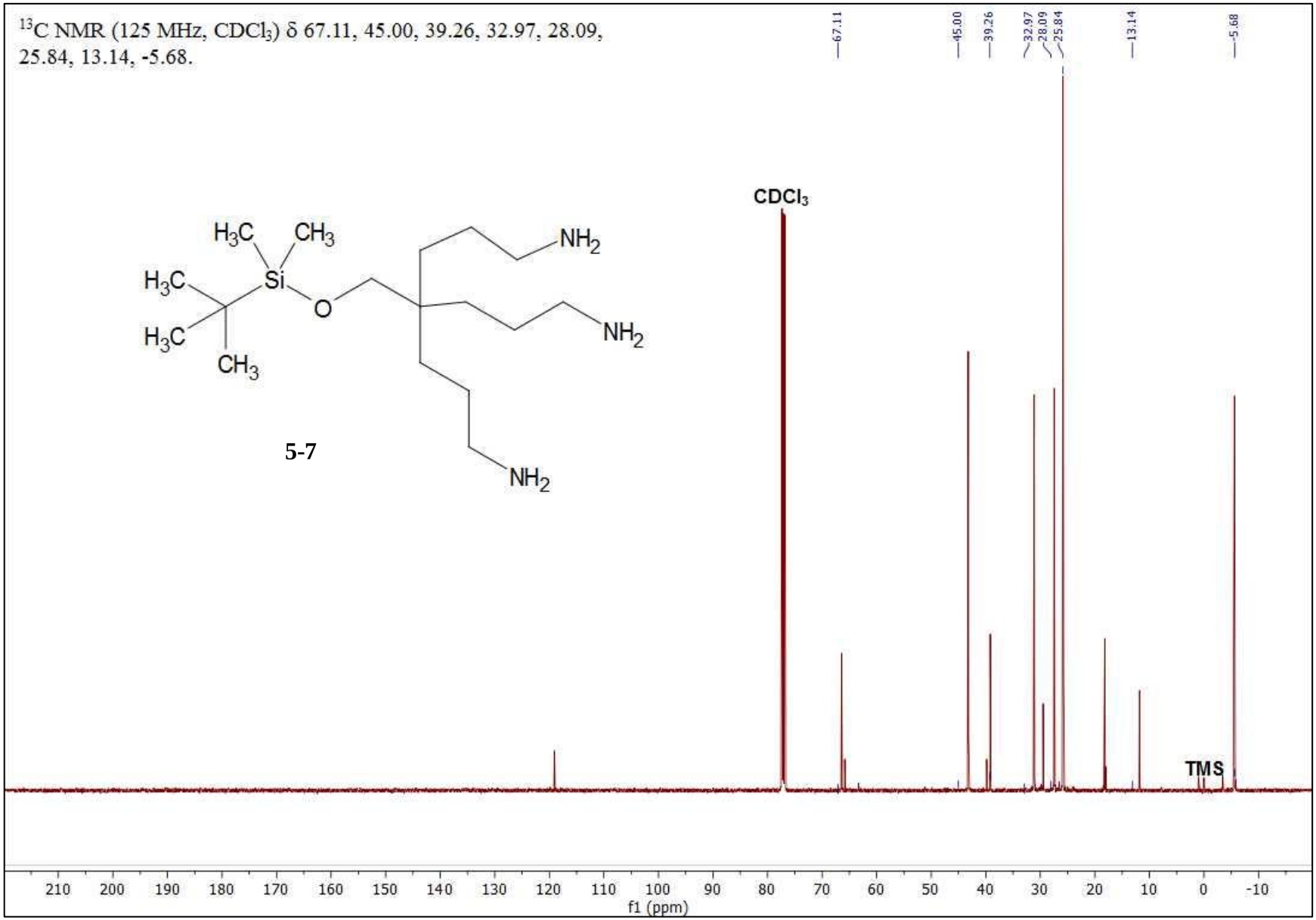

5-7